2016-10-25

Macrophages Are Regulators of Whole Body Metabolism: A Dissertation

Joseph C. Yawe

University of Massachusetts Medical School

MACROPHAGES ARE REGULATORS OF WHOLE BODY METABOLISM

A Dissertation Presented

By

JOSEPH C. YAWE

Submitted to the Faculty of the
University of Massachusetts School of Biomedical Sciences, Worcester
In partial fulfillment of the requirements for the degree of

DOCTOR OF PHILOSOPHY

OCTOBER 25, 2016

INTERDISCIPLINARY GRADUATE PROGRAM

MACROPHAGES ARE REGULATORS OF WHOLE BODY METABOLISM

A Dissertation Presented

By

JOSEPH C. YAWE

The signatures of the Dissertation Defense Committee signify completion and approval as to style and content of the Dissertation

_____

Michael P. Czech, Ph.D., Thesis Advisor

_____

Paul F. Pilch, Ph.D., Committee Member

_____

Roger J. Davis, Ph.D., Committee Member

_____

Yong-Xu Wang, Ph.D., Committee Member

_____

Kendall L. Knight, Ph.D., Committee Member

The signature of the Chair of the Committee signifies that the written dissertation meets the requirements of the Dissertation Committee

_____

Michael A. Brehm, Ph.D., Chair of Committee

The signature of the Dean of the Graduate School of Biomedical Sciences signifies that the student has met all graduation requirements of the school

_____

Anthony Carruthers, Ph.D.,
Dean of the Graduate School of Biomedical Sciences

Interdisciplinary Graduate Program

October 25, 2016

Acknowledgements

I would like to sincerely thank my mentor Michael Czech for taking me on as a student, and nurturing my love for science. He has provided guidance and a positive environment that has enabled me to grow as a research scientist. I will take away many lessons from his mentorship, and hope to pay them forward in the future. I would also like to thank my thesis committee for all their suggestions and feedback along the way. The amazing faculty members at UMASS are a major reason why I joined the program and I am grateful for the time and consideration than has gone into assisting me throughout my training.

I would also like to thank all members of the Czech lab, both past and present. Especially Myriam Aouadi for her strong mentorship early in the program and who continues to be trusted mentor and friend. Thank you to Rachel Roth Flach and Joe Virbasius for all the help with editing, experimental design and thoughtful discussions. Thank you to Pranitha Vangala, Sarah Nicoloro, Jessica Cohen, Yuefei Shen, Michaela Tencerova and Shinya Amano for all the excellent teamwork. I am glad to consider you all my lab family and good friends.

Finally I would like to thank my friends and family, who in various ways created a support system for me on this journey. Special thanks go to Djade Soumana, Laura Turyatemba, Vladimir Geneus and Caroline Duffy for your friendship and always cheering me on. Thank you to my parents for their love, patience, understanding, and pushing me to realize my true potential. Lastly,

thank you to my amazing brothers for believing in me and always having my back.

Abstract

Obesity is the top risk factor for the development of type 2 diabetes mellitus in humans. Obese adipose tissue, particularly visceral depots, exhibits an increase in macrophage accumulation and is described as being in a state of chronic low-grade inflammation. It is characterized by the increased expression and secretion of inflammatory cytokines produced by both macrophages and adipocytes, and is associated with the development of insulin resistance. Based on these observations, we investigated the potential role of macrophage infiltration on whole body metabolism, using genetic and diet-induced mouse models of obesity.

Using flow cytometry and immunofluorescence imaging we found that a significant percentage of macrophages proliferate locally in adipose tissue of obese mice. Importantly, we identified monocyte chemoattractant protein 1 (MCP-1) as the stimulating factor. We also found that ATMs can be targeted for specific gene silencing using glucan encapsulated siRNA particles (GeRPs). Knockdown of the cytokine osteopontin improved regulation of systemic glucose levels as well as insulin signaling in adipocytes. Conversely, targeting lipoprotein lipase (LPL) abrogated the buffering of lipid spillover from adipose tissue, resulting in increased hepatic glucose output. Finally, silencing of the master regulator of inflammation NF-κB in resident liver macrophages called Kupffer cells significantly improved hepatic insulin signaling. Thus this work demonstrates that macrophages can regulate whole body metabolism.

Table of Contents

List of Figures

List of Symbols, Abbreviations or Nomenclature

T2DM – Type 2 Diabetes Mellitus

TAG – Triacylglycerol

DAG – Diacylglycerol

FFA – Free Fatty Acid

ATM – Adipose Tissue Macrophage

KC – Kupffer Cell

WAT – White Adipose Tissue (visceral[VAT], subcutaneous[SAT]

GeRP – Glucan Encapsulated siRNA Particle

siRNA – short interfering RNA

KD – Knockdown

KO – Knockout

GTT – Glucose Tolerance Test

ITT – Insulin Tolerance Test

PTT – Pyruvate Tolerance Test

HFD – High Fat Diet

MCP-1 – Monocyte Chemoattractant Protein 1

OPN – Osteopontin

LPL – Lipoprotein Lipase

NF-κB - nuclear factor kappa

CHAPTER I: INTRODUCTION

PART 1: Insulin resistance and glucose metabolism

Insulin is an important hormone involved in regulating the utilization and storage or energy rich molecules such as glucose, glycogen and lipids. Part 1 will introduce major target organs for insulin, namely the liver and adipose tissue. It will also describe what happens when insulin signaling fails, particularly in the obese state, leading to type 2 diabetes mellitus (T2DM).

Insulin signaling pathway

Insulin is a peptide hormone that is produced and secreted by the pancreas, specifically in the Islets of Langerhans, which contain specialized insulin-producing beta cells (1). Owing to its importance in regulating whole body energy balance, particularly concerning carbohydrate and lipid metabolism, insulin expression, secretion and action have been extensively studied for almost a century. Although glucose is the primary stimulator of insulin secretion, other circulating nutrients such as amino acids and fatty acids can also act as insulin secretagogues (2). Translation of insulin does not result in the mature insulin protein, but instead a preproinsulin is synthesized on the rough endoplasmic reticulum (RER). Removal of the amino terminal sequence yields proinsulin, which is directed into the regulated secretory pathway and is further cleaved by endoproteases to produce insulin and C-peptide. The mature protein and C-peptide are finally stored in crystalline granules until secretion (3). Subsequent secretion of insulin in response to glucose is biphasic, owing to the existence of two distinct insulin granule pools. The readily releasable pool (RRP) is docked at

the cell surface, where calcium channels allow for rapid fusion with the plasma membrane and is therefore responsible for the initial or first phase of secretion (4). The second reserve pool is actively recruited to plasma membrane and results in a prolonged secretion of insulin called the second phase (5). Once insulin is secreted, it circulates to its target tissues where it binds and signals through its receptor.

The insulin receptor (IR) is a member of the receptor tyrosine kinase family of receptors and is expressed as two isoforms: IR-A and IR-B (6). IR-A is predominantly expressed during neonatal development, and has an affinity for another signaling molecule called insulin-like growth factor II (IGF-II) which is important for growth and development, and tends to be up-regulated in cancer cells (7). The IR-B isoform is more highly expressed in adult tissues such as adipose, muscle and liver, where it is involved in metabolic regulation (6). Insulin binding causes dimerization and autophosphorylation of the IR, thus activating the receptor. A number of IR substrates have been reported in the literature, however the most studied and metabolically relevant of those is the insulin receptor substrate (IRS) family, which number from IRS-1 to IRS-6 (8). They are phosphorylated on several tyrosine residues, and thus act as protein scaffolds for further downstream signaling complexes by binding proteins containing Src-homology 2 (SH2) domains (9). One such protein is phosphoinositide 3-kinase (PI3K). Binding of its regulatory subunit to IRS results in activation of its catalytic subunit, which phosphorylates phosphatidylinositol 4,5 bisphosphate (PIP_2) to

produce phosphatidylinositol (3,4,5) triphosphate (PIP_3), a lipid second messenger (8).

The proteins that mediate most of the physiological effects of PIP_3 belong to a subset of the AGC (PKA, PKG, PKC) family of kinases, which have a similar structure and are activated by phosphorylation of two serine and threonine residues (10). PIP_3 is anchored to the plasma membrane where it recruits and binds the pleckstrin homology (PH) domain of 3-phosphoinositide-dependent protein kinase 1 (PDK-1), which in turn phosphorylates and activates AGC kinases such as p70 ribosomal S6 kinase (S6K), serum- and glucocorticoid-induced protein kinase (SGK) and Akt/protein kinase B (PKB) (8). The family consists of three different isoforms Akt1, Akt2 and Akt3 encoded by different genes (11), with Akt2 being the most abundantly expressed and critical isoform in insulin-sensitive tissues (12). The Akt family of serine/threonine kinases represents a critical signaling node in the insulin pathway by regulating the activity and expression of a wide range of proteins such as transcription factors, enzymes and regulators of apoptosis, survival and the cell cycle (13). It is also important for mediating insulin's action in energy homeostasis, as will be discussed in subsequent sections.

Figure 1.1- The Insulin signaling pathway

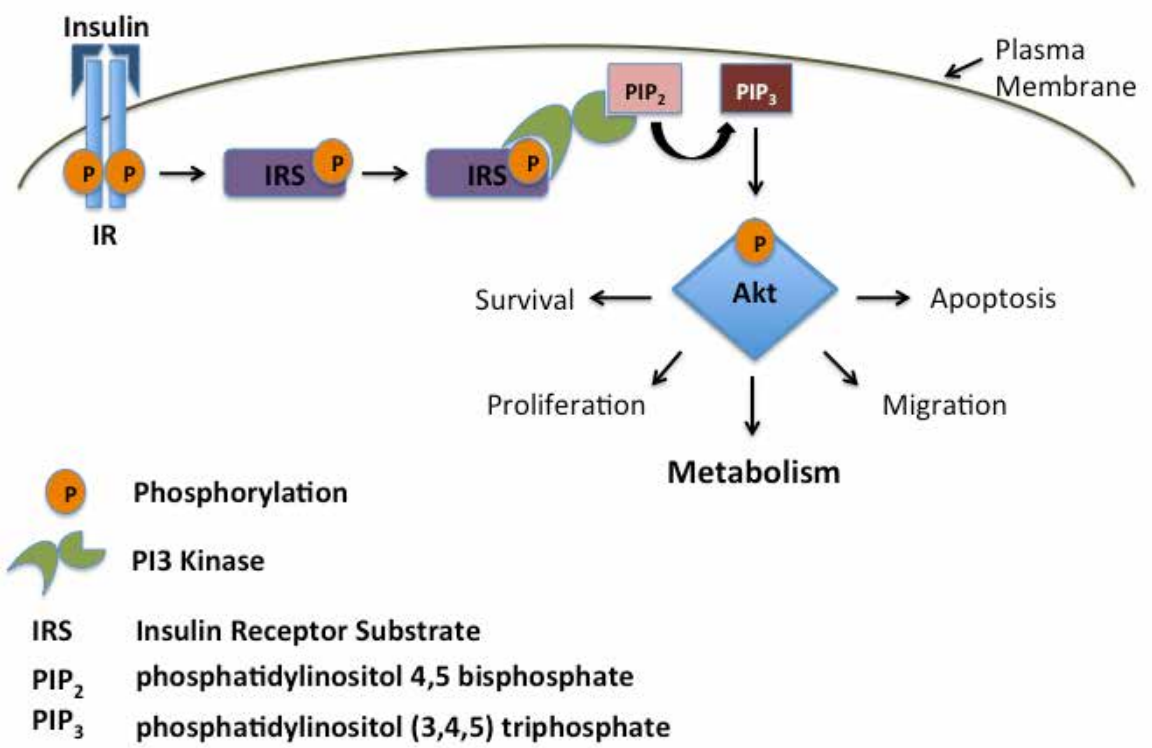

Figure 1.1 - The insulin signaling pathway
Insulin binding to its receptor results in dimerization and activation of the receptor via autophosphorylation. The activated receptor in turn phosphorylates one of its major targets, Insulin Receptor Substrate (IRS). IRS is bound by PI3 Kinase, which converts PIP_2 to PIP_3 at the plasma membrane. Finally PIP3 activates a class of kinases that includes Akt, which is a major signaling node and regulator of energy homeostasis.

Liver metabolism

Physiology and function of the liver

The liver is the largest organ in the human body and accounts for 2 to 3% of average body weight. It is highly vascularized and receives up to 25% of cardiac output at rest, which is more than any other organ. It is often described as having two lobes, which are characterized based on morphology and function (14). The liver is composed of five main cell types: hepatocytes, which constitute 80% of the cell population (15), endothelial cells, stem cells, biliary cells, stellate cells and immune cells (16). The liver's extensive access to the circulation is a feature that makes it uniquely adapted to its major functions. These include synthesis of plasma proteins and clotting factors such as albumin and fibrinogen respectively (17), systemic immune surveillance facilitated by robust innate and adaptive immune responses (16), detoxification of harmful molecules by xenobiotic biotransformation enzymes (18), and regulation of systemic glucose concentration as discussed below.

Maintaining blood glucose levels in the range of 4-6 mM is critical for sustained normal body function and homeostasis(19). The pancreas, which contains insulin-secreting β-cells and glucagon-secreting α-cells, serves an important role in modulating these levels (20). Secretion of the glucagon hormone is stimulated by a drop in the blood glucose levels, signaling the conversion of hepatic glycogen stores into glucose. This is also accompanied by increased gluconeogenesis, which altogether returns circulating levels to normal.

Conversely, a rise in blood glucose levels, typically postprandial, stimulates insulin secretion, which counteracts the action of glucagon in the liver by curbing glucose production (20, 21). In this way, the pancreas acts as a glucose-sensing organ, regulating liver glucose output as necessary.

Glucose and lipid metabolism

Glucose production is achieved via two different pathways, glycogenolysis and gluconeogenesis. Glycogenolysis involves the catalytic conversion of stored hepatic glycogen into glucose (22). Once glycogen is depleted, gluconeogenesis is stimulated and involves a series of enzymatic reactions that convert pyruvate into glucose. Pyruvate is generated in the cytosol from other metabolites such as amino acids and lactate and then converted to oxaloacetate by pyruvate carboxylase. Oxaloacetate is converted into phosphoenolpyruvate (PEP) by the gluconeogenic enzyme phosphoenolpyruvate carboxykinase (PEPCK). PEP is then sequentially converted into glucose-6-phosphate, which is the final precursor to glucose. It is converted into glucose by another key enzyme glucose-6-phosphatase (Glu-6-Pase) (22, 23).

Glucagon signaling increases the expression and enzymatic activity (by phosphorylation) of gluconeogenic enzymes by raising cAMP levels. This is a result of the activation of adenylate cyclase (AC), which is coupled to the glucagon receptor. cAMP-dependent kinase activity is thus increased, driving phosphorylation of gluconeogenic enzymes(22). Particularly, PEPCK gene transcription is rapidly induced by cAMP analogues (24) and there is evidence

that cAMP also blocks PEPCK mRNA transcript degradation(25). Conversely, insulin signaling stimulates glycolytic enzyme activation, shifts substrate concentrations in favor of glycogenesis and counteracts the transcription-inducing effects of cAMP (19, 21, 22, 24).

The liver is also an important organ for the handling and synthesis of triglycerides or triacylglycerol (TAG). These are neutral lipids that are composed of a glycerol backbone and three acyl chains, which are generated through the process of lipogenesis and released into the circulation (26). This process requires the esterification of fatty acids to the substrate glycerol-3-phosphate (G3P). G3P is generated first by phosphorylation of fructose-6-phosphate (F6P) by phosphofructo kinase (PFK) to fructose-1,6-bisphosphate (F16BP), which is subsequently hydrolyzed to produce G3P. For fatty acid production, pyruvate is first converted to citrate in the mitochondria and transported back into the cytosol where ATP-citrate Lyase (ACLY) subsequently converts it to acetyl CoA. Fatty acids are derived through a series of conversions by key lipogenic enzymes namely acetyl CoA carboxylase (ACC), fatty acid synthase (FAS), Fatty acyl-CoA elongases (Elovls) and finally stearoyl-CoA desaturases (SCDs)(23). This conversion of carbohydrates into fatty acids is also called de novo lipogenesis and is mostly carried out in the liver, though it occurs in adipose tissue as well (27). Free fatty acids (FFAs) can also be taken up from the circulation by the hydrolytic action of lipoprotein lipase (LPL) on circulating lipid-rich chylomicron particles (26). Insulin promotes lipogenesis by signaling through Akt to activate

transcription factors that up-regulate the expression of important enzymes as listed above (23). However, insulin-independent activation of lipogenesis is also observed and is thought to be driven by dietary carbohydrates (28).

Glucose and lipid metabolism in adipose tissue

Anatomy and Physiology of Adipose Tissue

Adipose tissue (AT) is a lipid storage organ that primarily acts as an energy reservoir and endocrine organ. AT is divided into two major depots: subcutaneous AT (SAT) is located under the skin and acts as cushion from mechanical stress, insulation from heat loss and a barrier against dermal infection, and visceral AT (VAT) is proximal to organs of the viscera or 'trunk' (29, 30). The parenchymal cell of the adipose tissue is the adipocyte, which adopts a different morphology and subcellular configuration depending on the primary function of the depot in which it is located. Other cell types that constitute AT include endothelial cells, immune cells, fibroblasts and adipocyte precursors. The cellular makeup as well as the morphology of AT can vary greatly with a number of genetic, metabolic, and environmental factors (30-35). Although originally thought of as just a fat storing organ, AT secretes a host of signaling molecules including hormones and cytokines, eliciting both local and systemic effects, thus establishing it as an important endocrine organ as well (35). This aspect of AT

function and its implications on whole body metabolism will be discussed in further detail in later sections.

There are three classifications of adipocytes to date: white adipocytes, brown adipocytes and the more recently characterized pink adipocytes (33). The white adipocyte is characterized by a single large lipid droplet (unilocular), which takes up 90% of the cell's volume thus confining the nucleus to a small area against the plasma membrane. The whitish/clear appearance of the lipid droplet under microscopy gives these cells their name. Brown adipocytes on the other hand are polygonal in morphology, have several lipid droplets in their cytoplasm (multilocular) and a more centralized roundish nucleus (29). Despite the name, pink adipocytes are not intermediates between the white and brown state, but rather they are subcutaneous white adipocytes that transdifferentiate into lipid laden epithelial cells during pregnancy to form the milk-secreting mammary gland in females (33). Since white and brown adipocytes are the most studied and metabolically active types, they will be discussed in further detail.

White Adipose Tissue

During times of positive energy balance, white adipose tissue (WAT) stores energy in the form of TAG, which can be hydrolyzed into fatty acids via lipolysis during times of energy demand. In this way WAT acts to maintain energy homeostasis (30). TAG is produced via lipogenesis, utilizing a similar pathway as described earlier (36). In adipocytes, insulin stimulates the uptake of glucose from the circulation by signaling the translocation of the primary adipocyte

glucose transporter GLUT4 from intracellular vesicles to the plasma membrane (37). In vitro data generated from 3T3-L1 adipocytes shows this to be dependent on Akt activation (38). Subsequently, glucose is converted into G3P for FFA esterification as seen in the liver. Fatty acids are mainly derived from the hydrolysis of circulating lipoproteins by LPL and uptake of resultant FFAs (27). These are subsequently re-esterified to the intracellular G3P pool. Aside from promoting glucose uptake, insulin also acts to promote lipogenesis in adipocytes by enhancing FFA uptake by increasing the gene expression and activity of LPL (39, 40), stimulating de novo lipogenesis, although to smaller scale than in the liver (27), and promoting the translocation of two proteins involved in FFA diffusion and capture, i.e., fatty acid transporter (CD36) and fatty acid transporter protein 1 (FATP1), to the plasma membrane (41). Furthermore, insulin-stimulated FATP1 translocation is blunted by PI3K and MAPK pathway blockade, suggesting a mechanism for this process (42). In addition, insulin has antilipolytic effects, which promote the storage of TAG.

Lipolysis is the opposite of esterification and involves the stepwise enzymatic breakdown of TAG back into glycerol and FFA during periods of negative energy balance (43). Lipolysis is driven by catecholamine and natriuretic peptide (NP) stimulation of β-adrenergic receptors (β-AR) (44) and natriuretic peptide receptor (NPR) (45), respectively. In the case of β-ARs, which are G-protein-coupled-receptors, catecholamine stimulation results in interaction of the stimulatory G_s subunit with AC, thus activating it to convert ATP to the

second messenger cAMP. This increase in intracellular cAMP activates protein kinase A (PKA) which phosphorylates a lipid droplet-associated protein perilipin 1 (PLIN1) (46) and hormone sensitive lipase (HSL) (47), so-called due to its tight regulation by catecholamines and insulin (48). PLIN1 phosphorylation promotes the release of a co-activator for adipose triglyceride lipase (ATGL) called comparative gene identification-58 (CGI-58), therefore activating ATGL, which is the rate-limiting step of lipolysis (49). ATGL hydrolyzes TAG to diacylglycerol (DAG), which releases one FFA and HSL hydrolyzes DAG to produce monoacylglycerol (MAG) and another FFA. The final step is MAG hydrolysis by monoglyceride lipase (MGL), yielding glycerol and a third FFA (43). NPR stimulation also results in PLIN1 and HSL phosphorylation; however, the kinase involved is cGMP-dependent kinase (PKG). PKG is activated by cGMP, the levels of which are increased by the guanylyl cyclase (GC)-mediated conversion of GTP to cGMP in response to NPR stimulation (45). Insulin exerts an antilipolytic effect that stems from IRS1/2 phosphorylation and subsequent PI3K/Akt activation of phosphodiestrase III B (PDE3B), which degrades cAMP to 5'-AMP. A drop in intracellular cAMP reduces PKA activity, resulting in decreased PLIN1 and HSL phosphorylation (50). The FFAs mobilized via lipolysis are released into the circulation, where they can be taken up and utilized as an energy source by other tissues such as the liver, muscle and brown adipose tissue.

Brown Adipose Tissue

Brown adipocytes are located in the brown adipose tissue (BAT), which has high mitochondrial content and is highly vascularized (33). Previously thought to only exist in in the interscapular region of rodents and human infants, recent evidence shows that adult humans also possess BAT primarily in the supraclavicular and neck region (51). Although brown adipocytes also contain lipid droplets, their main function is to utilize lipid and glucose as fuel for heat generation via non-shivering thermogenesis (31, 52). BAT is uniquely adapted for this role due to the presence of a high number of mitochondria and high expression of uncoupling protein 1 (UCP-1). UCP-1 generates heat by uncoupling oxidative phosphorylation from the production of ATP via ATP synthase. It provides an alternative route for release of the proton motive force built up by the electron transport chain across the mitochondrial inner membrane. This in turn increases substrate oxidation and the dissipation of resulting energy as heat (53). BAT thermogenic activity is controlled by beta-3 Adrenergic Receptor (β3-AR) signaling, and while a significant increase in activation is observed with cold exposure and re-feeding, it can also occur during starvation. Additionally, insulin appears to play a similar role in BAT as in WAT; promoting glucose uptake and the storage of lipid as TAG (52).

So whereas these tissues do share similarities, they are adapted to perform almost opposite functions: WAT stores energy while BAT burns energy. It is therefore also important to note that there is a growing interest in understanding

the recently observed phenomenon of “browning”. This involves the acquisition of brown adipocyte characteristics by white adipocytes under a number of stimuli including cold, exercise, catecholamines and PPARγ agonists (54). These beige or brite cells have more mitochondria, lipid droplets, and UCP1 expression than white adipocytes, and the mechanisms driving this adaptation are currently under vigorous investigation (54). The importance of understanding this phenomenon and its overall contribution to systemic insulin sensitivity and glucose disposal will be discussed in the next section.

Figure 1.2 - Lipogenesis and lipolysis pathways in the adipocyte.

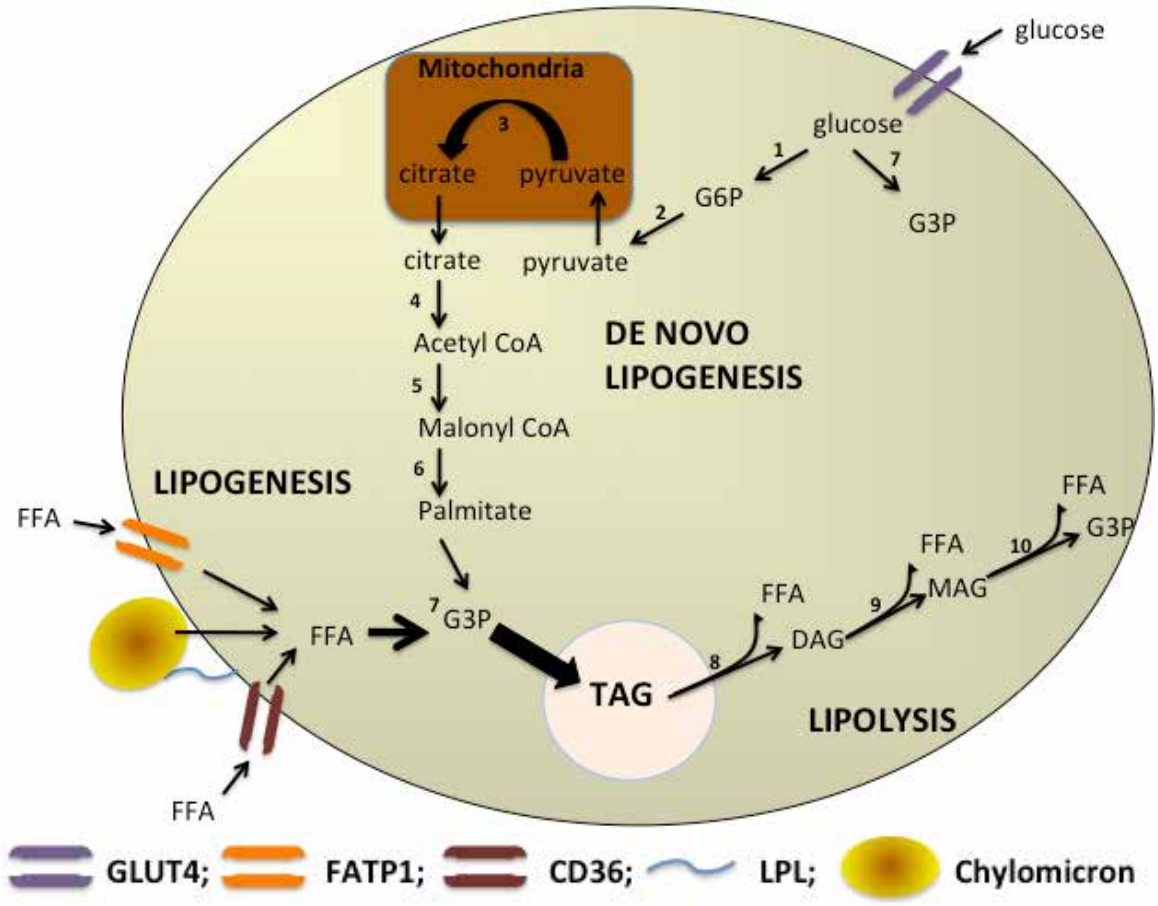

Figure 1.0-2 - Lipogenesis and lipolysis pathways in the adipocyte
1) Glucose taken up via GLUT4 is converted to glucose-6-phosphate (G6P) by hexokinase **2)** G6P is converted to pyruvate by pyruvate kinase **3)** Pyruvate is transported into the mitochondria where it is converted first to Acetyl CoA and then citrate, which is transported back to the cytosol **4)** Citrate is reverted to Acetyl CoA by ATP-citrate lyase **5)** Acetyl CoA is subsequently converted to Malonyl CoA by Acetyl CoA carboxylase **6)** Fatty acid synthase converts Malonyl CoA to palmitate **7)** Palmitate and other FFAs taken up from the extra cellular space and chylomicron hydrolysis are esterified to glycerol-3-phosphate (G3P). G3P is derived from glucose via glycolysis and phosphorylation of fructose-6-phosphate. G3P is also produced in the final step of lipolysis. **8)** Lipolysis is initiated by activation of adipose triglyceride lipase, which hydrolyzes TAG to DAG **9)** DAG is subsequently hydrolyzed to MAG by hormone stimulated lipase **10)** Finally MAG is hydrolyzed to FFA and G3P. One FFA is released at each step of hydrolysis.

Obesity and Type 2 Diabetes Mellitus

Obesity and adipose tissue expansion

Adipose tissue is a very plastic organ that has the ability to expand and adapt in situations of excess/surplus energy (55). This is often the result of a high caloric diet and a sedentary lifestyle, which results in high energy intake, low energy expenditure and weight gain attributed to increased fat mass (56). If unchecked, this energy imbalance results in the development of obesity. An individual is characterized to be obese if their body mass index (BMI) is above 30 kg/m^2. BMI is calculated by dividing the mass (in kilograms) of an individual by the square of their height (in meters). A BMI under 19 kg/m^2 is considered underweight, whereas19-24.9 kg/m^2 is the normal range, and 25-29.9 $kg/m^{2\ is}$ overweight (57).

The incidence of obesity in western societies, particularly here in the U.S, has been rising over the past four decades as a result of an increase in per capita energy intake (58). Indeed, recent data shows about one third of the U.S population is obese, with another third falling in the overweight category (59). This is problematic because obesity and its associated sequelae are currently the leading cause of morbidity, mortality and reduced quality of life. These sequelae are collectively referred to as the metabolic syndrome and include increased blood sugar, high blood pressure and abnormal triglyceride/cholesterol, which together raise the risk of diabetes, stroke and cardiovascular disease (60). And although diet and lifestyle play a central role in the development of obesity,

genetic factors must also be taken into account because 45-75% of BMI variability can be explained by heritable factors (61).

Adipose tissue expansion is observed in both SAT and VAT depots and is considered to be an adaptive response to a positive energy balance. However, in the extreme case of obesity it can become pathological as described above. Research into the underlying causes of metabolic syndrome has given rise to the hypothesis that although SAT and VAT both undergo this expansion, VAT expansion is maladaptive compared to SAT expansion (62). This so-called visceral obesity is associated with impaired glycemic and lipid control and the development of cardiovascular complications (63). Indeed, studies have also shown that men tend to gain more visceral than subcutaneous fat, which is associated with a higher cardiovascular risk. Conversely premenopausal women preferentially store subcutaneous fat, but switch to visceral deposition after menopause and thus increase their risk of cardiovascular events in a manner reminiscent to that of men (64).

The depot-dependent risk for driving the metabolic syndrome stems from the ability of each depot to adequately adapt to the storage of excess lipid. During expansion, AT adapts by increasing adipocyte size and adipocyte number, or hypertrophy and hyperplasia, respectively (65). SAT has more expandability than VAT, which is suggested to be the source of its protective effects (55). VAT primarily expands by hypertrophy, and adipocyte size correlates with insulin resistance (IR) and hyperglycemia, and also depots with

large adipocytes show increased inflammation and susceptibility to cell death (66, 67). Meanwhile, SAT expands via both hypertrophy and hyperplasia, which is believed to be protective as smaller, newer adipocytes are more insulin sensitive and have enhanced storage capacity (64). Two recent rodent studies showed that VAT expands first in response to a high fat diet (HFD), eventually reaching a maximum capacity, while SAT continues to expand (68, 69). Upon reaching maximum capacity, adipocyte dysfunction results in increased lipid circulation, which is detrimental to metabolic homeostasis (70). This will be discussed in further detail in the next section.

Ectopic lipid deposition

Adipose tissue expansion is typically sufficient to meet the requirements of excess energy storage. However, this adaptation is only viable up to a certain point when adipocytes fail to cope. This state is characterized by endoplasmic reticulum (ER) stress and mitochondrial dysfunction and results in increased intracellular and systemic levels of adipokines, free fatty acids and inflammatory mediators, which together drive adipocyte dysfunction (71). Lipogenesis is significantly reduced, as shown by the reduced expression of key lipogenic genes such as the adipogenic master regulator PPARγ (72). Conversely, there is an increase in lipolytic activity and lipid spillover from apoptotic adipocytes (67). The inability of AT to adequately store TAG results in ectopic deposition in other tissues such as liver and muscle.

Muscle is a highly metabolically active tissue and is the major site of insulin stimulated glucose uptake, accounting for 75% of glucose clearance (73). Similar to adipose tissue, this is GLUT4-dependent, although exercise-induced, insulin-independent expression of GLUT4 can also improve glucose clearance (74). Glucose is subsequently converted to glycogen and stored as a readily accessible source of energy. Once these glycogen stores are depleted, as is the case with exercise, there is a shift to glycolysis of fresh glucose taken up from the circulation (75). Muscle also stores a small amount of TAG as yet a third source of energy; however, increased circulating FFA in obesity causes excess deposition and an increase in TAG. Paradoxically, this phenomenon is also observed in endurance athletes with an active lifestyle (76). In obese patients, this increased lipid deposition is believed to promote IR in the muscle, impairing glucose clearance and contributing to a state of hyperglycemia (77).

In the liver, lipids are typically stored in hepatocytes only during fasting conditions; however, obesity increases hepatic lipid stores (78). This is thought to stem from increased circulating FFAs, and the resulting lipid accumulation has been associated with hepatic dysfunction, inflammation and ER stress (79). This pathological state called non-alcoholic fatty liver disease (NAFLD) can contribute to the development of type 2 diabetes (T2DM) if lipid accumulation goes unchecked (80). Fatty liver or steatosis is the first step on a spectrum of liver disorders that could result in cancer. The next step, non-alcoholic steatohepatitis (NASH), is promoted by prolonged steatosis, inflammation, cell death and

fibrosis. NASH predisposes the liver to cirrhosis, which is a high risk factor for the development of hepatocellular carcinoma (81). However, the spectrum of NAFLD is beyond the scope of this thesis and we will focus on the pathology of T2DM instead.

Insulin resistance and Type 2 Diabetes

Thus far, obesity has been characterized as an insult on the human body, with resulting sequelae associated with the metabolic syndrome. The body of work herein focuses on those factors that cause T2DM. T2DM is characterized by the inability to maintain fasting blood glucose levels within the normal range of 4-6 mM, resulting in hyperglycemia, hyperinsulinemia and dyslipidemia. The T2 diabetic state is also associated with a host of complications such as retinopathy, nephropathy and cardiovascular complications (82). Although there is a consensus that obesity predisposes one to develop T2DM, the underlying molecular mechanisms are still under rigorous investigation. A focal point for this research is the shift from insulin sensitivity to IR of insulin targets.

As discussed previously, adipocyte dysfunction and ectopic lipid deposition in muscle and liver are some of the factors believed to drive IR. In muscle, although TAG deposition is increased, it is increased intramyocellular DAG accumulation that is concomitant with IR and impaired glucose uptake (83, 84). These studies showed DAG signaling activates a novel PKC (nPKC) isoform PKCθ that blocked IRS-1-associated PI3K activity, and the data were later confirmed with human studies (85, 86). One mechanism proposed for hepatic

insulin resistance is an increase in pyruvate carboxylase activity due to increased levels of hepatic acetyl CoA derived from WAT-lipolysis. This results in the loss of insulin's ability to suppress HGP, resulting in hyperglycemia (87). Short chain FFAs can also inhibit glucose-stimulated insulin secretion by reducing glucose oxidation and thus reducing the ATP/ADP ratio (88).

Hyperglycemia triggers an increase in insulin secretion; however, the inability of target tissues to respond adequately creates a sustained feedback loop. This puts a strain on insulin-secreting β-cells, causing islet hyperplasia and a hyperinsulinemic state. Eventually, lipotoxicity, glucotoxicity, increased oxidative stress and inflammation result in β-cell failure (89, 90). Adipose tissue inflammation is also hypothesized to be an initiating factor in the development of IR (32). However, recent data from our lab suggests insulin itself is a driver of adipose tissue inflammation, therefore hyperinsulinemia is an early step in the development of obesity-associated diabetes (91). Whether inflammation is the chicken or the egg remains to be elucidated. Adipose tissue inflammation will be discussed in further detail in Part 2.

Figure 1.3 – Lean insulin sensitive versus Obese insulin resistant

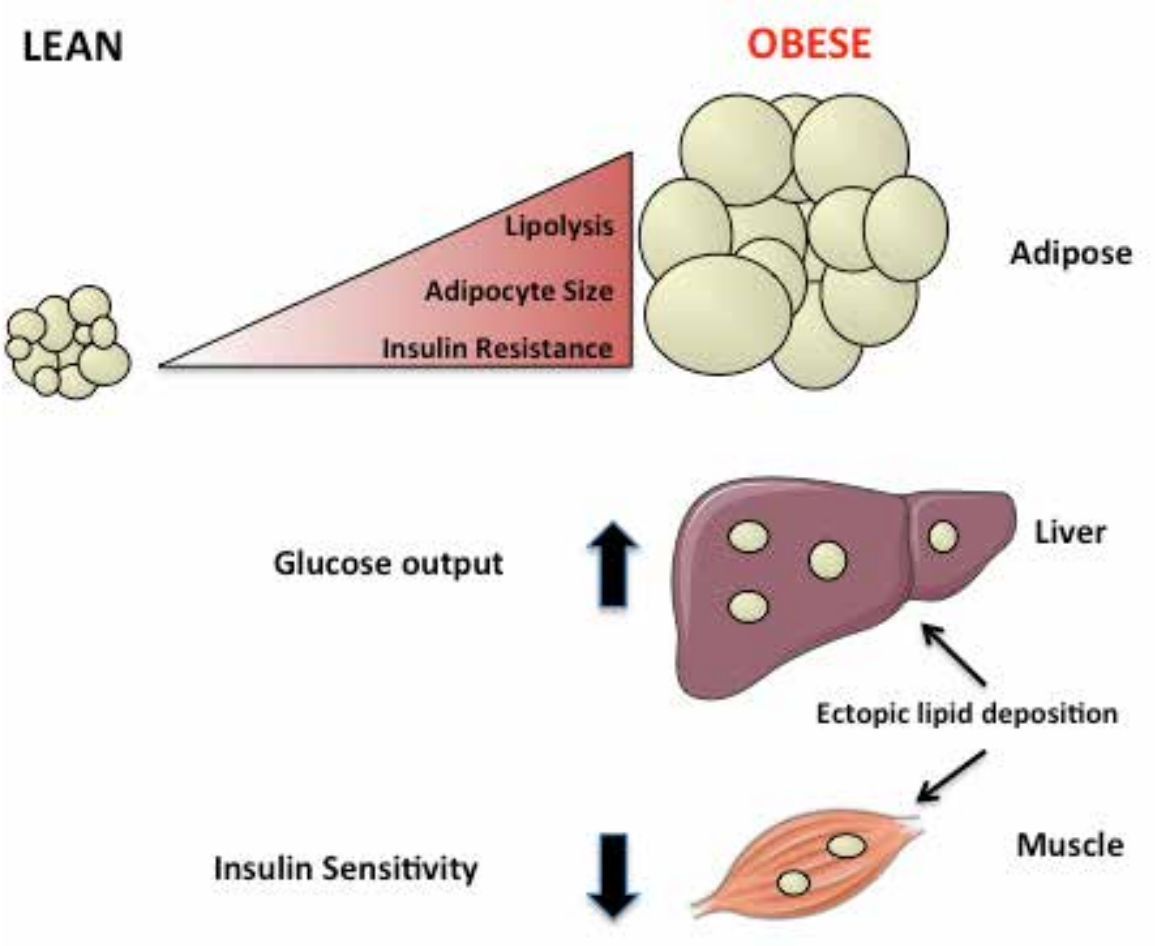

Figure 1.3 - Lean insulin sensitive versus obese insulin resistant
Increased caloric intake usually combined with a sedentary lifestyle results in increased energy storage in the form of fat in adipose tissue. Adipocytes undergo hypertrophy and proliferation to cope with excess lipid, eventually leading to adipocyte dysfunction, increased lipolysis and ectopic lipid deposition in other tissues such as liver and muscle. This is associated with decreased insulin sensitivity and hyperglycemia resulting from increased hepatic glucose output. These sequelae define the type 2 diabetic state in the context of obesity.

PART 2: Inflammation and insulin resistance

The adipose tissue of obese diabetic patients and rodents has been characterized as being in a state of chronic low-grade inflammation, with increased cytokine expression and immune cell accumulation, particularly macrophages. This has prompted speculation on the role of inflammation in the development of insulin resistance and T2DM. Part 2 will focus on the current understanding of how inflammation is involved in the regulation of adipose and liver function.

Immunometabolism

Adipose tissue inflammation

The immune cell population of AT is the second largest after adipocytes themselves and therefore plays an important role in maintaining AT homeostasis. Furthermore, AT has increasingly been recognized as an important organ that integrates metabolic, endocrine and immune functions that affect systemic homeostasis as well (92). Resident AT immune cells span almost the entire spectrum of innate and adaptive immune cells, and in the lean healthy state they carry out general housekeeping functions including immune surveillance and clearance of apoptotic debris (93). In acute inflammation, the typical immune response in to an insult involves resident macrophage and mast cell secretion of cytokines and chemokines. This attracts neutrophils first, then macrophages and lymphocytes from the circulation, which clear the inflammatory agent and

affected cells (94). Antigen presenting cells (APCs) then facilitate the transition from innate to adaptive response carried out by B and T lymphocytes (95). This generally results in increased local and systemic levels of chemokines and cytokines typical of sepsis. Obesity induces an immune response in AT, although it is defined as chronic low-grade inflammation that displays modest increases in circulating proinflammatory cytokines without the clinical indications of inflammation (96).

Though less severe, this low-grade inflammation has been reported to have significant effects on whole body metabolism and the development of IR. The first evidence of this was the rat study by Feingold *et al,* which showed increased blood glucose levels with administration of the proinflammatory cytokine tumor necrosis factor alpha (TNFα) almost 30 years ago (97). Later studies showed that obese rodents and humans have elevated TNFα levels, and that knockout (KO) mice or mice administered with neutralizing antibodies against the protein had improved insulin sensitivity (98-100). Furthermore, evidence that obesity stimulated activity of the canonical inflammatory nuclear factor kappa B (NF-κB) pathway can drive IR helped strengthen the hypothesis of a metabolism-inflammation connection (101, 102). Finally, these data together with the implication of another important class of proinflammatory signaling molecules, the c-Jun N-terminal kinases (JNK), served as the foundation for the field of immunometabolism (103, 104).

AT immune cell composition and number is significantly altered by obesity, and in turn the immune response and function of AT is changed. Specifically, there is an increase in number and activity of macrophages, mast cells, B and T lymphocytes, and neutrophils, while a decrease in the number of other cell types such as eosinophils and subsets of T lymphocytes is observed (94). This shift of balance is typically observed in VAT rather than SAT, lending weight to the argument that VAT immune derangement is an important initiator of IR and T2DM (105). However, an acute decrease in fat mass such as that induced by caloric restriction also appears to trigger AT inflammation (106). This could be explained by increased AT lipolysis and secretion of lipid signaling molecules that activate or recruit AT immune cells (107).

The unequivocal immune response in AT in response to changes in energy balance suggests an evolutionary adaptation linking metabolism and immunology. Indeed the heavy presence of immune cells in AT suggests immunological control of this energy store (93). For example, adipokines and FFA release from perinodal AT (PAT) can control activation and proliferation of lymphocytes, and conversely, activated lymphocytes can induce lipolysis in PAT to fuel an immune response (108). One hypothesis that has arisen to explain this phenomenon is the ‘energy-on-demand hypothesis’. It offers the argument that AT inflammation and IR raise circulating nutrient levels, allowing rapid access to energy to mount an immune response against bacterial pathogens. On the other hand, parasite infestation requires starving the parasite by sequestering

nutrients. The diverse immune cell population therefore serves to alternate between these two states depending on the threat (109). Regardless of whether this is the case, AT inflammation continues to be a fertile area for research due to the number of different immune cells involved, particularly macrophages. Our understanding of the contribution of each of these cell types will be reviewed in next few sections of this chapter.

Myeloid cells

Adipose Tissue Macrophages

In lean rodents, adipose tissue macrophages (ATMs) constitute the largest number of AT immune cells, accounting for 10-15% of cells in VAT and rising to as much as 50% with obesity (110, 111). While lower in humans, the expansion of this population with obesity is still significant: from 4% to 12% (112). Further studies showed that this increase was associated with visceral obesity and the development of atherosclerosis, IR and hepatic dysfunction (113, 114). Adipocyte size and stromal vascular fraction (SVF) expression of pro-inflammatory elements such as TNFα also correlate with ATM infiltration (115, 116). Conversely, weight loss was shown to reduce the number of ATMs (117). However, without identifying the relevant macrophage phenotype involved, the link between ATM accumulation and IR cannot readily be deduced.

Ever since Weisberg *et al* showed that obesity induced ATM accumulation in rodents is a result of infiltrating macrophages from the circulation, this view has

been widely accepted (110). Other groups have reported on potential chemokine signals that recruit macrophages to obese AT, driving inflammation and IR. Most of the data points toward monocyte-chemoattracting protein 1/chemokine C-C motif ligand 2 (MCP-1/CCL2), which is secreted by adipocytes and binds the CCR2 receptor on macrophages to stimulate migration (110, 118, 119). Data demonstrated that MCP-1 overexpression promoted ATM accumulation, AT inflammation, hepatic steatosis and IR, strengthening this observation. Conversely, a dominant negative mutant attenuated these effects (120). Furthermore, there are also data to suggest other targets such as CCL3, CCL5, CCL7, CCL8, CCL11 and CCL13 are responsible (121-123). Chapter 2 will show evidence that MCP-1 is important for inducing local macrophage proliferation, which has been disregarded as a significant source of ATMs until recently.

M1 and M2 ATMs

Macrophages are innate immune cells derived from the pool of mononuclear phagocytes generated in the bone marrow (124). Depending on the nature of the immune response, their lifespan can vary from hours to years (125). Resident tissue macrophages are closely related to dendritic cells (DC). However they are distinguished by their expression of Fc receptors, F4/80 and CD11b upon differentiation from circulating monocytes (126). Macrophages have a number of important duties that range from serving as sentinels that phagocytose invading pathogens, to tissue remodeling after injury and scavenging dead cells and detritus (127, 128). There are a number of macrophage populations in the body,

typically named for their anatomical location such as microglia in the brain, alveolar macrophages in the lung, osteoclasts in bone, histiocytes in interstitial connective tissue and Kupffer cells in the liver (126). Despite their location and phenotypic differences, they all perform macrophage-like functions with appropriate stimulation (129). Still, macrophages can further be described by their phenotypic function: M1 or classically activated, M2 or alternatively activated, regulatory macrophages, tumor associated macrophages, and others. M1 macrophages mediate host defense, antitumor immunity and inflammatory responses, whereas M2, regulator and tumor associated macrophages suppress those functions (130). However, in the context of obesity-stimulated AT inflammation and IR, M1 and M2 seem to be the most important players (32).

Polarization of macrophages to the M1 phenotype involves pathogen- and damage-associated molecular patterns that synergize with interferon-γ (IFNγ). This results in the production of reactive nitrogen and oxygen species, which have antimicrobial properties (130). *In vitro*, bone marrow derived macrophages (BMDMs) can be induced to M1 polarity by stimulating with proinflammatory factors such as bacterial polysaccharides (LPS), IFNγ and granulocyte-macrophage colony-stimulating factor (GM-CSF) (130). M2 polarization on the other hand is facilitated by anti-inflammatory cytokines interleukin-4 (IL-4), IL-10 and IL-13, and macrophage colony-stimulating factor (M-CSF), which activate the signal transducer and activator of transcription 6 (STAT6) program. These

suppressor macrophages are involved in the antiparasitic response, wound repair and tissue remodeling (126, 130).

Lean adipose tissue is predominantly populated by anti-inflammatory M2 macrophages, which secrete IL-10 and IL-1 receptor antagonist (IL1Ra), and they express M2 antigens CD206, Cd209 and CD301 as well as arginase 1 enzyme, which blocks inducible nitric oxide synthase (iNOS) activity (32, 109). They carry out housekeeping functions that maintain AT homeostasis such as extra cellular matrix (ECM) remodeling, clearing cellular debris, regulating thermogenesis and preadipocyte proliferation and differentiation (109, 131, 132). Obesity induces a shift from M2 to M1 by decreasing the expression of important M2 maintenance factors such as IL-4 and IL-13 while increasing the expression of proinflammatory markers such as F4/80, CD11c, TNFα and IL-6 (115). These macrophages are recruited from the circulation rather than conversion of the resident M2 population (133). Unlike M2 macrophages that are diffusely located in AT, M1 macrophages tend to aggregate around necrotic adipocytes in crown-like structures (CLS) and take up lipids to become foam cells. Furthermore, lipid signaling is also thought to play a role in the accumulation and polarization of M1 macrophages (134). Chapter 4 will focus on the role of CLS macrophages in lipid buffering and how it affects systemic insulin sensitivity.

M1/M2 axis in insulin resistance

The presence of M1 ATMs is strongly associated with systemic inflammation and IR, and there is also evidence showing that ablation of this population is protective (135, 136). A number of mechanisms explaining this relationship have been proposed including recruitment and activation of other immune cells, TNFα-mediated inhibition of insulin signaling, and increased collagen expression leading to fibrosis (135, 137-139). The polarization of macrophages from M2 to M1 is driven by a number of different factors such as LPS, which binds to toll-like receptor 4 (TLR4), a member of a pattern recognition receptor family that activates an innate immune response against pathogens. Obese rodents and humans exhibit increased systemic LPS levels, and interfering with TLR4 signaling ameliorates ATM accumulation and M1 polarization (140, 141). Lipid spillover from dysfunctional adipocytes also shifts macrophage polarity as saturated FFAs can also bind TLR4 as well as induce ER stress and inflammasome activation (142-144). Additionally, evidence suggests the important adipokine adiponectin has M2 polarizing effects. The reduced levels observed with increasing obesity could be another contributing factor to the M2 to M1 shift (145).

Though macrophages can exist as either M1 or M2, and this polarization can be recapitulated in vitro, closer inspection of in vivo populations suggests a continuum rather than a dichotomy. ATMs from both rodents and humans can simultaneously express F4/80 and CD11c, which are M1 markers, as well as

CD206 and CD301 (mannose receptor and Mgl1/2), which are M2 markers (146, 147). Additionally, human ATMs also exhibit decreased expression of some M1 markers while increasing the expression of the M2 marker lymphatic vessel endothelial hyaluronan receptor 1 (LYVE1) with obesity. Furthermore, these macrophages are also capable of secreting both pro- and anti-inflammatory factors (148). Interestingly, ATMs have also been shown to repolarize from one state to another. Switching rodents from a HFD to a normal diet can shift polarity back to M2, a change that is mimicked by adiponectin as well as administration of omega-3 FFAs (149-151). Thus, although useful for understanding inflammatory status of AT at a specific time, the M1/M2 classification is an oversimplification that should be approached cautiously.

Dendritic cells

DCs share a common progenitor with macrophages and act as the primary APCs that present antigens to T cell receptors via major histocompatibility complexes I and II (MHCI, MHCII), thus facilitating the innate to adaptive immunity transition (152). They are also involved in promoting helper T cell 1 (Th1) differentiation and the proliferation of CD8+ and natural killer cells. These responses are driven by cytokines IL12 and IL15, which are produced by DCs (95). Their identification and study in AT is complicated by the fact that they share a common primary marker CD11c with proinflammatory M1 macrophages. In flow cytometry, this is countered by defining macrophages as $F4/80^{+}CD11b^{+}CD11c^{+}$ and DCs as $F4/80^{-/low}CD11b^{-}CD11C^{+}$ (153). In mice, HFD

feeding increases DC counts in AT, while humans exhibit increased levels of DC antigens in obese SAT and demonstrated ability of isolated cells to induce Th17 cell differentiation. This creates a proinflammatory environment that favors an M1 polarization of ATMs (154).

Mast cells

Mast cells act as first line of defense against pathogens and maintain a heavy presence in barrier layers such as the mucosa and the skin. However, asthma, allergies and anaphylaxis responses are also associated with the uncontrolled activation of these cells (92). Once activated, they secrete a number of inflammatory factors including proteases, histamine, lipid mediators, and pro- and anti-inflammatory cytokines (155). AT mast cells are increased by obesity, and depletion of this population reduces ATM infiltration, prevents DIO and improves insulin sensitivity. Interestingly, data suggests these effects are mediated by IL-6 and IFNγ, affecting body weight and adiposity instead of AT inflammation (156).

Neutrophils

Neutrophils are the first immune cells recruited to a site of inflammation or damage and are responsible for coordinating acute inflammatory responses. They are phagocytes and contain cytoplasmic granules of biologically active molecules such as myeloperoxidase (MPO), which is important for antimicrobial defense (92). Additionally, they secrete chemoattractants that recruit other

immune cells including DCs, macrophages and lymphocytes (157). Obese individuals have elevated plasma levels of neutrophil markers like MPO, and HFD feeding causes a transient (1week) 20-fold increase in AT neutrophil number preceding ATM infiltration (133, 158, 159). Neutrophil elastase has also been implicated in IR, potentially via the degradation of IRS-1 or TLR activation (160).

Eosinophils

These granulocytes are involved in the antiparasitic response and secrete a host of cytokines, including IL-4 and IL-13, which mediate Th2 immunity (161). They are responsible for 90% of AT-associated IL-4 expression despite being present at very low numbers. They have also been linked to the M2 polarizing effects of IL-4 and IL-13, and their obesity-induced depletion is associated with the development of IR (162). However, administration of exogenous IL-4 can improve insulin sensitivity, further strengthening the idea of eosinophils playing a beneficial role (163).

Lymphocytes

CD4+ T cells

T cells are important for driving adaptive immunity and are classified as either CD4+ or CD8+ based on the expression of these two surface markers (92). CD4+ cells can be further subdivided into subclasses including but not limited to Th1, Th2, Th17 and regulatory T cells (Tregs) depending on which

cytokines they produce (164). Obesity increases the number of Th1 cells, which secrete the proinflammatory cytokine interferon gamma (IFNγ). This cytokine polarizes ATMs to M1, thus promoting AT inflammation and IR. Indeed IFNγ deletion or modulating CD4+ cells into Tregs protects mice from these derangements (165, 166). The increase in Th1 cells is also accompanied by the decrease in Th2 cells, which maintain macrophages in an M2 state by secreting the anti-inflammatory cytokines IL-4, IL-5 and IL-13. Therefore maintaining an appropriate Th1/Th2 ratio is an important aspect of preventing AT inflammation (166).

CD8+ T cells

CD8+ T cells are responsible for the antiviral response, and in addition to cytokines, they also release cytolytic factors (92). Similar to CD4+ cells, CD8+ infiltration is significantly increased with obesity and precedes macrophage infiltration. They are also responsible for polarizing macrophages to the M1 phenotype as shown *in vitro* and *in vivo* (167). Furthermore, adoptive transfer of CD8+ cells into CD8-deficient rodents increases the M1 ATM polarization, whereas ablating this cell population in obese rodents ameliorates AT inflammation and prevents the development of IR (166, 168).

Th17 cells

Typically involved in autoimmune pathogenesis, increased cell counts and associated cytokines IL-17 and IL-23 can be found in obese patients regardless

of insulin sensitivity status. This is accompanied by a concomitant decrease in Tregs, which are responsible for regulating the action and proliferation of Th17 cells (169-171). The discovery of an increase in this cell population in both diabetic and non-diabetic obese subjects has likewise spawned two contradicting hypotheses. One argues that IL-17 promotes IR by blocking IRS-1 signaling through JNK activation (172), while the other suggests that IL-17 prevents weight gain and decreases fasting glucose (169). Further investigation is warranted to tease out the actual role of Th17 cells in obesity and T2DM.

Regulatory T cells

Tregs have a unique cell marker signature CD4+CD25+Foxp3+. They are responsible for suppressing inflammation, thereby allowing for a controlled immune response by antagonizing Th1 and Th17 responses (92). In obesity, AT Treg numbers are decreased along with anti-inflammatory cytokine IL-10, causing local and systemic pro-inflammatory cytokine presence, which promotes IR. Administration of recombinant IL-2 is sufficient to reverse these insults by stimulating an increase in Tregs (173). The beneficial role of Tregs is thought to stem from their ability to dampen the Th1 response in AT and prevent M1 polarization of ATMs (174).

Natural Killer T cells

NKT cells respond to lipid antigens presented by CD1d rather than peptide antigens presented by MHCI or MHCII and can participate in both Th1 and Th2

responses since they secrete both pro- and anti-inflammatory cytokines (95, 175). Given their dual nature, it is not surprising that there are conflicting reports of their role in AT inflammation and associated IR. Rodent studies in which this cell population is depleted in the context of diet induced obesity report beneficial, neutral and detrimental effects (175-180). More evidence is required to build a more cohesive understanding of these cells.

B cells

Although B cells can act as APCs, their primary function is the production of antibodies to help target foreign antigens (92). Obesity induces an increase in the number of AT B cells and indeed B cell depletion has been shown to improve IR in obese rodents (166, 181). Furthermore, IgG2c antibodies are elevated in obesity, stimulate M1 polarization of ATMs in obese AT and can promote AT inflammation and IR in lean mice (166, 182).

Figure 1.4: Crosstalk between adipose tissue and liver

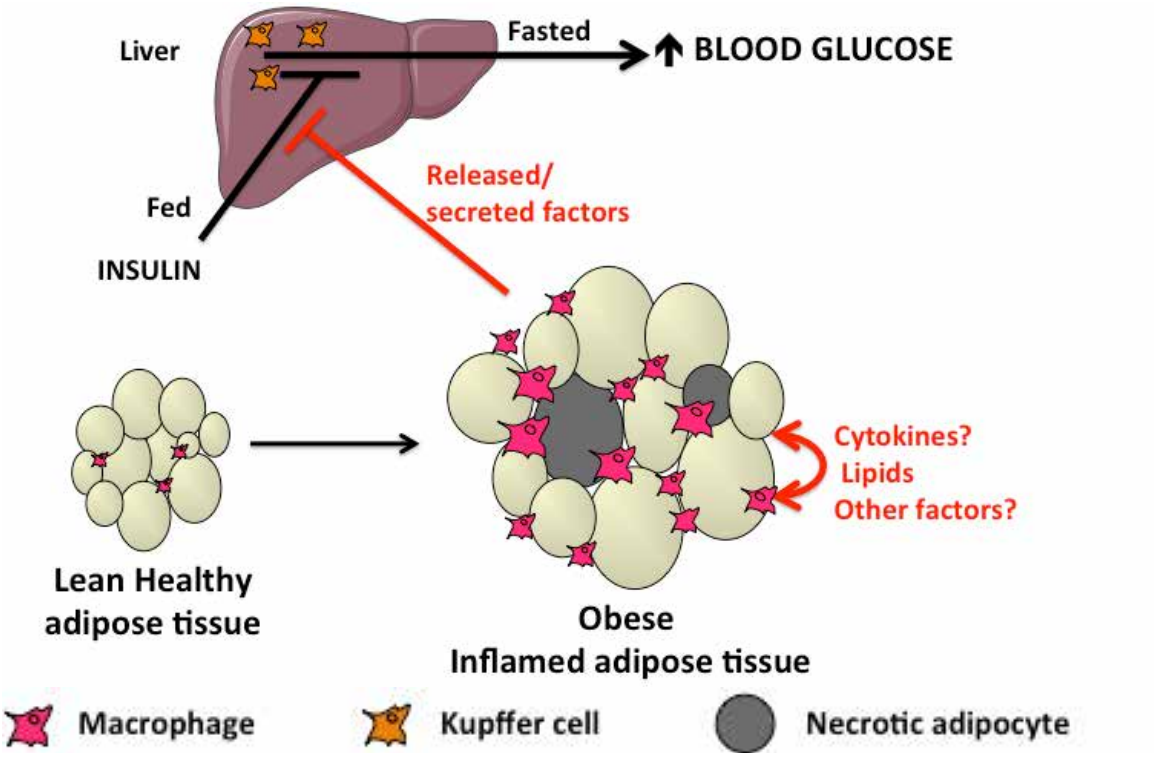

Figure 1.4 - Crosstalk between adipose tissue and liver

A chronic low-grade inflammation characterizes the obese T2DM adipose tissue, especially in visceral fat. There is an increase in immune cell content and activation, particularly macrophages. These phagocytes also help in remodeling and debris clearance, as is the case with dead and dying adipocytes, which are unable to cope with excess lipid storage. Under healthy conditions, insulin acts on the liver to lower postprandial glucose production. Macrophage infiltration is associated with increased cytokine production and impaired systemic insulin sensitivity. Kupffer cell activation has also been implicated in dysregulated hepatic glucose production.

Inflammation in other tissues

Liver

As mentioned earlier, hepatocytes are the parenchymal cell type of the liver, however there is also a large immune cell population. This includes macrophages, T and B lymphocytes, DCs and NKs (183). In the context of obesity and IR however, macrophages are the most studied population. Kupffer cells (KCs) are resident macrophages in the liver, making up 80-90% of all tissue macrophages and over 10% of the liver cell population (184). Their main functions include phagocytosis of microbes and other toxic agents in the circulation and serving as APCs (185). Exposure to these agents results in activation of KCs and subsequent production of pro-inflammatory mediators such as cytokines and chemokines. These contribute to immune cell recruitment to the liver, but can also cause hepatic toxicity and impairment of liver function (186-189).

Unlike AT, obesity does not increase KC number in the liver, but rather their activation state changes. Similar to AT however, in lean individuals, KCs have an M2 polarity, and perform tissue homeostasis functions (190). In obesity, the development of NAFLD and hepatic IR are associated with increased production of inflammatory cytokines such as TNFα, IL-6 and IL-1β by KCs (191, 192). Rodent studies show that KCs are activated by lipid and cholesterol derivative overload, and isolated KCs from HFD-fed mice are also more responsive to LPS-induced activation compared to those from chow-fed mice (184). On the other

hand, alternative activation of KCs to an M2 phenotype can prevent insulin resistance as well as delay the progression to NASH (192). There is evidence suggesting that obesity induces KCs or hepatocytes to produce MCP-1, which attracts monocytes that differentiate into hepatic macrophages and exacerbate hepatic inflammation and IR. However, whether these recruited macrophages become KCs is still unclear (193, 194). Chapter 5 will highlight the role of NF-κB-mediated activation of KCs in the development of IR

Skeletal muscle

Obesity-induced inflammation and macrophage infiltration has also been observed in murine skeletal muscle, particularly in inter-muscular adipose depots, though to a much smaller extent than AT or liver (110). Like ATMs and KCs, these macrophages appear to also be polarized to the M1 phenotype and are associated with increased muscle IR and expression of proinflammatory factors (110, 133). Furthermore, in human skeletal muscle there is a correlation between insulin sensitivity and the expression of M1 and M2 macrophage markers (195).

Pancreas

In the pancreas, inflammation is associated with β cell failure, resulting in decreased insulin production and hyperglycemia (196). The presence of amyloid deposits, fibrosis, β cell apoptosis and macrophage infiltration in islets of T2DM patients together with increased cytokine and chemokine expression indicate

pancreatic inflammation is a driver of IR (197). Endocannabinoid activation of the inflammasome in macrophages has also been implicated in β cell loss (90). Finally, macrophage infiltration seems to precede the onset of T2DM, and the cytokine IL-1β appears to be the master regulator of immune cell recruitment (198, 199).

Hypothalamus

Most recently, DIO has been linked with the development of inflammation in the hypothalamus, particularly the arcuate nucleus (ARC) (200). This is notable because the ARC is involved in regulating energy homeostasis by modulating food intake and energy expenditure (201). Inflammation in the ARC is thought to be FFA-associated, since FFAs can access the ARC through its fenestrated vascularization. These FFAs induce inflammation and neuronal injury, resulting in increased pro-inflammatory gene expression, leading to the accumulation and activation of resident macrophages (202). Although the initial mechanism of inflammation is still incompletely understood, understanding how ARC inflammation affects satiety and energy imbalance is a fertile area of research for developing obesity therapeutics (203).

PART 3: Targeting adipose and liver macrophages

In part 2 we discussed the role of inflammation, particularly adipose tissue macrophage accumulation, in the development of diabetes. This discovery has been a driving force for research into ways of curbing ATM accumulation and inflammation. These methods have largely taken a whole body approach of targeting macrophages. Part 3 will introduce these techniques and their limitations and describe a novel technique that achieves specific macrophage targeting in adipose tissue.

Reducing macrophage infiltration and activation

Cytokine depletion

Given the data implicating ATMs and AT inflammation in obesity-induced IR, preventing macrophage activation has emerged as an attractive investigative and therapeutic approach (204). In order to achieve this, pathways associated with macrophage recruitment and activation including cytokine and chemokine signals, receptors for inflammatory factors, and intracellular mediators of inflammation have been targeted. Most studies however, have focused on blocking cytokine action. The earliest report of this, from Hotamisligil *et al*, involved the administration of a neutralizing antibody against TNFα to obese rats. This resulted in an increase in insulin-stimulated glucose uptake in peripheral tissues (99). Following up on these results Uysal *et al.* generated whole-body TNFα KO mice and placed them on a HFD. They also generated whole-body

KOs on an ob/ob background to test the effects of genetically induced obesity. KO animals showed improved insulin sensitivity and lower circulating free fatty acid levels compared to the control groups. Furthermore, they obtained similar results by deleting the genes encoding the two TNFα receptors (100). However, these benefits could not be replicated in human trials, as systemic administration of the TNF inhibitor Etanercept resulted in reduced systemic levels of inflammatory factors without any improvement in insulin sensitivity in obese patients (205). This data suggests that local TNFα activity in AT rather than systemic activity is important for inflammation-driven IR.

A different study focused on CCR2, the receptor for the MCP-1 cytokine which stimulates macrophage recruitment (119). By genetically deleting CCR2 and putting the mice on a HFD, Christiansen *et al.* were able to show CCR2 deficiency attenuated the development of obesity and reduced ATM infiltration. This was accompanied by protection from hepatic steatosis and improved whole-body glucose metabolism and insulin sensitivity. Additionally, there was a surprising reduction in food intake. To determine the effects of CCR2 blockade in already established obesity, they administered a receptor antagonist, which also reduced ATM numbers and improved insulin sensitivity. However, this was not accompanied by any changes in weight or hepatic steatosis (206). These results, though compelling, require careful interpretation. CCR2 appears to play a significant role in ATM accumulation and AT inflammation, but its additional effect on food intake confounds those of ATMs on insulin sensitivity. It should be noted

that the apparent function of CCR2 in appetite regulation might be tied to ARC inflammation in the hypothalamus (200).

Another cytokine that has been targeted in ATM recruitment and inflammation is osteopontin (OPN). Osteopontin is a glycophosphoprotein expressed by a variety of cell types, most notably macrophages, which is involved in a number of macrophage functions including cytokine expression, phagocytosis, migration and expression of iNOS (207). Importantly, DIO raises circulating and AT levels of OPN in murine models and obese humans exhibit similar increases in expression. These increases have been associated with the infiltration of macrophages into VAT (208-211). Global OPN KO mice fed a HFD have reduced macrophage infiltration into AT, decreased expression of inflammatory markers both locally and systemically, and improved insulin sensitivity without any effect on obesity (208). Using a neutralizing antibody, Kiefer *et al.* reported similar results, as well as attenuation of liver inflammation and steatosis, which they attribute to increased macrophage apoptosis (212). Interestingly, they also propose that OPN deficiency in the liver shifts lipid storage back to AT, thereby attenuating hepatic steatosis and decreasing hepatic glucose output (213). There are clear benefits to blocking OPN action in the context of obesity, however these whole-body studies do not address the specific role of OPN secreted from the ATMs. Chapter 3 will address this issue and present data on macrophage-specific OPN depletion.

Targeting intracellular mediators

Rather than interfering with the extracellular signal, some studies have instead focused on disrupting inflammatory signaling by genetically altering major intracellular drivers of inflammation, i.e., JNK and NF-κB (104, 214, 215). In the case of JNK, reciprocal bone marrow transplants were performed between whole-body KO mice and wild type mice (104). Using this technique serves two purposes: first, any developmental defects or confounding effects are avoided, and secondly only hematopoietic cells possess the genetic mutation leaving the rest of the system unaltered. In this way the role of macrophages can be addressed more specifically. On a HFD, chimeric wild type mice that received JNK-depleted bone marrow were protected from AT and liver inflammation and also exhibited improved insulin sensitivity (104). However, according to a different study, JNK deletion in the non-hematopoietic population is required for the insulin-sensitizing effects of hematopoietic JNK deletion (214). Since JNK was deleted in all myeloid cells, this approach still fails to address how ATMs are specifically involved.

Arkan *et al* took an approach that is more precise and strategically different by indirectly targeting the master regulator of inflammation NF-κB (215). They used the LyzM-Cre conditional KO system to attain macrophage-specific deletion of IκB kinase β (IKKβ), which activates NF-κB by phosphorylating its inhibitors and thus promoting their degradation. IKKb deletion conferred partial protection from systemic insulin resistance without significant changes in adiposity (215).

Although this technique appears to primarily offer macrophage-specific gene deletion, LyzM-Cre also deletes in neutrophils and dendritic cells, and therefore does not allow for a true distinction between myeloid cell types (216). Interestingly, LyzM-Cre-mediated deletion of the insulin receptor improves glucose metabolism and protects against obesity-induced inflammation (217).

Macrophage depletion

Another approach toward ameliorating or preventing AT inflammation centers on reducing the macrophage numbers as a whole. In studies of obesity-induced inflammation, hepatic steatosis and IR, several studies have reported on the effects of depleting macrophage populations (135, 192, 218-226). Two methods have been reported in this regard, with the first one focusing on the conditional ablation of activated CD11c+ macrophages (135). The system relies on CD11c promoter-driven transgenic expression of the simian diphtheria toxin receptor (DTR). Injecting mice with diphtheria toxin specifically induces apoptosis in cells expressing this DTR. CD11c+ depletion resulted in reduced macrophage infiltration, lower proinflammatory cytokine levels and normalization of insulin sensitivity in AT, muscle and liver in mice fed a HFD (135).

The second method involves the use of liposomes to deliver toxic compounds to circulating monocytes and tissue macrophages. The most commonly used chemical compound for liposome macrophage depletion is a bisphosphonate called clodronate. In solution, this compound is unable to cross the plasma membrane, however liposomes are actively phagocytosed by

macrophages and allow clodronate to accumulate to toxic levels within the cell, thus triggering apoptosis (227). Intraperitoneal injections are used to target ATMs in mice on a HFD, and results show reduced weight gain, de-repression of adipocyte thermogenesis and improvement in insulin sensitivity (221, 222, 226). However, most studies report on intravenous injection of clodronate liposomes to target Kupffer cells in the liver, with mostly positive results. KC depletion appears to decrease hepatic lipogenesis, thereby ameliorating hepatic steatosis and improving systemic insulin sensitivity (192, 219, 223, 224). Another study showed that KC depletion prevented obesity and AT inflammation, but once established there was no therapeutic effect on IR (220). Only one group has reported detrimental effects of KC ablation in the context of obesity, citing the loss of KC-derived IL-10, which exacerbates HFD-induced steatosis and IR (218). Gadolinium (III) chloride is another compound used to deplete KCs via liposome delivery, and the beneficial results mimic those of clodronate, with the added effect of improved autophagy (225).

Given all the evidence up to this point, macrophages engage in numerous processes and functions involving different cells and environmental contexts. Therefore completely ablating this population is likely to create unintended effects that could confound our understanding of a particular sub-population. A more specific and less toxic method of targeting our macrophages of interest, providing the necessary precision and level of safety is required.

Glucan-encapsulated siRNA Particles (GeRPs)

Based on the reports above, our lab generated a tool that could fill the technological gap in ATM targeting. In collaboration with the laboratory of Gary Ostroff, we developed a novel method of delivering siRNA oligonucleotides specifically to macrophages for targeted gene knockdown (KD). (228). The system relies on the use of β-3, 1-D-glucan microparticles derived from baker's yeast, loaded with an siRNA sequence against the gene of interest. The first generation included a tRNA core, polyethyleneimine (PEI) and an amphipathic peptide called Endo-Porter in the formulation (228). These glucan-encapsulated siRNA particles (GeRPs) were delivered orally, taken up by macrophages systemically and facilitated targeted gene KD of mitogen activated protein kinase kinase kinase kinase 4 (MAPK4) (228). Using this formulation, another group also achieved specific downregulation of a different gene in peritoneal macrophages after intraperitoneal injection (229). These initial studies provided proof of concept, and a second generation of particles with fewer components was developed, eliminating PEI and tRNA, while retaining Endo-Porter (230).

These new particles, though simpler, also show macrophage-specific downregulation of genes, as reported by our lab and another. Importantly, this KD is tissue specific, homing in on particular sub-populations of macrophages depending on the route of administration (90, 230-233). The specificity of GeRPs is conferred by the β-3, 1-D-glucan, which is recognized by the Dectin 1 receptor expressed by phagocytic cells (234). The Endo-Porter peptide is a transfection

reagent of low toxicity that binds siRNA, creating a stable nanocomplex that anchors siRNA in the particles and also catalyzes endosomal escape (230). Chapters 3,4 and 5 will provide detailed information on studies conducted in our lab targeting ATMs and KCs for GeRP-mediated gene KD in the context of obesity, including tissue specificity and effects on whole body metabolism.

Project Goals

In obesity, inflammation has been implicated in the development of insulin resistance and impaired glucose metabolism resulting in T2DM. Particularly, macrophage infiltration into adipose tissue and activation of liver Kupffer cells are believed to play important roles in this pathology. However, direct evidence to support ATM and KC involvement is incomplete due to the lack of a methodology that specifically ties the function of these macrophage populations to disrupted whole-body metabolic homeostasis. As such, the experiments described in this thesis are aimed at **describing the role of resident tissue macrophages in the regulation of insulin signaling, the effect on energy homeostasis, and how the functions of adipose tissue and liver are altered.**

There are three major aims addressed in this thesis:

1. **To determine how macrophages accumulate in AT:** What is the source of macrophage accumulation in obese adipose tissue? Are macrophages solely recruited from the circulation or do they proliferate locally in adipose tissue?

2. **To determine how ATM-specific gene targeting affects systemic metabolic function:** Does ATM-derived OPN promote impaired glucose metabolism? Is LPL important for ATM lipid buffering?
3. **To determine how Kupffer cell-specific targeting affects systemic metabolic function:** How does targeted knockdown of NF-κB in Kupffer cells affect liver function? Does changing the activation state of Kupffer cells affect systemic insulin sensitivity in obesity?

To answer these questions, studies in this thesis utilize in vitro and in vivo experimentation to determine the role of macrophages on whole body metabolsim. First, we discovered that in addition to infiltration, macrophages proliferate locally in VAT of genetic and diet-induced models of obesity. Importantly, MCP-1 was identified as the cytokine with a direct role in promoting proliferation, particularly in CLS (Chapter 2). OPN was also significantly upregulated in VAT and was associated with increased macrophage proliferation. By administering GeRPs loaded with siRNA against OPN via intraperitoneal injection, significant downregulation of OPN was achieved in ATMs. GeRP-mediated knockdown of ATM-derived OPN resulted in improved glucose disposal and insulin signaling as determined by glucose and insulin tolerance tests as well as increased AKT phosphorylation and lipogenic gene expression in adipose tissue (Chapter 3). On the other hand, GeRP-mediated knockdown of LPL in ATMs resulted in the loss of AT foam cells which led to increased circulating FFA and a concomitant increase in hepatic glucose output and decrease in hepatic

insulin sensitivity (Chapter 4). To assess the importance of Kupffer cell activation state on hepatic function, GeRPs were delivered to Kupffer cells via intravenous injection. Depletion of NF-κB by this method decreased inflammatory markers in the liver, which was associated with an improvement in insulin signaling and decreased hepatic glucose output (Chapter 5). These data show that initial accumulation of macrophages in AT might be an adaptive response to AT remodeling and lipid spillover. However, with increasing accumulation, a chronic low-grade inflammation develops, exerting detrimental effects that lead to insulin resistance. Similarly, activated Kupffer cells promote hepatic inflammation, dysfunction and insulin resistance.

CHAPTER II: Local proliferation of macrophages contributes to obesity-associated adipose tissue inflammation

This chapter is derived from an article of the same title published in the journal of Cell Metabolism.

Amano, S. U., Cohen, J. L., Vangala, P., Tencerova, M., Nicoloro, S. M., Yawe, J. C., Shen, Y., Czech, M. P., and Aouadi, M. (2014) Local proliferation of macrophages contributes to obesity-associated adipose tissue inflammation. *Cell Metab* **19**, 162-171

Author contributions

- **Figure 2.1 and 2.2 Flow cytometry** – Animals were maintained on a high fat diet by Shinya Amano. Cell isolation was performed by Shinya Amano, Jessica Cohen, Pranitha Vangala, Michaela Tencerova, Sarah Nicoloro, Myriam Aouadi and Joseph Yawe (GeRP team, Czech lab). CD11b and Ki67 staining and cell sorting were performed by Shinya Amano and Jessica Cohen
- **Figure 2.3 Liposome injections, EdU administration, Flow cytometry and Microscopy** – Liposomes were prepared and injected by Shinya Amano. EdU water was prepared and administered by Shinya Amano, Jessica Cohen and Pranitha Vangala. Cell isolation was performed by the GeRP team.. F4/80 and EdU staining were performed by Pranitha Vangala. Microscopic analysis was conducted by Myriam Aouadi.
- **Figure 2.4 RT-PCR and MCP-1 treatment** – Tissue isolation was performed by the GeRP team. RT-PCR analysis of gene expression was performed by Pranitha Vangala, Jessica Cohen and Joseph Yawe. Shinya Amano and Jessica Cohen prepared explants and conducted MCP-1 treatment experiments.

SUMMARY

Adipose tissue (AT) of obese mice and humans accumulates immune cells, which secrete cytokines that can promote insulin resistance. ATM are thought to originate from bone-marrow-derived monocytes, which infiltrate the tissue from the circulation. Here, we show that a major fraction of macrophages unexpectedly undergo cell division locally within AT, as detected by Ki67 expression and 5-ethynyl-2**0** -deoxyuridine (EdU) incorporation. Macrophages within the VAT, but not those in other tissues (including liver), displayed increased proliferation in obesity. Importantly, depletion of blood monocytes had no impact on ATM content, whereas their proliferation in situ continued. Treatment with monocyte chemotactic protein 1 (MCP-1) induced macrophage cell division in AT explants. These results reveal that, in addition to blood monocyte recruitment, in situ proliferation driven by MCP-1 is an important process by which macrophages accumulate in the VAT in obesity.

INTRODUCTION

Obesity can induce an insulin-resistant state in AT, liver, and muscle and is a strong risk factor for the development of T2D (32, 70). It is increasingly appreciated that accumulation of macrophages and other immune cell types in AT correlates with a chronic inflammatory state that ultimately impairs adipocyte function and may contribute to the development of insulin resistance (32, 110,

231, 235). Consistent with this theory, decreasing AT inflammation improves insulin sensitivity (231).

The origin of ATMs has previously been attributed to recruitment of blood monocytes into AT based on one study using irradiation followed by bone marrow transplant (110). Therefore, strategies to decrease ATM accumulation have been particularly focused on decreasing macrophage migration into the adipose tissue by depleting blood monocytes or genes encoding chemokines that attract macrophages into the AT (206, 208). However, studies using these approaches have shown modest and variable results. One interpretation could be that a process other than migration contributes to maintain or increase macrophage content in the AT.

Although mature mammalian cells have a reduced proliferative capacity, there is evidence that immune cells, including macrophages, can divide even at the adult stage (236, 237). Indeed, local macrophage proliferation has been demonstrated in kidney, atherosclerotic plaques, skin and lung in animals and humans (238-243). Interestingly, it has been shown that in tissues, such as lung, that are shielded from radiation, resident macrophages remain completely host-derived for at least 8 months despite reconstitution with donor marrow (239). These studies showed that resident macrophage proliferate *in situ* independently of bone marrow derived monocytes.

The present study was designed to determine whether significant macrophage cell division also occurs within epididymal AT in mice. Indeed, a

significant fraction of ATMs in obese mice display active proliferation, as detected by incorporation of 5-ethynyl-2'-deoxyuridine into DNA, even when circulating monocytes are depleted. These results suggest the unexpected concept that local macrophage proliferation contributes to the overall macrophage accumulation and VAT inflammation in the insulin resistant state.

MATERALS AND METHODS

Animals, Diets and Treatments: 8 to 12 week-old male wild-type C57BL/6J (WT) and B6.V-*Lepob*/*J* (*ob*/*ob*) mice were obtained from Jackson Laboratory (Bar Harbor, Maine, USA) and maintained on a 12-hour light/dark cycle. Animals were given free access to food and water. C57BL/6J wild-type mice were fed a high-fat diet (45% calories from lipids; D12451; Research Diets Inc., New Brunswick, New Jersey) for 7 weeks beginning at 8 weeks of age. All other mice were fed normal chow diet (Prolab 5P76 Isopro 3000, LabDiet, St. Louis, Missouri, USA). Intraperitoneal GTTs were performed as previously described (Fitzgibbons et al., 2011). Animals were weighed, sacrificed by cervical dislocation, and adipose tissues (epididymal and inguinal depots), livers and spleen were harvested at age 7-14 weeks. For the *in vivo* EdU injection studies, 8-12 week-old mice were intraperitoneally injected with 1 mg EdU in 200 μl phosphate-buffered saline (PBS) and three hours later mice were sacrificed by asphyxiation with carbon dioxide and immediately bled by cardiac puncture prior to tissue dissection. For the *in vivo* EdU drinking water studies mice were given

free access to water containing 1 mg/ml EdU and 2% sucrose to offset taste aversion. All procedures were performed in accordance with protocols approved by the University of Massachusetts Medical School's Institutional Animal Care and Use Committee. See Supplemental Methods for animal procedures.

Isolation of macrophages from adipose tissue SVF: Adipose tissue SVF cells were prepared from collagenase-digested adipose tissue. Briefly, epididymal or inguinal fat pads were mechanically dissociated using the gentleMACS Dissociator (Miltenyi Biotec) and digested with collagenase at 37°C for 45 minutes in Hank's buffered saline solution (HBSS) (Gibco, Life Technologies) containing 2% bovine serum albumin (American Bioanalytical) and 2 mg/ml collagenase (collagenase from clostridium histolyticum, Sigma). Samples were then filtered through 100 μm BD falcon cell strainers and spun at 300 *g* for 10 minutes at room temperature. The adipocyte layer and the supernatant were aspirated and the pelleted cells were collected as the SVF. The cells were then treated with red blood cell (RBC) lysis buffer, and then stained for flow cytometry.

Liver and spleen cell isolation: Liver cells were isolated as previously described (244). Briefly, the livers of freshly asphyxiated mice were perused with collagenase 4mg/ml in 1% BSA in HBSS via the inferior vena cava and/or portal vein until livers were blanched. Small incisions at the edges of the liver were made to assist in complete blanching. After several minutes of perfusion, livers were placed in collagenase solution at 37 deg C with gentle rocking for 20-30

minutes. The resulting cell digest was filtered through a 100um mesh filter and several 30g centrifugation steps pelleted out hepatocytes. The remaining cells were pelleted by centrifugation at 500g and washed several times with HBSS. The cells were treated with RBC lysis buffer and then stained for flow cytometry. Spleens were manually dissociated using the plunger of a 1 ml plastic syringe in cold HBSS. The resultant cell suspension was centrifuged at 500g and the cell pellet was treated with RBC lysis buffer. A portion of the splenocytes was then taken for flow cytometry staining.

Flow cytometry: Cells were resuspended in PBS containing 1% BSA (FACS buffer) containing Fc block (clone 2.4G2, eBioscience, San Diego, California, USA) and allowed to block non-specific binding for 15 minutes at 4°C. Cells were then counted and incubated for an additional 20 minutes in the dark at 4°C with fluorophore-conjugated primary antibodies or isotype control antibodies. Antibodies used in these studies included: F4/80-APC (clone Cl:A3-1, AbD Serotec, Raleigh, North Carolina, USA), CD11b-PerCP-Cy5.5 (clone M1/70), Gr-1-APC-Cy7 (clone RB6-8C5), Siglec-f-PE (clone E50-2440), Ly6C-PE-Cy7 (clone AL-21), Ki67-FITC (clone B56) and IgG1κ-FITC (clone MOPC-21, BD Pharmingen San Diego, California, USA), and CD11c-V450 (clone HL-3, BD Horizon, San Jose, California, USA). For the EdU experiments, cells were surface stained according to manufacturer's instructions. Following incubation with primary antibodies, cells were washed and fixed with

fixation/permeabilization buffer (eBioscience) and then permeabilized with permeabilization buffer (eBioscience). EdU was chemically conjugated to Alexa 405 or Alexa 647 fluorophore according to the instructions of the manufacturer (Invitrogen). Sample data were acquired on a BD LSRII (BD Biosciences) and analyzed with FlowJo software (Tree Star). Sample data were initially gated on forward and side scatter, followed by a singlet cell gate, and then a gate to remove auto-fluorescent debris (see Figure S1 for complete gating scheme).

Immunohistochemistry: Adipose tissue SVF cells were plated overnight on glass coverslips in complete DMEM and then fixed for 15 min at room temperature in 4% paraformaldehyde. Cells were washed twice with PBS containing 0.3% Triton x-100 (American Bioanalytical, Natick, Massachusetts, USA) and blocked with 10% normal goat serum and were then incubated with the following antibodies: rat anti-mouse F4/80 (AbD Serotec, Raleigh, North Carolina, USA; 1:50 dilution), and goat-anti-mouse Ki67 (Abcam, Cambridge, Massachusetts, USA; 1:200 dilution) overnight at 4°C. After washing, the cells were incubated with secondary antibodies (1:200 dilution) for 30 minutes at room temperature. Cells were mounted in ProLong Gold antifade reagent containing 4',6-diamidino-2-phenylindole (DAPI) (Molecular Probes, Eugene, Oregon, USA). Adipose tissue sections were blocked with 10% normal goat serum and were then incubated with anti-Ki67 antibodies and hematoxylin stained. Images

were captured on a Zeiss Axiovert 200M microscope using Axiovision software (Carl Zeiss, Thornwood, New York, USA).

Isolation of RNA and Real Time PCR: RNA isolation was performed according to the Trizol Reagent Protocol (Invitrogen). cDNA was synthesized from 0.5-1 µg of total RNA using iScript cDNA Synthesis Kit (Bio-Rad) according to the manufacturer's instructions. For real time PCR, synthesized cDNA forward and reverse primers along with the iQ SYBR Green Supermix were run on the CFX96 Real-time PCR System (Bio-Rad). The ribosomal mRNA, 36B4 was used as an internal loading control, as its expression did not change over a 24 h period with the addition of LPS or siRNA against the genes used in this study. Primer sequences used are as follows: 36B4 (5'-TCCAGGCTTTGGGCATCA-3', 5'-CTTTATCAGCTGCACATCACTCAGA-3'); mcp1 (5'-GCTGGAGAGCTACAAGAGGATCACC-3', 5'-TCCTTCTTGGGGTCAGCACAGAC-3'); opn (5'-AGCAAGAAACTCTTCCAAGCAA-3', 5'-GTGAGATTCGTCAGATTCATCCG-3'); il4 (5'-GGTCTCAACCCCCAGCTAGT-3', 5'-GCCGATGATCTCTCTCAAGTGAT-3'); mcsf (5′-GACTTCATGCCAGATTGCC-3′, 5′-GGTGGCTTTAGGGTACAGG-3′)

Statistical analysis: All values are shown as means ± SEM. Student's *t*-test for two-tailed distributions with equal variances was used for comparison between

two groups. Differences $p \leq 0.05$ were considered significant. Statistical analyses were performed with Graph Pad Prism 5.

RESULTS

Macrophages proliferate locally within the adipose tissue

To confirm macrophage accumulation in AT of obese mice, we used 8 to 12-week old genetically obese (*ob*/*ob*) male mice and their lean control wild-type (WT) littermates. Stromal-vascular fraction (SVF) from subcutaneous and visceral epididymal fat pads, which contains all cells of the AT except adipocytes, was stained with antibodies against macrophage markers, F4/80 and CD11b, an eosinophil marker, Siglec-f, and a neutrophil marker, Gr-1 and analyzed by flow cytometry. The macrophage population in the AT was defined as $F4/80^{+}/CD11b^{+}/Siglec\text{-}f^{-}/Gr\text{-}1^{-}$. Consistent with published studies, macrophage content was significantly increased in the epididymal adipose depot of *ob*/*ob* compared to WT mice (WT 140 ± 35 $x10^3$ *vs. ob/ob* 959 ± 69 $x10^3$ macrophages/g of epididymal fat, $p<0.001$ and **Figure 2.1A-B**). The number as well as the percentage of macrophage was also increased in the subcutaneous AT of *ob/ob* compared to WT mice but to a lower extent than in epididymal AT (WT 109 ± 12 $x10^3$ *vs. ob/ob* 192 ± 31 $x10^3$ macrophages/g of epididymal fat, $p=0.04$ and **Figure 2.1E**).

To test whether ATM proliferation increases in the inflammatory setting of obesity, SVF cells were stained with an antibody against the proliferation marker

Ki67, which is a protein expressed during all active phases of the cell cycle (245). Ki67 signal was detected in approximately 2.3% of epididymal ATMs of lean WT mice, and in 10% of ATMs of *ob*/*ob* mice (WT 7.6 ± 3.2 x10^3 *vs.* 94 ± 7 x10^3 macrophages/g of epididymal fat, p<0.001 and **Figure 2.1C-D**). The percentage of Ki67$^+$ macrophages was also increased in subcutaneous adipose tissue from *ob/ob* compared to WT mice (**Figure 2.1F**). However, the number of Ki67$^+$ macrophages was lower in subcutaneous compared to epididymal fat pad in ob/ob mice (subcutaneous 20.0 ± 3.3 x10^3 *vs.* epididymal 94 ± 7 x10^3 macrophages/g, p<0.001).

We next measured the proliferation rate of ATMs in mice with diet-induced obesity. Mice were fed a high fat diet (HFD) for 7 weeks and SVF isolated from the epididymal fat pad was stained with antibodies against macrophages markers and Ki67. Similar to genetically induced obesity, diet-induced obesity increased macrophage content in the AT **(Figure 2.2A-B)**. ATM number was significantly higher in SVF of epididymal AT in mice fed a high fat diet (HFD) compared to normal chow diet (ND) (ND 140 ± 35.10^3 *vs.* HFD 1,045 ± 131 x10^3 macrophages/g of epididymal fat, p<0.001). More importantly, in mice fed a HFD 17% of ATMs were Ki67$^+$ compared to 3% in mice fed a ND (ND 7.6 ± 3.2 x10^3 *vs.* HFD 183 ± 21 x10^3 macrophages/g of epididymal fat, p<0.001) (**Figure 2.2 C-D**).

Fig 2.1 – Genetic Obesity induces macrophage proliferation in AT

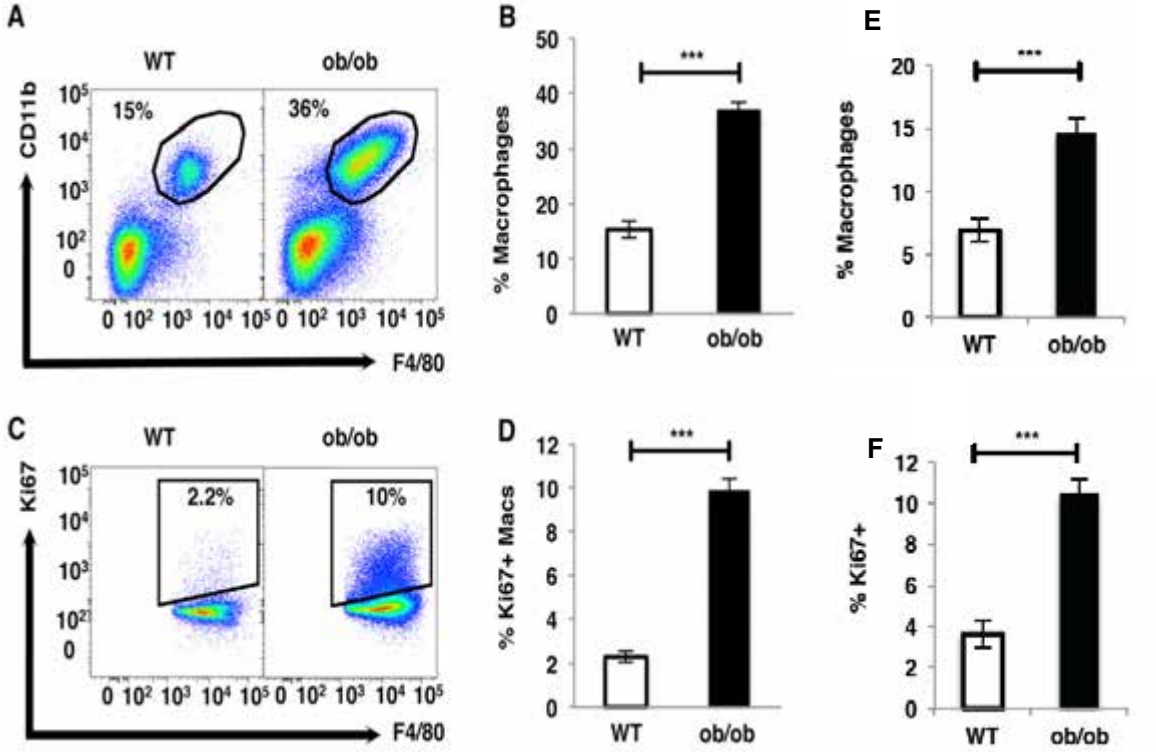

Figure 2.1 Genetic obesity induces macrophage proliferation in VAT
(**A-B**) Percentage of CD11b+F4/80+ macrophages from SVF of WT vs. Ob/Ob. (**C-D**) Percentage of macrophages expressing Ki67 in VAT of WT vs. Ob/Ob mice; n=10. **(E)** Percentage of macrophages in SVF from SAT of WT vs. Ob/Ob mice. (**F**) Percentage of macrophages expressing Ki67 in SAT of WT vs. Ob/Ob mice; n=10. All graphs are expressed as mean ±s.e.m. Statistical significance was determined by Student's t-test. ***P<0.001

Figure 2.2 – HFD induces macrophage proliferation in VAT

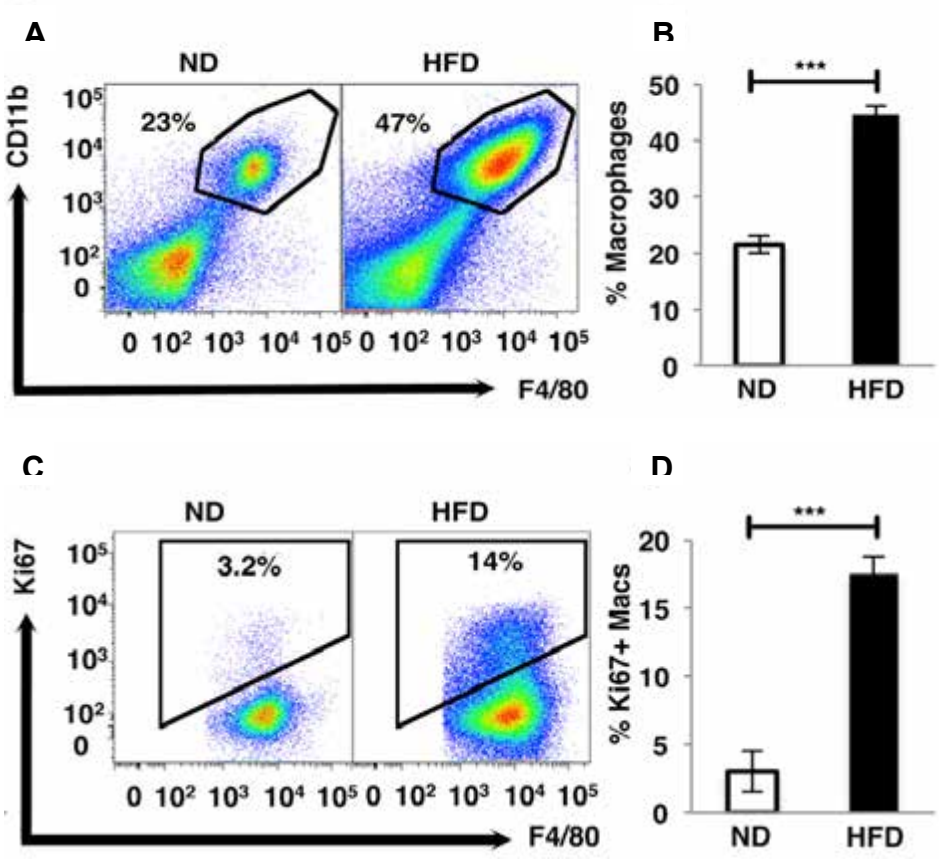

Figure 2.2 HFD induces macrophage proliferation in VAT
(**A-B**) Percentage of macrophages in SVF from VAT of mice fed a ND or a HFD for 10 weeks. (**C-D**) Percentage of macrophages expressing Ki67 in VAT of mice fed a ND or a HFD; n=18. All graphs are expressed as mean ± s.e.m. Statistical significance was determined by Student's t-test. ***P<0.001

Macrophage proliferation contributes to adipose tissue inflammation independently of monocyte recruitment

To test this hypothesis that macrophages proliferate independently of monocyte recruitment, we depleted blood monocytes in *ob/ob* mice by intravenous (i.v.) injection of clodronate-loaded liposomes, which induce apoptosis once ingested by monocytes (227). *ob/ob* mice were given EdU in drinking water during monocyte depletion as depicted in diagram in **Figure 2.3A**. Thirty-two hours after EdU exposure, approximately 28% of macrophages were EdU^+ in the AT of ob/ob mice injected with PBS-liposomes (**Figure 2.3B-C**). Eighty hours after EdU exposure, about half of the macrophages in the AT of *ob/ob* mice injected with PBS-liposomes had incorporated EdU (**Figure 2.3B-C**). Importantly, depletion of blood monocyte had no effect on macrophage proliferation as observed by the EdU incorporation in the epididymal AT of *ob/ob* mice injected with clodronate-liposomes (26% after 32 hrs. and 46% after 80 hrs.) (**Figure 2.3B-C**).

We next analyzed the proliferative capacity of macrophages in the epididymal AT depot, where most of the macrophage expansion occurs in obesity, versus the subcutaneous AT depot (**Figure 2.3D**). EdU incorporation by macrophages was significantly higher in the epididymal AT of *ob/ob* compared to WT mice. However, no difference in EdU incorporation was observed in macrophages in subcutaneous AT of *ob/ob* compared to WT mice after 80 hours of EdU exposure (**Figure 2.3D**). This suggested that macrophage proliferation

plays a major role in epididymal AT macrophage expansion in obesity. It has been previously showed that CLS density is higher in visceral fat compared to subcutaneous depot in obese mice (246). Interestingly, microscopic analysis of epididymal AT section showed that EdU was mostly incorporated in macrophages in CLS (**Figure 2.3E**).

Fig 2.3 – ATMs proliferate independent of monocyte recruitment

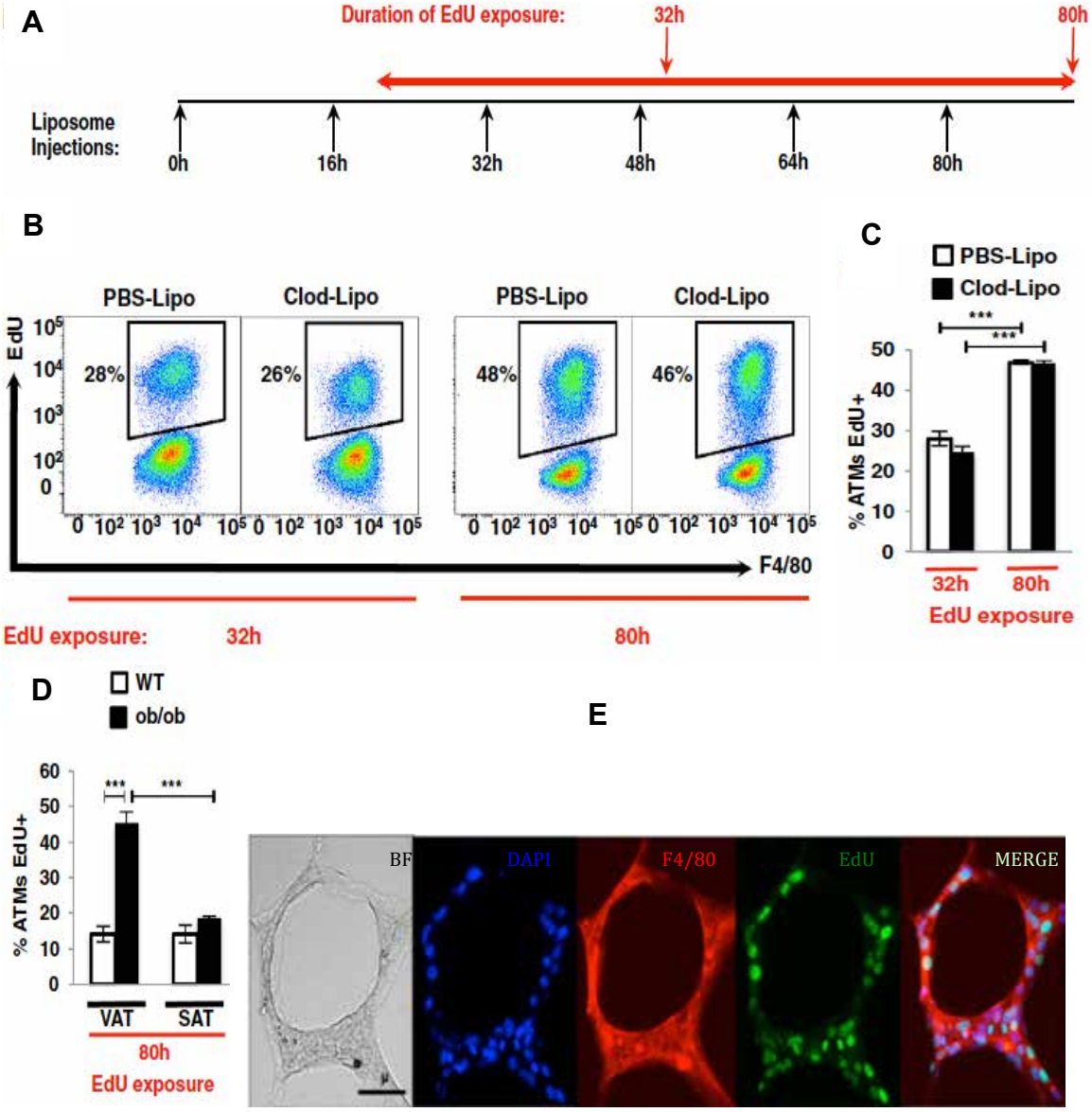

Figure 2.3 ATMs proliferate independent of monocyte recruitment
(**A**) Schematic representation of experimental design. (**B**) Representative flow cytograms (**C**) and quantification (**D**) of EdU incorporation into ATMs during 32 and 80 hrs. of exposure to EdU drinking water in PBS-Lipo-treated and monocyte-depleted Clod-Lipo-treated ob/ob mice; n=5 (**E**) VAT of ob/ob mice containing CLS stained with antibodies against F4/80 (red) and EdU (green). Nuclei were stained with DAPI (blue). 20x magnification images. The scale bar represents 40 μm.

MCP-1 stimulates adipose tissue macrophage proliferation

To investigate the mechanism by which obesity stimulates macrophage proliferation selectively in the AT, we measured, in AT and liver of lean (ND and WT) and obese (HFD and *ob/ob*) mice, the expression of multiple cytokines known to play a role in macrophage proliferation, IL-4 (239), M-CSF (242), and macrophage infiltration, OPN (208) and MCP-1 (120, 206)(**Figure 2.4A-D**). While IL-4 and M-CSF expression in the epididymal AT was either decreased or unchanged with obesity, OPN and MCP-1 expression was significantly increased in *ob/ob* mice or mice fed a HFD compared to control lean mice (**Figure 2.4A-D**).

As described in figure 1 and 2, macrophage proliferation was mainly increased in epididymal AT in obese compared to lean mice, therefore we next measured the expression of OPN and MCP-1 in this fat depot compared to subcutaneous AT and liver, where ATM proliferation is minimal (**Figure 2.4E-F**). Although OPN expression was unchanged in subcutaneous AT in obese compared to lean mice, it was significantly increased in liver (**Figure 2.4E**). In addition OPN expression was similar in liver and epididymal AT in mice fed a HFD (**Figure 2.4E**). In contrast, MCP-1 expression was significantly higher in epididymal AT compared to liver and subcutaneous fat in obese mice (**Figure 2.4F**).

Although macrophage subpopulations in the AT may have overlapping marker expression profiles, it is generally thought that CD11c expression is characteristic of proinflammatory macrophage subtypes (247). Therefore, we

analyzed the rate of proliferation of proinflammatory (CD11c+) and anti-inflammatory (CD11c**-**) macrophages (data not shown). We failed to observe any difference in the rate of proliferation of macrophage population subtypes. This suggests that obesity increases macrophage proliferation rate independently of their inflammatory state.

MCP-1 has been extensively described as a chemokine attracting macrophages from the blood to the AT in obese mice (120, 206). Thus, to test whether MCP-1 regulates ATM proliferation independently of macrophage recruitment, epididymal AT explants from *ob/ob* mice were treated with 1 and 10 ng/ml of MCP-1 and EdU incorporation in ATM was measured by flow cytometry. 10 ng/ml MCP-1 treatment significantly increased the number of macrophages in the AT explants independently of monocyte recruitment (**Figure 2.4G**). More importantly, MCP-1 treatment significantly increased the number of EdU^+ ATMs (**Figure 2.4H**). These results suggested that MCP-1 could regulate macrophage proliferation in AT. We then compared the expression of MCP-1 in adipocytes and SVF from epididymal AT of mice fed a HFD. Although MCP-1 expression was high in both fractions, it was significantly higher in the adipocytes (**Figure 2.4I**)

Fig 2.4 – MCP-1 stimulates macrophage proliferation in VAT

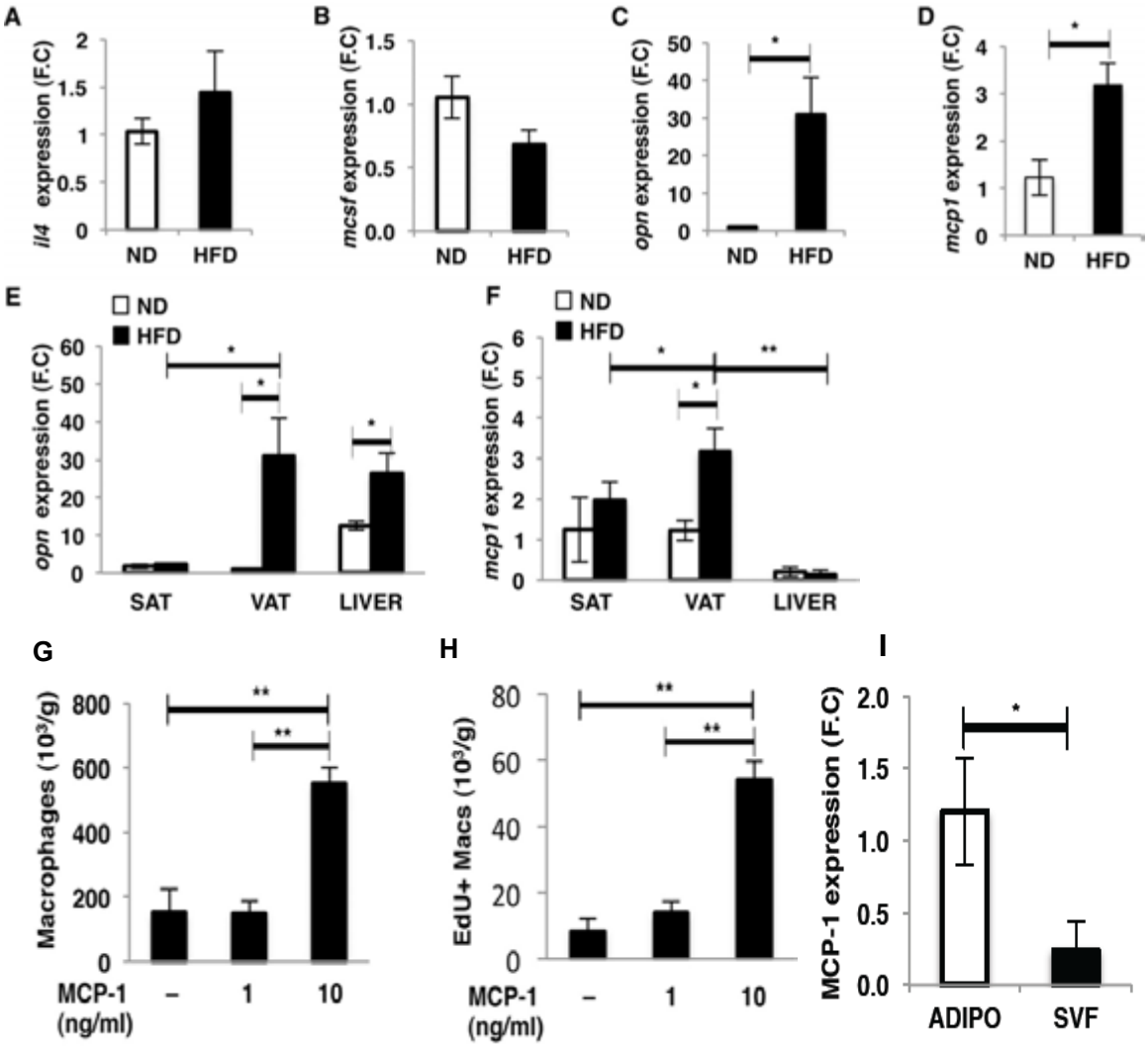

Figure 2.4 MCP-1 stimulates macrophage proliferation in VAT
il4 (**A**), mcsf (**B**), opn (**C**), and mcp-1 (**D**) expression was measured by RT-PCR; n = 5. (**E-F**) Expression of opn (**E**) and mcp-1 (**F**) in SAT, VAT, and liver from mice fed an ND or HFD for 7 weeks; n = 5. (**M-N**) Explants from VAT of five ob/ob mice were treated with 1 and 10 ng/ml of MCP-1 in presence of 10 mM of EdU for 48 hr. Graph represents the number of macrophages (**G**) and EdU+ (**H**) macrophages in explants. (**I**) Expression of mcp1 in adipocytes and SVF from epididymal AT of HFD fed mice; n = 5. Statistical significance was determined by Student's t-test. ***P<0.001; **P<0.01; *P<0.05.

DISCUSSION

Macrophages have been shown to accumulate in massive numbers in the AT of obese mice and human subjects (110, 111). We confirmed that macrophages accumulate in AT of both genetically and diet induced models of obesity (**Figure 2.1 and 2.2**). FACS analysis showed an increase in both the percentage and number of macrophages in subcutaneous and visceral AT depots of obese mice; with VAT showing a more significant increase. These results confirmed that macrophages accumulate mostly in the epididymal AT in mice in response to obesity caused by either genetic mutation or a diet high in fat (**Figure 2.1 and 2.2**). Importantly, further analysis of the macrophage populations in these depots also revealed that they expressed the proliferation marker Ki67 in both lean and obese states. However, obese mice displayed an increase in Ki67 expression that was concomitant with macrophage accumulation. In addition, this increase in Ki67 expression was more significant in the visceral compared to subcutaneous AT of obese mice (**Figure 2.1 and 2.2**). Collectively, these results show that macrophages express the proliferation marker Ki67 in the AT in mice and humans and to a higher degree in response to obesity in mice caused by either genetic mutation or a diet high in fat.

By performing irradiation and transplant studies Weisberg *et al.* demonstrated that ATMs are derived from the bone marrow, subsequently migrating to and differentiating in the AT (110). They concluded that the ATM population increases as a result of monocyte recruitment, but did not rule out

proliferation of resident macrophages. By utilizing clodronate-liposomes and EdU incorporation we found that macrophage proliferation is unaffected by depletion of blood monocytes (**Figure 2.3**). These results suggest that resident macrophages proliferate independently of monocyte recruitment. However, recently recruited macrophages may also proliferate in AT of obese mice since a recent study showed that 5% of labeled blood monocytes, transferred from donor into recipient mice, express Ki67 in the host AT two days after transfer (248). We also found that consistent with higher Ki67 expression in VAT than SAT, EdU incorporation was also increased in VAT but did not change in SAT of obese mice (**Figure 2.3**). This data is in line with the observation that obesity-induced macrophage accumulation occurs primarily in VAT (**Chapter 1**). It is also important to note that proliferating macrophages were localized to crown like structures, around dead and dying adipocytes (**Figure 2.3**). This implies a mechanism whereby the AT responds to adipocyte dysfunction by locally stimulating macrophage proliferation, in order to facilitate remodeling and clearing of debris.

In attempting to understand this mechanism of obesity-induced proliferation in AT, we measured the expression of cytokines IL-4, M-CSF, OPN and MCP-1, and found that only MCP-1 and OPN were significantly increased by obesity in VAT (**Figure 2.4**). However, OPN was increased in both VAT and liver, whereas MCP-1 was only increased in VAT, where we also see increased proliferation (**Figure 2.4**). This suggests a positive regulation between MCP-1 expression and

macrophage proliferation in mice. Furthermore, treatment of explants from Ob/Ob mice *ex vivo* elicited a strong proliferative response of ATMs. The MCP-1 receptor CCR2 has also been shown to be mostly expressed in macrophages in CLS where most of proliferating ATMs were observed (115). These results suggested that MCP-1 released by adipocytes in CLS could stimulate proliferation of surrounding ATMs. Although proliferation may be regulated by multiple factors, MCP-1 plays a major role in regulating macrophage proliferation in the AT of obese mice.

In summary, we show here that macrophage proliferation within epididymal AT is a dynamic mechanism that increases with obesity. Given the high proportion of macrophages (about 50%) that incorporate EdU over 80 hours, proliferation therefore likely contributes significantly to the accumulation of macrophages and the inflammation of AT in obesity. At the molecular level, this study revealed MCP-1 as a potential stimulus for macrophage proliferation in obese adipose tissue.

Chapter III: Silencing osteopontin in adipose tissue macrophages regulates whole-body metabolism in obese mice

This chapter is derived from an article published in Proceedings of the National Academy of Sciences.

Aouadi, M., Tencerova, M., Vangala, P., Yawe, J. C., Nicoloro, S. M., Amano, S. U., Cohen, J. L., and Czech, M. P. (2013) Gene silencing in adipose tissue macrophages regulates whole-body metabolism in obese mice. *Proc Natl Acad Sci U S A* **110**, 8278-8283

Author Contributions

- **Figure 3.1 GeRP biodistribution** – Biodistribution studies were performed by Myriam Aouadi, Michaela Tencerova, Pranitha Vangala, Sarah Nicoloro, Shinya Amano, Jessica Cohen and Joseph Yawe (GeRP team, Czech lab).
- **Figure 3.2 Macrophage uptake of GeRPs** – The GeRP team isolated adipose tissue and SVF. F4/80 staining and flow cytometry analysis were performed by Shinya Amano, Myriam Aouadi and Pranitha Vangala.
- **Figure 3.3 Osteopontin expression and siRNA test** – RT-PCR analysis was performed by Myriam Aouadi, Sarah Nicoloro and Joseph Yawe. In vitro siRNA testing was performed by Myriam Aouadi and Joseph Yawe.
- **Figure 3.4 GeRP mediated osteopontin knockdown** – Knockdown experiments were performed by the GeRP team. RT-PCR analysis of inflammatory gene expression was performed by Joseph Yawe.
- **Figure 3.5 Metabolic studies** – The administration of GeRPs, subsequent metabolic studies and osteopontin ELISA were performed by Pranitha Vangala and Joseph Yawe.
- **Figure 3**.6 Insulin signaling and adipocyte gene expression analysis – Serum parameters were measured by Pranitha Vangala and Joseph Yawe. AKT phosphorylation was measured by Michaela Tencerova and Joseph Yawe. All RT-PCR analysis was conducted by Joseph Yawe.

- **Figure 3.7 Osteopontin knockout animals**. Joseph Yawe conducted all experiments in this figure with assistance from Pranitha Vangala during metabolic studies.

SUMMARY

Adipose tissue inflammation and infiltration by macrophages is associated with insulin resistance and T2DM in obese humans, offering a potential target for therapeutics. However, whether ATMs directly contribute to systemic glucose intolerance has not been determined. The reason is the lack of methods to ablate inflammatory genes expressed in macrophages specifically localized within AT depots, leaving macrophages in other tissues unaffected. Here we report that i.p. administration of siRNA encapsulated by glucan shells in obese mice selectively silences genes in epididymal ATMs, whereas macrophages within lung, spleen, kidney, heart, skeletal muscle, subcutaneous (SubQ) adipose, and liver are not targeted. Such administration of GeRPs to silence the inflammatory cytokine osteopontin in epididymal ATMs of obese mice caused significant improvement in glucose tolerance. These data are consistent with the hypothesis that cytokines produced by ATMs can exacerbate whole-body glucose intolerance.

INTRODUCTION

The rapidly rising prevalence of obesity and T2DM over the past several decades has highlighted a pressing need to develop new therapeutics for these metabolic diseases (249). In obese human subjects, the inability to appropriately expand subcutaneous adipose tissue leads to ectopic lipid deposition in liver and muscle and may be an underlying cause of insulin resistance (70, 250, 251). It is well appreciated that infiltration and activation of macrophages in the visceral AT

correlate with a chronic inflammatory state. These macrophages secrete cytokines and other factors that could impair the ability of adipocytes to secrete beneficial adipokines or store lipid, leading to lipid deposition in nonadipose tissues and insulin resistance (32, 110, 252). Consistent with this concept, macrophage numbers in visceral AT correlate with systemic insulin resistance even in obese human subjects that are matched for body mass index (253, 254). In light of this evidence, it has been suggested that therapeutics that can attenuate visceral AT inflammation may alleviate the diabetic state (Chapter 1).

Despite abundant literature consistent with the paradigm that AT inflammation contributes to systemic insulin resistance and glucose intolerance, direct data actually addressing this issue is difficult to obtain. The limitation has been a lack of available methodology to ablate inflammatory genes expressed in macrophages specifically localized within AT depots while leaving these immune cells in other tissues unaffected. This was discussed in detail in chapter 1, as well as the introduction of a methodology designed to overcome this limitation i.e. GeRPs. We show here that in contrast to lean mice, in which i.p.-injected GeRPs are phagocytosed by macrophages throughout the body (228, 230), i.p. injection of GeRPs into obese mice results in their accumulation and silencing of genes mostly in macrophages found in the VAT. Under the same conditions, we could not detect GeRPs in these immune cells within other tissues.

Using this approach, we targeted the inflammatory cytokine osteopontin, whose expression is upregulated by obesity. It is also thought to play a role in the

development of insulin resistance in rodents and humans (208-211). Attenuation of OPN expression improved whole-body glucose tolerance. These results reveal i.p. administration of GeRPs as a unique tool to study the specific role of visceral ATMs in the development of insulin resistance induced by obesity.

MATERIALS AND METHODS

Animals: All mice were purchased from Jackson Laboratory. Mice were housed on a 12-h light/dark schedule and had free access to water and food. High fat diets were obtained from Research Diets: 45% kcal fat (D12451) and 60% kcal fat (D12492). All procedures involving animals were approved by the Institutional Animal Care and
Use Committee at the University of Massachusetts Medical School.

Preparation of Glucan Shells: β-1,3-D-glucan particles were prepared by suspending Saccharomyces cerevisiae (100 g of SAF-Mannan, SAF Agri) in 1 L of 0.5 M NaOH and heating to 80 °C for 1 h. The insoluble material containing the yeast cell walls was collected by centrifugation, suspended in 1 L of 0.5 M NaOH, and incubated at 80 °C for 1 h. The insoluble residue was again collected by centrifugation and washed three times with 1 L of water, three times with 200 mL of isopropanol, and three times with 200 mL of acetone. The resulting slurry was placed in a glass tray and dried at room temperature to produce 16.2 g of a fine, slightly off-white powder.

Fluorescein labeling of Glucan Shells: Glucan shells (1 g) were washed with sodium carbonate buffer (0.1 M, pH 9.2) and resuspended in 0.1 L carbonate buffer. Then 5-(4,6-dichlorotriazinyl) aminofluorescein (Invitrogen; 1 mg/mL in ethanol) was added to the buffered glucan shell suspension (10% vol/vol) and mixed at room temperature in the dark overnight. Tris buffer (2 mM) was added, incubated for 15 min, and glucan shells washed with sterile pyrogen-free water until the supernatant was clear. The glucan shells were then flash-frozen and lyophilized in the dark.

Preparation of GeRPs: To load siRNA in glucan shells, 3 nmol siRNA (Dharmacon) were incubated with 50nmoles Endo-Porter (EP; Gene Tools) in 30 mM sodium acetate pH 4.8 for 15 min at room temperature in a final volume of 20 **µ**L. The siRNA/EP solution was added to 1 mg (~10^9) of glucan shells and then vortexed and incubated for 1 h. The siRNA-loaded GeRPs were then resuspended in PBS and sonicated to ensure homogeneity of the GeRP preparation. GeRPs were kept at 4 °C. siRNA sequences used are as follows: Scrambled (SCR) (5'-CAGUCGCGUUUGCGACUGGUU-3'); anti-OPN1 (5'-CAACUAAAGAAGAGGCAAAUU-3'); anti-OPN2 (5'-CCACAUGGCUGGUGCCUGAUU-3')

GeRP Administration and Tissue Isolation: Five-week-old C57BL6 ob/ob male

mice were i.p. injected once a day for 5 or 10 d with 5.6 mg/kg GeRPs loaded with 2.1 mg/kg EP and 0.262 mg/kg siRNA. Twenty-four hours after the last injection, mice were killed and tissues were isolated and used for RT-PCR and microscopy.

Metabolic Studies: Glucose and insulin tolerance tests were performed on ob/ob animals at 5 or 10 d after GeRP treatment. Glucose (1 g/kg) and insulin (1 IU/kg) were administrated by i.p. injection. Blood samples were withdrawn from the tail vein at the indicated time, and glycemia was determined using glucometers (Bayer and alpha-trak).

Isolation of Macrophages From Adipose Stromal-Vascular Fraction: Epididymal fat pads were mechanically dissociated using the gentleMACS Dissociator (Miltenyi Biotec) and collagenase digested at 37 °C for 45 min in HBSS (Gibco, Life Technologies) containing 2% BSA (American Bioanalytical) and 2 mg/mL collagenase (Sigma-Aldrich). Samples were then filtered through 100-μm-diameter pore nylon mesh and centrifuged. The adipocyte layer and the supernatant were aspirated and the pelleted cells were collected as the stromal-vascular fraction (SVF). The cells were then treated with red blood cell lysis buffer and washed in PBS and plated or directly harvested for further analysis.

Isolation of RNA and Real-Time PCR: RNA isolation was performed according to the TRIzol Reagent Protocol (Invitrogen). cDNA was synthesized from 0.5 to 1

μg of total RNA using iScript cDNA Synthesis Kit (Bio-Rad) according to the manufacturer's instructions. For real-time PCR, synthesized cDNA forward and reverse primers along with the iQ SYBR Green Supermix were run on the CFX96 Real-time PCR System (Bio-Rad). The ribosomal mRNA 36B4 was used as an internal loading control be- cause its expression did not change over a 24-h period with the addition of LPS or siRNA against the genes used in this study. Primer sequences are as follows: 36B4 (5'TCCAGGCTTTGGGCATCA-3', 5'-CTTTATCAGCTGCACATCACTCAGA-3'); mcp1 (5'-GCTGGAGAGCTACAAGAGGATCACC-3', 5'-TCCTTCTTGGGGTCAGCACAGAC-3'); opn (5'-AGCAAGAAACTCTTCCAAGCAA-3', 5'- GTGAGATTCGTCAGATTCATCCG-3'); il4 (5'- GGTCTCAACCCCCAGCTAGT-3', 5'-GCCGATGATCTCTCTCAAGTGAT-3'); il6 (5'-TAGTCCTTCCTACCCCAATTTCC-3', 5'-TTGGTCCTTAGCCACTCCTTC-3'); il10 (5'-CTGGACAACATACTGCTAACCG-3', 5'-GGGCATCACTTCTACCAGGTAA-3'); il1b (5'-GCAACTGTTCCTGAACTCAACT-3', 5'-ATCTTTTGGGGTCCGTCAACT-3'); cd11b (5'-ATGGACGCTGATGGCAATACC-3', 5'-TCCCCATTCACGTCTCCCA-3'); cd11c (5'-CTGGATAGCCTTTCTTCTGCTG-3', 5'-GCACACTGTGTCCGAACTCA-3'); f4/80 (5'-CCCCAGTGTCCTTACAGAGTG-3', 5'-GTGCCCAGAGTGGATGTCT -3'); cd68 (5'-GGACCCACAACTGTCACTCA-3', 5'-AAGCCCCACTTTAGCTTTACC-3'); ccr2 (5'-

ATCCACGGCATACTATCAACATC-3', 5'-CAAGGCTCACCATCATCGTAG-3'); ap2 (5'-AAGGTGAAGAGCATCATAACCCT-3', 5'-TCACGCCTTTCATAACACATTCC-3'); pparg (5'-GGAAGACCACTCGCATTCCTT-3', 5'-GTAATCAGCAACCATTGGGTCA-3'); fasn (5'-GGAGGTGGTGATAGCCGGTAT-3', 5'-TGGGTAATCCATAGAGCCCAG-3'); glut4 (

Srebp-1c (5'-GGAGCCATGGATTGCACATT-3', 5'-GGCCCGGGAAGTCACTGT-3');

Scd1 (5'-TTCTTGCGATACACTCTGGTGC-3', 5'-CGGGATTGAATGTTCTTGTCGT-3'); adiponectin (5'-AGAGAAGGGAGAGAAAGGAGATGC-3', 5'-TGGTCGTAGGTGAAGAGAACGG-3'); cpt1b (5'-GCTTTGGCTGCCTGTGTCAGTATGC-3', '5-GCTGCTTCCCCTCACAAGTTCC-3')

Flow Cytometry: SVF cells from mice treated with fluorescein-GeRPs were incubated for 20 min in blocking buffer containing 1% BSA and Fc block (eBioscience) and allowed to block nonspecific binding for 15 min at 4 °C. Cells were then counted and incubated for an additional 20 min in the dark at 4 °C with fluorophore-conjugated primary antibodies or isotype control antibodies (AbD Serotec). Antibodies used in these studies included: F4/80-allophycocyanin (APC), CD11b-peridinin chlorophyll protein-Cyano 5.5(PErCP- Cy5.5), Gr-1-

APC-Cyano (Cy)7, Siglec-f-PE, lymphocyte antigen 6C (Ly6C)-phycoerythrin-Cyano 7 (PE-Cy7), and CD3-PE-Cy7. Subsequently cells were analyzed by flow cytometry in an LSRII cytometer (BD Bioscience). FlowJo software (Treestar) was used to identify the different cell populations. A total of 10,000 events were recorded. For sorting experiments, SVF cells were run through a FACS Vantage (BD Bioscience). Both FITC+ and FITC− populations were collected and RNA was harvested for RT-PCR.

ELISA: PECs were treated for 6 h with 1 μg/mL LPS, and TNF-α levels in the media were measured using mouse ELISA kits (Pierce) as recommended by the vendor. Osteopontin (OPN) levels in the media and serum were measured using an ELISA kit (R&D Systems).

Microscopy: Fixed SVF cells from in vivo experiments were incubated with rat anti-mouse F4/80 primary antibody (AbD-Serotec) followed by goat anti-rat Alexafluor 594 secondary antibody (Invitrogen). Cells were mounted in Prolong Gold anti-fade with DAPI (Invitrogen). Cell images were obtained with a Solamere CSU10 Spinning Disk confocal system mounted on a Nikon TE2000-E2 inverted microscope. Images were taken with a multi-immersion 20× objective with a numerical aperture (N.A.) 0.75; oil: Working distance (W.D.) = 0.35 mm, or a 100× Plan Apo VC objective N.A. 1.4, oil: W.D. = 0.13 mm. For tissues, fixed sections were H&E stained. Images were obtained using a Zeiss Axiovert 200

inverted microscope equipped with a Zeiss AxioCam HR CCD camera with 1,300 × 1,030 pixels basic resolution and a Zeiss Plan NeoFluar 20×/0.50 Ph2 (DIC II) objective. For crown-like structures, fixed sections were incubated with rat anti-mouse F4/80 primary antibody (AbD- Serotec) followed by goat anti-rat secondary antibody conjugated to horseradish peroxidase (AbD-Serotec). Images were obtained with a Solamere CSU10 Spinning Disk confocal system mounted on a Nikon TE2000-E2 inverted microscope. Images were taken with a 40× objective.

Immunoblot Analysis: Tissue extracts were prepared using Triton Lysis Buffer [20 mM Tris (pH 7.4), 1% Triton X-100, 10% glycerol, 137 mM NaCl, 2 mM EDTA, 25 mM β-glycerophosphate, 1 mM sodium orthovanadate, 1 mM phenylmethylsulfonyl fluoride, and 10 μg/mL of aprotinin plus leupeptin]. Protein concentration was measured using BCA assay (Thermo Scientific). Extracts (25 μg of protein) were examined by protein immunoblot analysis by probing with antibodies to AKT, pSer473AKT (Cell Signaling), α-Tubulin (Sigma), and α-Actin (Sigma). Immunocomplexes were detected by enhanced chemiluminescence.

Multiplexed ELISA of Protein Phosphorylation: Quantitative analysis of pSer473-AKT/AKT was performed using Bioplex kits (Bio- Rad) and a Luminex 200 machine (Millipore).

Statistics: t-test or one-way or two-way ANOVA analysis and Bonferroni or

Tukey posttests using GraphPad Prism 5.0a software determined the statistical significance of the differences in the means of experimental groups. The data are presented as the means ± SEM.

RESULTS

Biodistribution of GeRPs in Obese Mice.

Previous studies from our lab have demonstrated that GeRPs are systemically distributed when injected into lean mice (228, 230). To study the localization of i.p.-injected GeRPs in obese mice, we used FITC-labeled GeRPs loaded with non-targeting scrambled (SCR) siRNA. Five-wk-old ob/ob mice were administered GeRPs by i.p. injection daily for 5 d and various tissues, including liver, lung, spleen, pancreas, heart, and kidney and SubQ, mesenteric, perirenal, and epididymal ATs were analyzed by microscopy (**Figure 3.1A–J**). FITC-GeRPs were only observed in cells within the epididymal AT and not in the other organs (**Figure 3.1A–F**) or other adipose depots (**Figure 3.1G–I**). Similar results were obtained when mice were treated with GeRPs for 10 d. These data document that GeRPs injected i.p. are mostly found in cells within the epididymal AT in obese ob/ob mice.

Figure 3.1 GeRPs injected i.p. localize in epididymal ATMs in obese mice

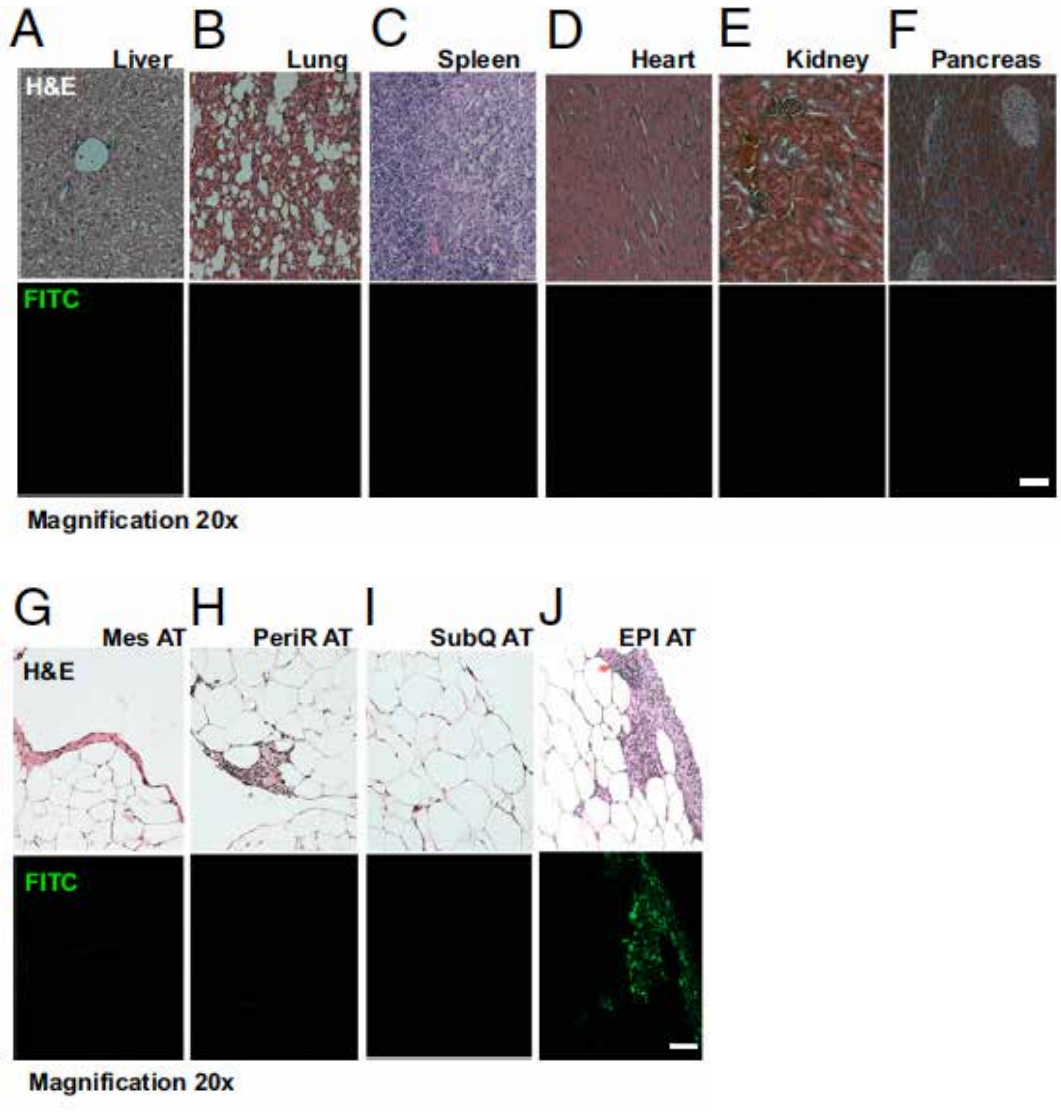

Figure 3.1 GeRPs injected i.p. localize in epididymal ATMs in obese mice (**A–J**) Five-week-old ob/ob mice were i.p. injected once a day for 5 d with 5.6 mg/kg FITC-labeled GeRPs loaded with 2.1 mg/kg EP and 0.262 mg/kg SCR siRNA. On day 6, liver, lung, spleen, pancreas, heart, kidney, and (SubQ AT), mesenteric (Mes AT), perirenal (PeriR AT), and epididymal AT (EPI AT) were isolated. Tissues were fixed, sectioned, and then stained with H&E. Tissues were then analyzed by fluorescent microscopy. Images were obtained using a Zeiss Axiovert 200 inverted microscope. (Scale bar: 50 **μ**m.)

GeRP Uptake in the Epididymal ATMs in Obese Mice.

To study the profile of cells in the epididymal AT that internalize GeRPs, we performed fluorescence microscopy and flow cytometry analysis. The ob/ob mice were i.p. injected daily for 5 d with FITC-GeRPs. On day 6, epididymal AT sections were stained with an antibody against the macrophage marker F4/80 and analyzed by microscopy. **Figure 3.2A** shows FITC-GeRPs in F4/80-positive cells in a region of the epididymal AT macrophage rich CLS. We next performed fluorescence microscopy on cells isolated from the SVF, which contains all cells in the AT that do not float upon centrifugation, unlike lipid-laden adipocytes (**Figure 3.2B**). SVF cells were isolated from the AT and stained with the F4/80 antibody (red) and the nuclear stain, DAPI (blue) (**Figure 3.2B**). Images in **Figure 3.2B**, **Left** show cells containing FITC-GeRPs only in GeRP-treated mice. Analyses at higher magnification (**Figure 3.2B**, **Right**) show F4/80-positive cells containing multiple FITC-GeRPs. Flow cytometry analysis confirmed the presence of FITC-GeRPs in F4/80-positive cells in the epididymal AT **(Figure 3.2C**, **Upper Right**). Importantly, an FITC signal was detected in phagocytic cells, including F4/80-positive macrophages and F4/80 intermediate and negative monocytes and neutrophils (**Figure 3.2C**, **Lower Right**). Similar results were obtained when mice were treated with GeRPs for 10 d. These results show that GeRPs injected i.p. are specifically delivered to phagocytes in the epididymal AT of obese ob/ob mice.

Figure 3.2 – ATMs in obese mice phagocytose GeRPs

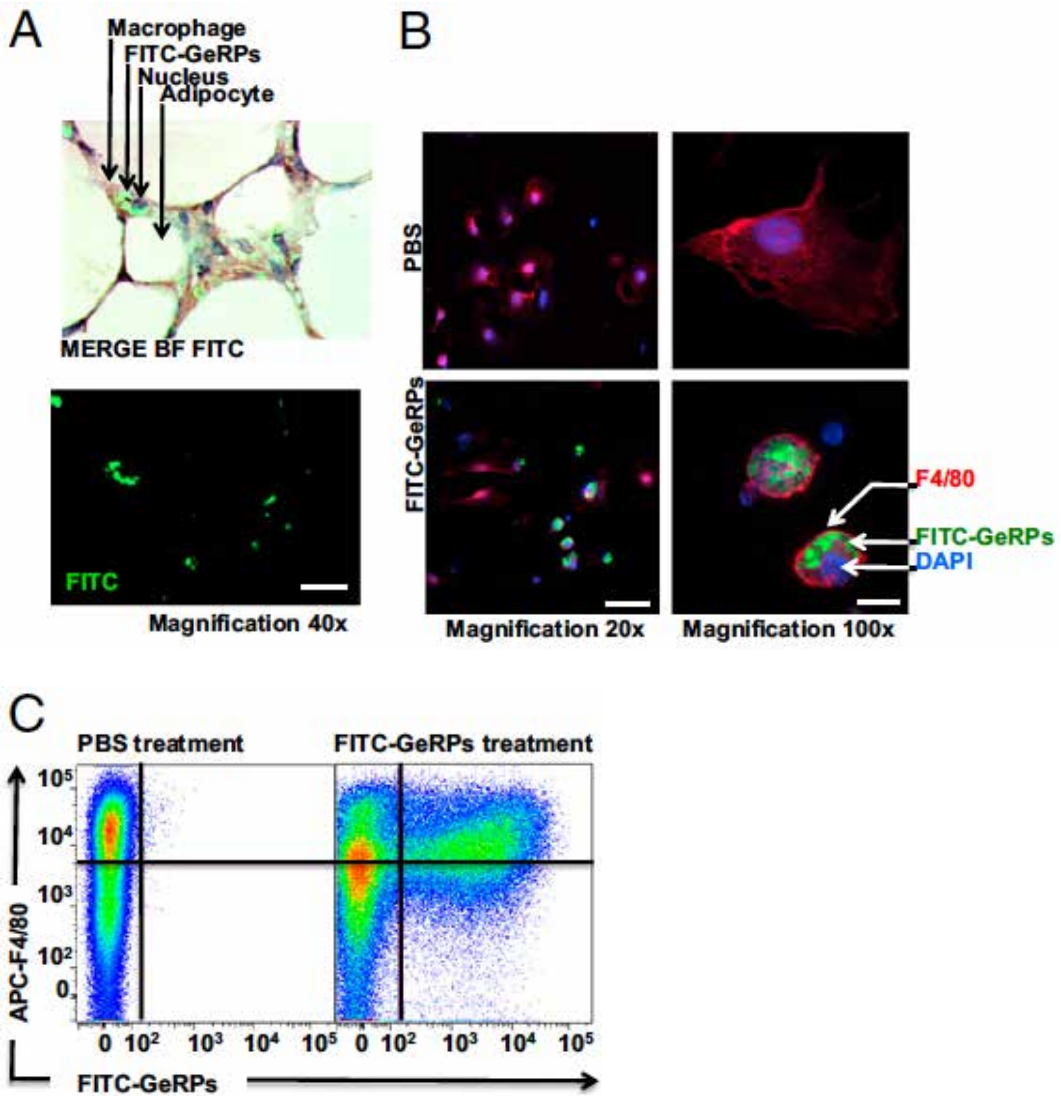

Figure 3.2 ATMs in obese mice phagocytose GeRPs

(**A**) Five-week-old ob/ob mice were i.p. injected once a day for 5 d with 5.6 mg/kg FITC-labeled GeRPs loaded with 2.1 mg/kg EP and 0.262 mg/kg SCR siRNA. On day 6, epididymal AT was isolated, fixed, sectioned, and stained with F4/80 antibody. Tissues were also counterstained with hematoxylin. Tissues were then analyzed by fluorescent microscopy. Spinning disk confocal microscopy showing crown-like structures composed of macrophages (dark brown) containing FITC GeRPs (green). (Scale bar: 20 μm.) (**B**) Confocal microscopy showing F4/80 (red) and GeRPs (green) present in SVF cells 24 h after treatment. Nuclei were stained with DAPI (blue). (Scale bar: Left, 50 μm; Right, 10 μm.) (**C**) FACS analysis showing SVF cells isolated from mice treated with FITC-labeled GeRPs (FITC-GeRPs) and stained with F4/80 antibody. APC: allophycocyanin.

Gene Silencing in Primary Macrophages.

We first measured the expression of OPN in epididymal and SubQ ATMs of 7-wk-old obese ob/ob mice and found strong increases of expression of these genes in epididymal ATMs of ob/ob mice compared with their lean WT littermates (**Figure 3.3A**). The increase in OPN expression in epididymal ATMs confirmed that the increase in macrophage content occurs mainly in the VAT in the obese state. Primary peritoneal macrophages were used to screen for potent siRNAs against OPN, and two were chosen for (**Figure 3.3B**). Both siRNA sequences potently silenced the expression of OPN. Furthermore, secretion of OPN was significantly silenced by the targeting siRNAs compared with SCR or untreated cells (**Figure 3.3C**). The data reveal that OPN could be silenced in primary macrophages *in vitro* both at the mRNA and protein levels.

Figure 3.3 – Silencing OPN in primary macrophages *in vitro.*

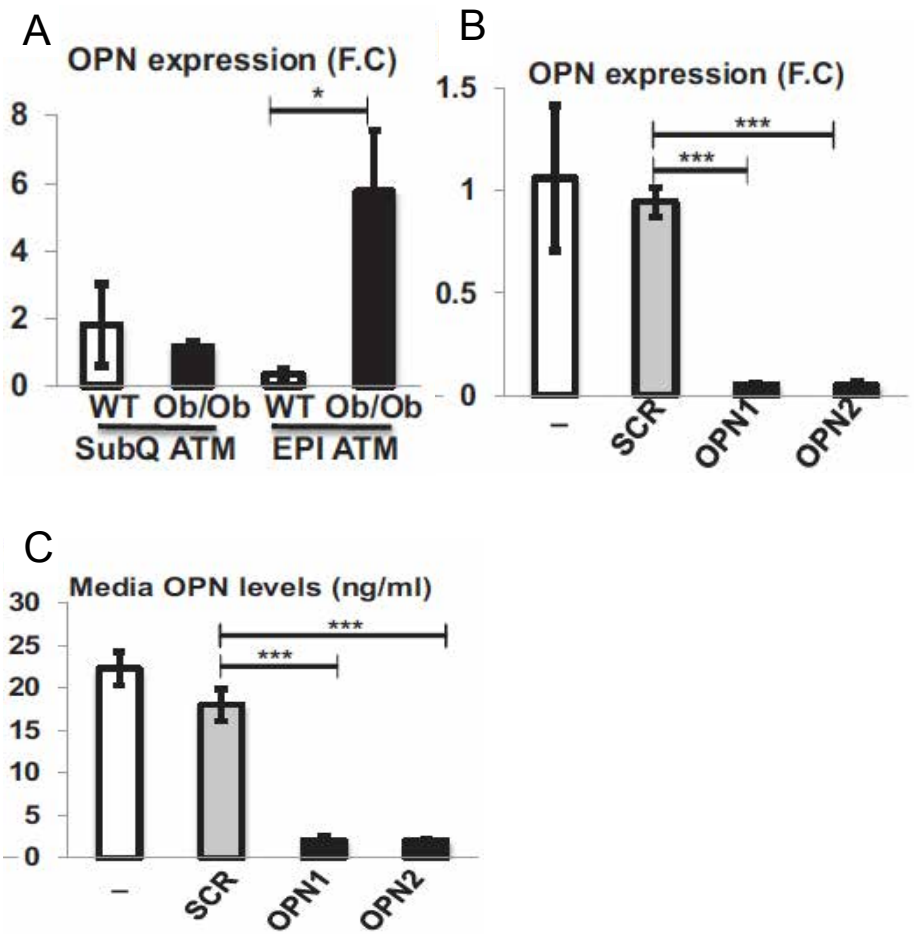

Figure 3.3 Silencing OPN in primary macrophages in vitro
(**A**) Expression of OPN measured by RT-PCR in isolated macrophages from epididymal and SubQ AT of 7-wk-old genetically obese ob/ob mice. Macrophages were isolated using CD11b antibody bound to magnetic beads; n = 4. Statistical significance was determined by t test. ***P < 0.001; *P < 0.05. Results are means expressed in fold change (F.C.) ± SEM. (**B**) 1 x 10^6 peritoneal macrophages were treated with particles made with a mixture of160 pmoles siRNA and 3 nmol EP. Forty-eight hours after the treatment, mRNA levels were measured by RT-PCR. (**C**) OPN protein basal levels in media measured by ELISA; n = 3 with three technical replicates for each experiment. Statistical significance was determined by ANOVA and Tukey post test. ***P < 0.001. Results are mean ± SEM.

Gene Silencing in Epididymal ATMs in Obese Mice.

To test the ability of GeRPs to deliver functional siRNA and silence OPN *in vivo*, 5-wk-old ob/ob mice were injected daily for 5 d with GeRPs loaded with SCR or OPN siRNA, validated as shown in **Figure 3.3**.The day after the last injection, OPN expression was measured in epididymal AT (**Figure 3.4A**). OPN expression was significantly knocked down by 70% in the epididymal AT of ob/ob mice treated with OPN- GeRPs compared with SCR-GeRPs (**Figure 3.4A**). To confirm the specificity of the siRNA-mediated knockdown, the expression of several other macrophage and immune cell factors was measured, including CD11b, CD11c, F4/80, CD68, IL-1β, IL-6, IL-10, IL-4, CC-motif chemokine receptor-2 (CCR2), monocyte chemoattractant protein 1 (MCP-1), and adipocyte protein 2 (aP2). Expression of these markers was unchanged in mice treated with OPN-GeRPs compared with SCR-GeRPs (**Figure 3.4B**). This result confirmed the specificity of siRNA-mediated knockdown and suggested that silencing OPN expression had no effect on global AT inflammation during the experiment.

Consistent with the biodistribution studies showing GeRPs were present only in phagocytic cells of epididymal AT and not in liver, no depletion of the target gene products was observed in liver of treated mice (**Figure 3.4C**). Mice treated with OPN-GeRPs had a significant 81% decrease of OPN secretion in SVF isolated from epididymal AT compared with mice treated with SCR-GeRPs (**Figure 3.4D**). FACS was performed to analyze the knockdown of OPN in ATMs

containing FITC-labeled GeRPs (Fig. 4**J**). OPN expression was significantly silenced in sorted F4/80**+**/FITC**+** ATMs in mice treated with OPN-GeRPs, compared with SCR-GeRPs (**Figure 3.4E**). Taken together, these data reveal that i.p.-injected GeRPs can specifically silence genes in epididymal ATMs *in vivo* without affecting gene expression in macrophages in other major organs such as liver.

Figure 3.4 – Specific silencing of OPN in ATMs of epididymal AT

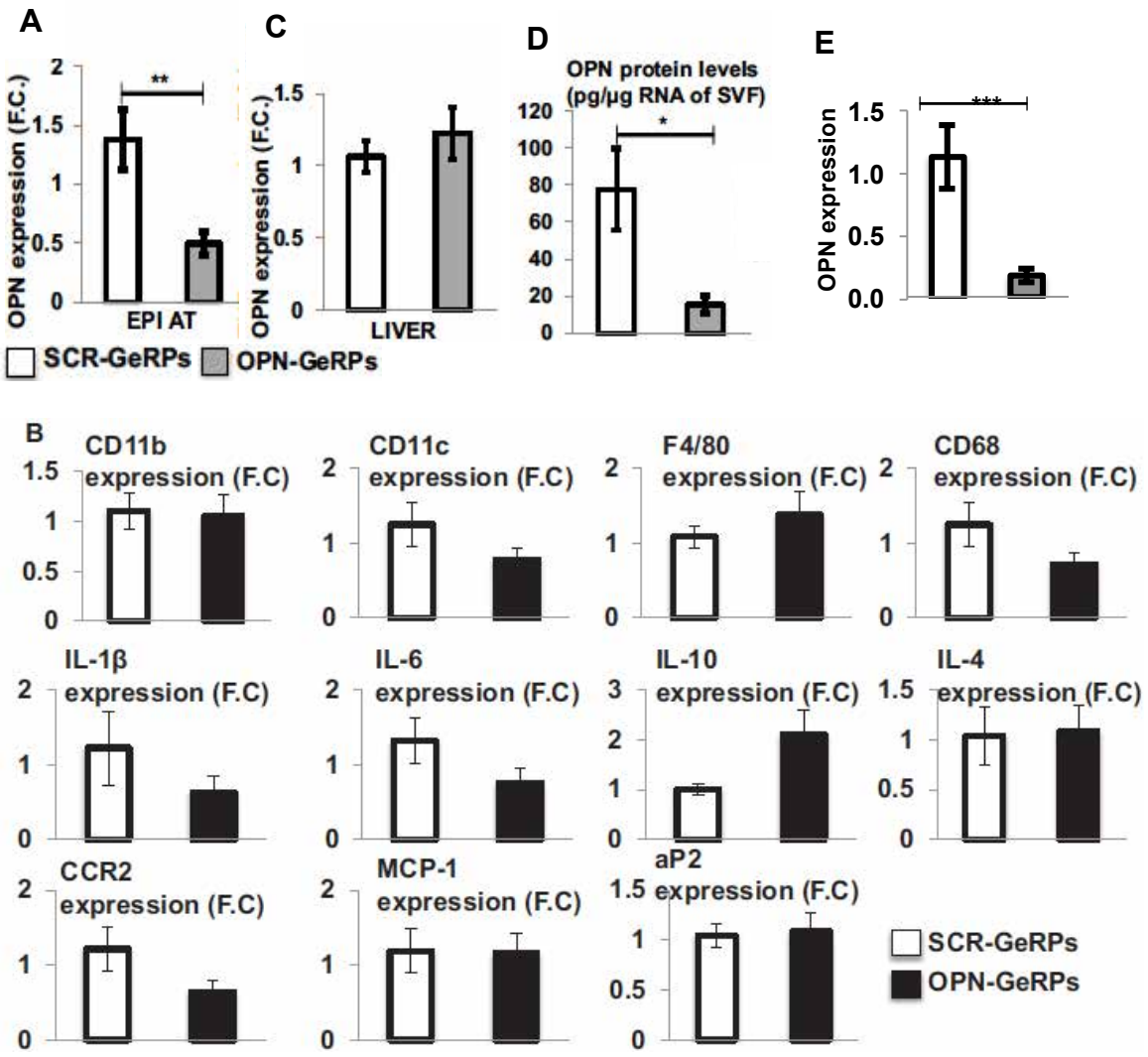

Figure 3.4 Specific silencing of OPN in ATMs of epididymal AT
Expression of OPN in (**A**) epididymal AT and (**C**) liver from mice treated for 5 d with SCR- or OPN-GeRPs. (**B**) Expression of inflammatory genes in AT of ob/ob mice treated with SCR- or OPN-GeRPs; **n** = 28. Statistical significance was determined by **t** test. ***$P < 0.001$; *$P < 0.05$. Results are means in F.C. ± SEM. (**D**) OPN protein levels in epididymal SVF media of mice treated with SCR- or OPN-GeRPs; **n** = 10. Statistical significance was determined by t-test. **$P < 0.01$; *$P < 0.05$. (**J**) Mice were treated with FITC-labeled SCR- or OPN-GeRPs for 5 d. F4/80+ cells containing GeRPs were sorted by FACS and mRNA levels were measured by RT-PCR; **n** = 3 groups of three mice pooled together. Statistical significance was determined by t-test. ***$P < 0.001$.

Silencing Inflammatory Genes in Epididymal ATMs Affects Whole-Body Metabolism in ob/ob Mice.

To test the effect of GeRP-mediated gene silencing in epididymal ATMs on whole-body metabolism, glucose tolerance tests were performed in ob/ob mice treated with OPN-GeRPs or SCR-GeRPs (**Figure 3.5A**). OPN silencing in epididymal ATMs improved glucose tolerance in obese mice (**Figure 3.5A**). Area under the glucose tolerance test curve showed that mice treated with OPN-GeRPs were significantly more glucose tolerant compared with mice treated with PBS or SCR-GeRPs (**Figure 3.5B**). Importantly, this occurred without affecting OPN expression in other tissues or protein levels in serum, where OPN levels unchanged (**Figure 3.4C and Figure 3.5C**). The effect of OPN silencing on glucose tolerance was independent of an effect on weight gain during treatments (**Figure 3.5D**). Taken together, these results suggest that decreasing production of these cytokines specifically in epididymal ATMs has a beneficial effect on whole-body metabolism.

To study the effect of OPN silencing in ATMs on systemic insulin sensitivity, we performed insulin tolerance tests in mice treated with PBS-, SCR-, or OPN-GeRPs (**Figure 3.5E and F**). Mice treated with OPN-GeRPs had a significant improvement in insulin response compared with mice treated with PBS or SCR-GeRPs (**Figure 3.5E and F**). Measurement of fasting insulin levels showed that mice showed no differences between the groups (**Figure 3.5G**). These results suggested that OPN silencing in ATMs increases systemic insulin sensitivity.

Figure 3.5 – OPN silencing in ATMs in obese mice regulates whole-body metabolism

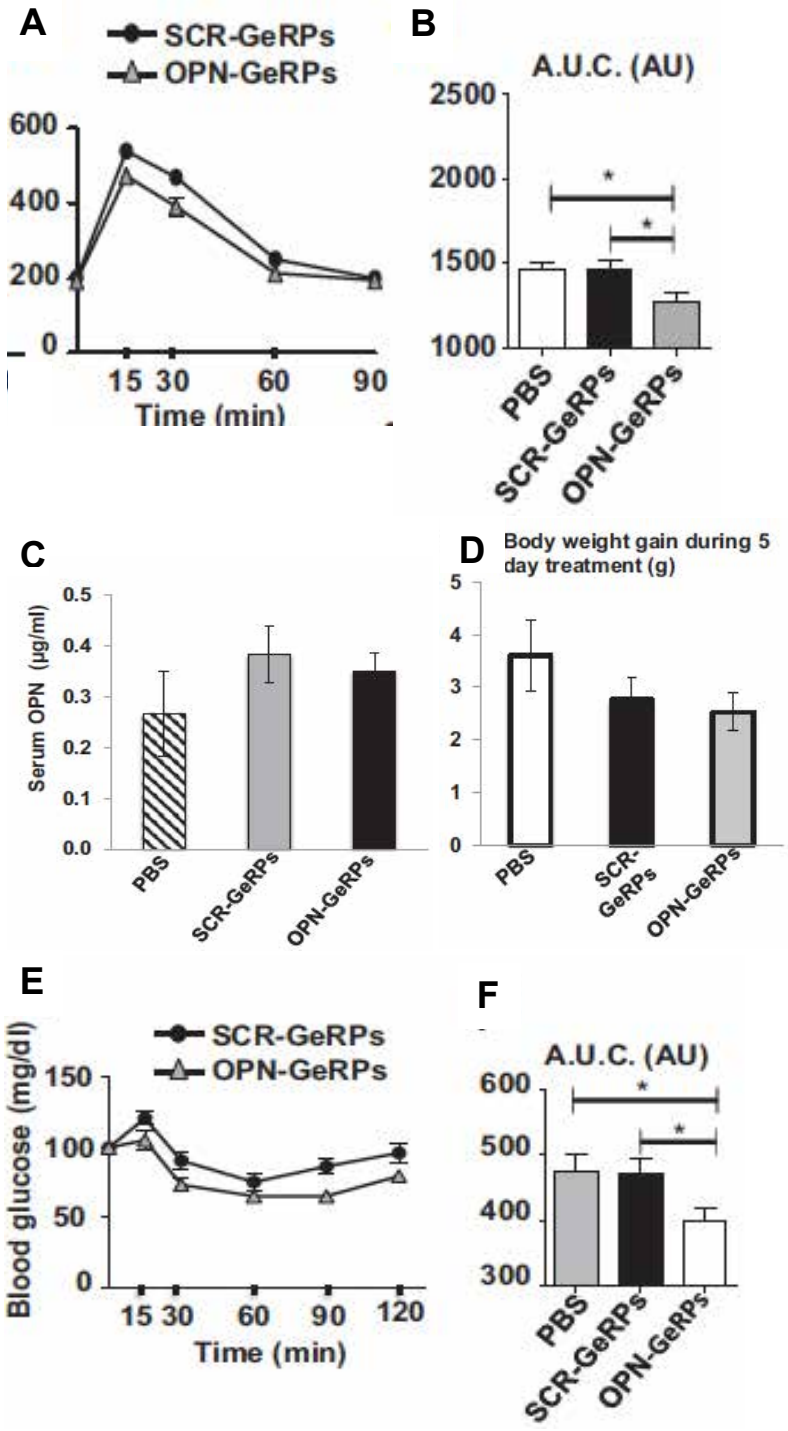

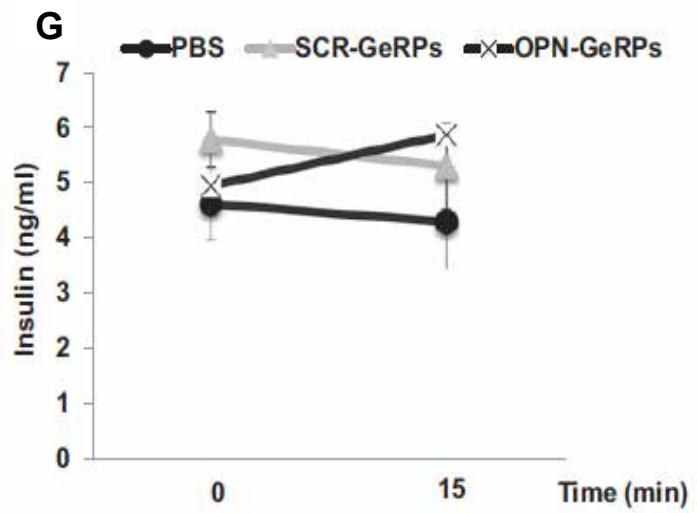

Figure 3.5 OPN silencing in ATMs in obese mice regulates whole-body metabolism

(**A**) Five-week-old ob/ob mice were treated as described in Figure 4.4. Twenty-four hours after the last injection, glucose tolerance tests (GTT) were performed on mice that were fasted for 16 h. Mice were treated with SCR-GeRPs or OPN-GeRPs. (**B**) Area under the curve (AUC) of GTT graph; **n** = 10**–**18. Statistical significance was determined by ANOVA and Tukey posttest. ***P** < 0.05. Results are mean ± SEM. **(C)** Serum OPN levels in ob/ob mice treated for 5 d with PBS or SCR- or OPN-GeRPs; n = 10–15. (**D**) Total body weight gain in ob/ob mice treated for 5 d with PBS or SCR- or OPN-GeRPs; n = 10**–**15 (**E**) Insulin tolerance tests (ITT) were performed on day 6 in ob/ob mice treated with PBS or SCR- or OPN-GeRPs by injecting 1 U/kg of insulin. (**F**) AUC of ITT graph; **n** = 15. Statistical significance was determined by ANOVA and Tukey posttest. ***P** < 0.05. Results are mean ± SEM. (**G**) Serum insulin levels during GTT in mice treated with PBS or SCR- or OPN-GeRPs; n = 10.

ATM-derived OPN affects insulin signaling and adipocyte biology

The role of OPN in the development of insulin resistance has been attributed to its role in attracting macrophages in the epididymal AT (21, 22). To test this, macrophage content was analyzed in the epididymal AT of mice treated with OPN-GeRPs compared with SCR-GeRPs (**Figure 3.6A**). Epididymal ATM content was unchanged in OPN-GeRP**–**treated mice compared with mice treated with SCR-GeRPs (**Figure 3.6A**). This suggests that OPN silencing in epididymal ATMs prevents obesity-induced insulin resistance independently of macrophage recruitment. Analysis of circulating lipids showed that OPN silencing in epididymal AT had no effect on lipolysis (**Figure 3.6B and C**). Therefore, we also performed biochemical studies to investigate insulin-stimulated AKT activation in mice treated with PBS, SCR-GeRPs, or OPN-GeRPs (**Figure 3.6D**). Obesity suppressed insulin-stimulated AKT activation in liver, AT, and skeletal muscle of mice treated with PBS or SCR-GeRPs but not in AT of mice treated with OPN-GeRPs (**Figure 3.6D**). Together, these data demonstrate that silencing OPN in ATMs improves insulin sensitivity in AT. Furthermore, OPN levels were specifically decreased in epididymal AT and not in other tissues or serum (**Figure 3.4**), suggesting that it may play a paracrine role in the AT. To determine whether OPN knockdown affected adipocyte function, we measured the expression of a number of adipocyte genes in adipocytes from mice treated with SCR- or OPN-GeRPs. By RT-PCR two genes showed a significant increase in gene expression: PPARγ and FASN. As discussed in Chapter 1, these genes are key

regulators of adipogenesis and lipogenesis respectively. This data taken together suggests ATM-OPN negatively affects adipocyte function and insulin signaling in obese mice.

Figure 3.6 – OPN knockdown in ATMs affects adipocyte biology and insulin signaling

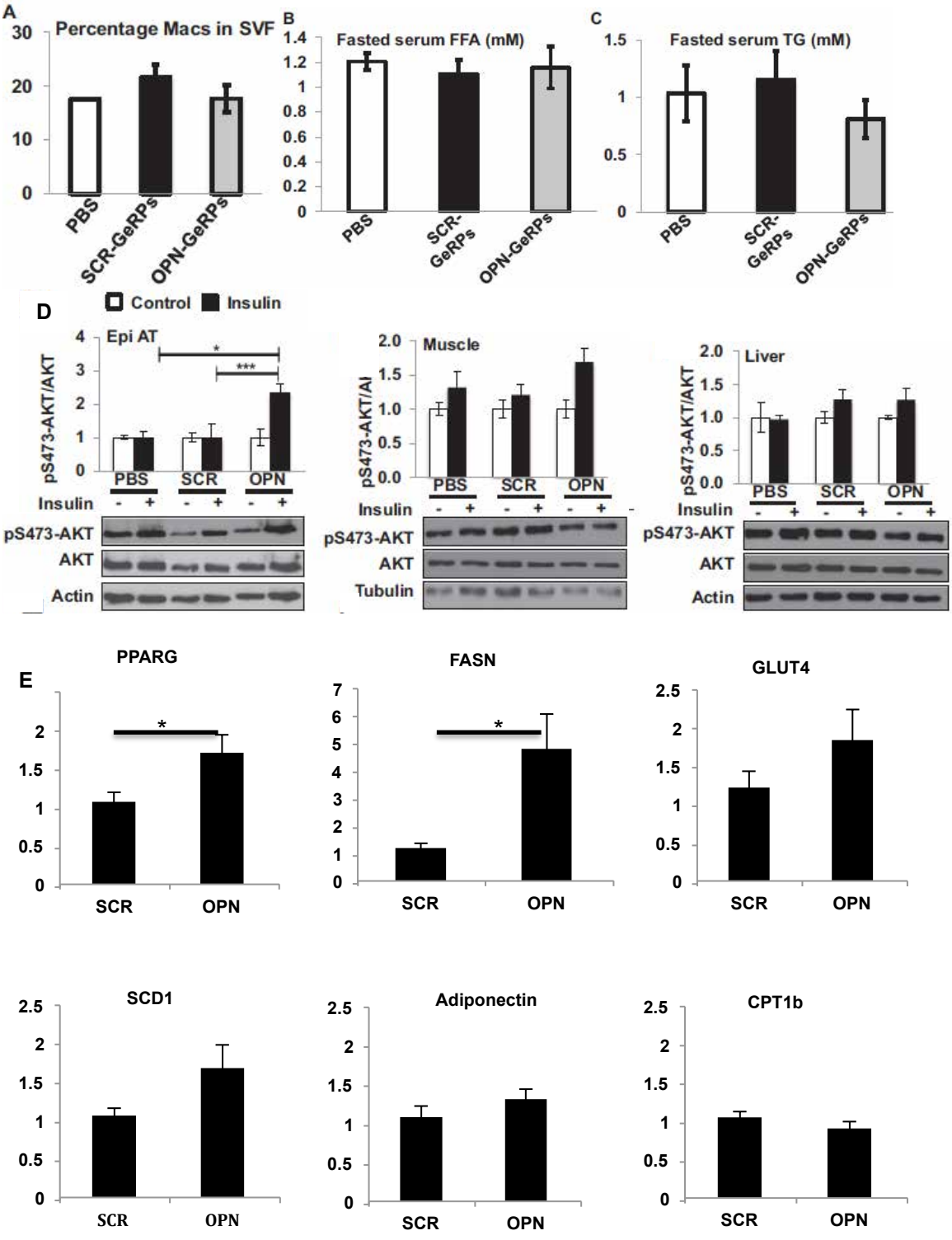

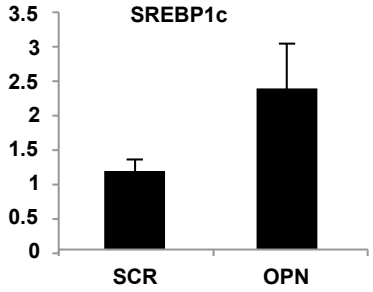

Figure 3.6 OPN Knockdown in ATMs affects adipocyte biology and insulin signaling

(**A**) Macrophage content in the epididymal SVF of mice treated with PBS or SCR- or OPN-GeRPs measured by flow cytometry. (**B**) Fasted FFA and (**C**) TG serum levels in ob/ob mice treated with PBS or SCR- or OPN-GeRPs; n = 5–10. (**D**) PBS or SCR- or OPN-GeRPs treated mice were also fasted for 4 h and then treated by i.p. injection with 1 U/kg of insulin (15 min). Western blotting and multiplexed ELISA were used to detect AKT and activated (pSer473) AKT in epididymal AT (EPI AT), gastrocnemius muscle and liver; **n** = 5**–**6. Statistical significance was determined by ANOVA and Tukey posttest. ***$P < 0.001$; *$P < 0.05$. Results are mean ± SEM. (**E**) Expression of adipocyte genes in isolated adipocytes of ob/ob mice treated with SCR- or OPN-GeRPs; **n** = 14-15. Statistical significance was determined by **t** test. *$P < 0.05$.

Osteopontin deficient mice are not protected from diet induced obesity and systemic glucose metabolism.

To test whether the effects of GeRP-mediated OPN KD in obese mice could be reproduced in OPN-deficient mice, I obtained global OPN KO mice from Jackson Labs. Heterozygous mice were bred together to generate KO animals and WT controls to be used in subsequent experiments. Opn-/- and WT mice were placed on either the 45%HFD or the 60%HFD for 19 weeks and 10 weeks respectively (**Figure 3.7A and B**). There was no significant difference in weight gain between KO and WT groups on either the chow diet or the two different HFDs, although there as a trend toward less weight gain in KO on the 45%HFD (**Figure 3.7A**) These mice were then subjected to glucose tolerance tests to determine whether OPN deficiency had any effect on systemic glucose metabolism. OPN KO animals did not show any improvement in glucose tolerance when placed on either of the HFDs (**Figure 3.7C and D**), and interestingly there was a trend toward worse glucose tolerance in the KO animals on the 60%HFD (**Figure 3.7D**). In order to confirm the depletion of OPN in the KO mice blood was collected from all animals at the time of dissection, and an OPN ELISA was performed on the serum using a commercially available kit and per the manufacturer's instruction. WT controls showed a circulating concentration in the range of 230-246ng/mL while in the KO mice, OPN could not be detected (**Figure 3.7E**).

Figure 3.7 – OPN KO mice develop diet induced obesity and glucose intolerance

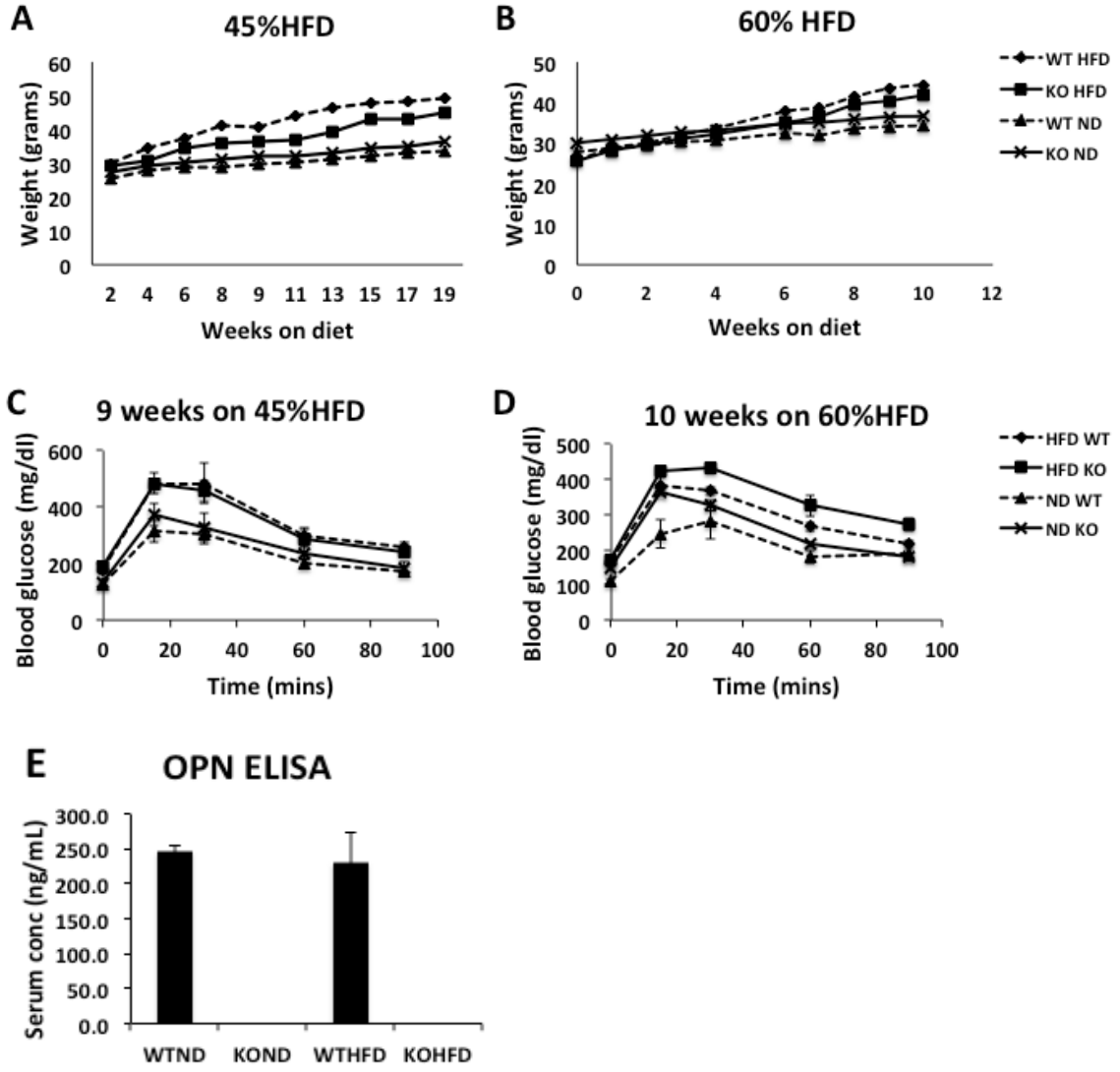

Figure 3.7 OPN KO mice develop diet-induced obesity and glucose intolerance

(**A**) Eight-week-old opn-/- and WT controls were placed on either a chow diet or a diet of 45%kcal fat for 19 wks. (**B**) Ten-week-old opn-/- and WT controls were placed on either a chow diet or a diet of 60%kcal fat for 10 wks. (**C**) GTTs were performed on mice that were fasted for 16 h; n=5 (**D**) GTTs were performed on mice that were fasted for 16 h; n=4-10 (**E**) OPN ELISA was performed on serum samples from opn-/- and WT controls on either chow diet or a diet of 60%kcal fat for 10 wks; n=4-10. Results are mean ± SEM.

DISCUSSION

The major findings reported here include the development of a powerful RNAi-based method to selectively silence genes in epididymal ATMs in obese mice while leaving such cells unperturbed in other tissues (**Figures 3.1 and 3.2**). This selective biodistribution profile of i.p.-injected GeRPs in obese mice is in keeping with the known high accumulation of macrophages in visceral AT compared with other adipose depots and metabolic tissues in obese rodents and humans (254-256). In previous studies using lean healthy animals, i.p.-injected GeRPs were internalized by macrophages that could be detected throughout the body (228, 230). In contrast, using obese insulin-resistant animals, we detected GeRPs mostly in the epididymal ATMs following i.p. injection. One explanation for the different patterns of GeRP distribution observed in lean versus obese mice could be the increase in AT chemoattractants in obesity. Adipocytes produce a wide range of such factors, such as MCP-1, which may recruit monocytes expressing its receptor CCR2 to adipose tissue in obese mice (257, 258).

Although multiple siRNA delivery systems have been recently described in the literature (259, 260), none has been used in an obese, insulin-resistant animal model. A previous study described delivery of lipidoid nanoparticles carrying siRNA to immune cells, including lymphocytes, in spleen, blood, and bone marrow following i.v. injection in lean mice (261). In contrast, we show here that GeRPs are only found in phagocytes, which could represent a major clinical

advantage. This important feature of the GeRPs is conferred by their size (2–4 μm) and the β-1,3-D-glucan that is specifically recognized by receptors expressed by phagocytic cells (234).

Decreasing inflammation in obese rodents often results in improvement of insulin sensitivity (102). However, blocking cytokines by injection of antibodies or antagonists has yielded mixed results in alleviating insulin resistance in humans (205, 262-265). An explanation for the frequently observed absence of effects of these drugs on insulin resistance in obese subjects may be their low penetrance in AT in which the endogenous cytokines act in a paracrine fashion (266). However, no study has actually shown a direct role of macrophages in the AT in the regulation of systemic metabolism because experimental anti-inflammatory gene knockouts and other procedures are not restricted to AT, but in general act on immune cells within all tissues. Macrophages in particular are present in all tissues, and cytokines are highly expressed by various immune and nonimmune cells (Chapter 1). Therefore, the physiological role of ATMs has been a key unanswered question in the field, and is particularly important considering the variable results obtained with cytokine blockers in human subjects.

The specificity of GeRPs in targeting epididymal ATMs when administered i.p. permitted us to address this critical question **(Figures 3.4 and 3.5).** The motivation for targeting OPN in epididymal ATMs in our studies was based on three major points: (i) OPN−/− mice are protected from obesity-induced insulin resistance (208); (ii) the expression OPN is high in AT from obese mice (**Figure**

3.3) (208, 212); and (iii) anti-OPN neutralizing antibody reverses obesity-induced insulin resistance in rodents (212). Based on these considerations, GeRPs were loaded with siRNAs to silence OPN in genetically obese ob/ob mice. Although previous work by our laboratory and others demonstrated that GeRPs can mediate potent gene silencing in peritoneal macrophages in lean mice (228-230), here we found specific gene knockdown within epididymal ATMs in obese mice.

Importantly, GeRP-mediated OPN silencing in epididymal ATMs improved the glucose tolerance of ob/ob mice (**Figure 3.5**). Silencing OPN had no effect on the expression of CD11b, CD11c, F4/80, CD68, IL-1β, IL-6, IL-10, IL-4, CCR2, MCP-1, or aP2 in AT, suggesting that none of these inflammatory mediators is downstream of OPN in this context. Thus, the selective depletion of OPN in the absence of changes in these other factors was sufficient to improve glucose tolerance (**Figure 3.4**). Notably, OPN silencing in ATMs specifically increased PPARγ and FASN expression, as well as insulin-stimulated AKT activation in AT. This suggests a paracrine role of macrophage OPN in improving insulin signaling and adipocyte function (**Figure 3.6**). Thus, this study shows a direct link between epididymal ATM-derived cytokines and insulin resistance.

Previous studies have demonstrated that OPN-deficient mice are protected from the complications associated with DIO and T2DM such as insulin resistance, hyperglycemia and hepatic steatosis (208, 213). We therefore sought to reproduce this protective effect as well as confirm the beneficial effects of our OPN-GeRPs by challenging OPN KO mice with two different high fat diets.

However, we were surprisingly unable to show any benefits to global depletion of OPN in obese mice (**Figure 3.7**). A possible reason for this could be the differences in housing facilities between previous studies and ours. In recent years the hypothesis that gut microbiota could play an important and unrecognized role in whole body metabolism has been generating a lot of interest. Differences in the microbiome could determine the metabolic response in humans and rodents, regardless or in addition to genetic and environmental factors (267). Therefore the microbes unique to our facility could have played a role in the data we obtained from our KO animals, which is inconsistent with that in other previously published studies.

This study illustrates the crucial role of macrophage local environment and emphasizes the importance of studying macrophage function within a specific tissue. Although additional work is needed to define the molecular mechanisms by which these macrophage proteins regulate whole-body metabolism, the GeRP siRNA delivery system provides a unique tool for such studies**.**

Chapter IV: Lipid storage by adipose tissue macrophages regulates systemic glucose tolerance

This chapter is derived from an article by the same name published in the

Journal of Lipid Research.

Aouadi, M., Vangala, P., Yawe, J. C., Tencerova, M., Nicoloro, S. M., Cohen, J. L., Shen Y and Czech, M. P. (2014) Lipid storage by adipose tissue macrophages regulates systemic glucose tolerance. *Am J Physiol Endocrinol Metab* **307**, E374-383

Author Contributions

- **Figure 4.1 Flow cytometry, microscopy and RT-PCR** – All staining and sorting of foam cells were performed by Pranitha Vangala and Myriam Aouadi. Immunofluorescence staining and microscopy were performed by Pranitha Vangala. All electron micrograhs were prepared by Gregory Hendricks and Lara Strittmatter at UMASS Medical School. Gene expression analysis was performed by Pranitha Vangala and Joseph Yawe.
- **Figure 4.2 GeRP-mediated LPL Knockdown, microscopy and flow cytometry** – Myriam Aouadi, Pranitha Vangala, Michaela Tencerova, Sarah Nicoloro, Jessica Cohen, Yuefei Shen and Joseph Yawe (GeRP team, Czech lab) conducted all knockdown studies.
- **Figure 4.3 Serum Lipids** – Pranitha Vangala and Joseph Yawe performed all measurements of serum TG, Cholesterol and FFA.
- **Figure 4**.4 Metabolic studies – Glucose and pyruvate tolerance tests were performed by Pranitha Vangala and Joseph Yawe.

SUMMARY

Proinflammatory pathways in ATMs can impair glucose tolerance in obesity, but ATMs may also be beneficial as repositories for excess lipid that adipocytes are unable to store. To test this hypothesis, we selectively targeted visceral ATMs in obese mice with siRNA against lipoprotein lipase (LPL), leaving macrophages within other organs unaffected. Selective silencing of ATM LPL decreased foam cell formation in visceral adipose tissue of obese mice, consistent with a reduced supply of fatty acids from VLDL hydrolysis. Unexpectedly, silencing LPL also decreased the expression of genes involved in fatty acid uptake (CD36) and esterification in ATMs. This deficit in fatty acid uptake capacity was associated with increased circulating serum free fatty acids. Additionally, obese mice with LPL-depleted ATMs exhibited higher hepatic glucose production from pyruvate and glucose intolerance. Silencing
Taken together, the data indicate that LPL secreted by ATMs enhances their ability to sequester excess lipid in obese mice, promoting systemic glucose tolerance.

INTRODUCTION

The inability to appropriately expand AT in human obesity may lead to ectopic lipid deposition in liver and skeletal muscle and may be an underlying cause of insulin resistance (70, 250, 251). Accumulation of immune cells including macrophages in the visceral AT of obese mice and humans creates a

chronic inflammatory state that correlates with insulin resistance (32, 110, 252). These AT macrophages (ATMs) secrete cytokines and other factors that may impair adipocyte capacity to store lipids (32, 110, 252), promoting the ectopic deposition of lipid in nonadipose tissues. However, some data indicate a beneficial role of ATMs, for example, in increasing adipose lipid storage (268). ATMs are also required for maintenance of AT homeostasis by regulating angiogenesis, extracellular matrix remodeling, and clearance of dead cells in AT (132, 269-272). It is therefore likely that macrophages exert multiple, even opposing effects on adipocytes, depending upon physiological conditions.

To determine whether ATMs contribute to lipid storage and glucose tolerance, we silenced the expression of lipoprotein lipase (LPL) by ATMs. LPL is released by cells within AT and is translocated to the lumen of adipose capillaries, where it binds the glycosylphosphatidylinositol-anchored high-density lipoprotein-binding protein-1 (GPIHBP1) (273, 274). LPL is known to control localized VLDL triglyceride (TG) hydrolysis and uptake of fatty acids into the tissue (273, 274). The contribution of macrophage-LPL in this function is suggested by experiments showing that depletion of macrophage LPL is effective in reducing lipid-laden foam cell formation in arteries of LDL receptor-null mice (275). Here, we employed GeRPs to silence gene expression of LPL specifically in ATMs in obese mice without perturbing macrophages in other tissues, including liver. Such selective silencing of LPL in ATMs of obese mice decreased foam cell formation in AT and caused a marked impairment in glucose tolerance,

indicating that ATMs contribute to beneficial lipid storage within AT.

MATERIALS AND METHODS

All procedures involving animals were approved by the Institutional Animal Care and Use Committee at the University of Massachusetts Medical School.

Preparation of GeRPs: As described previously (**Chapter 3**).

Peritoneal macrophage preparation: As described previously (**Chapter 3**), using Eight-week-old C57BL6/J male mice.

Gene silencing by siRNA/EP particles in vitro in cell culture: As described previously (**Chapter 3**).

GeRP administration and tissue isolation: Eight-week-old C57BL6/J or 5-wk-old ob/ob male mice were injected once a day for five days with 5.6 mg/kg GeRPs ip loaded with 2.1 mg/kg EP and 0.262 mg/kg siRNA. Further analyses were performed 24 h after the last injection. siRNA sequences used are as follows: Scrambled (SCR) 5'-CAGUCGCGUUUGCGACUGGUU-3'; anti-LPL (5'-UCUCAGACAUCGAAAGCAAUU-3')

Isolation of adipocytes, stromal vascular fraction (SVF) cells, and ATMs: Epididymal fat pads were mechanically dissociated using the GentleMACS Dissociator (Miltenyi Biotec) and collagenase was digested at 37°C for 45 min in Hank's buffered saline solution (HBSS; GIBCO, Life technologies), containing 2% bovine serum albumin (American Bioanalytical) and 2 mg/ml collagenase (Sigma-Aldrich). Samples were then filtered through 100μm diameter pore nylon mesh and centrifuged. The adipocyte layer was collected and washed for further analysis. The pelleted cells were collected as the SVF. The SVF cells were then treated with red blood cell lysis buffer and washed in PBS and plated or directly harvested for further analysis. For ATM isolation, the SVF pellet was resuspended in 1 ml of selection buffer (PBS, 2 mmol/l EDTA, and 0.5% BSA), and the CD11b-positive cells were selected using CD11b microbeads (Miltenyi Biotec), according to the manufacturer's instructions.

Isolation of RNA and real-time PCR: As described previously (**Chapter 2**). Primer sequences used were as follows: 36B4 (5'TCCAGGCTTTGGGCATCA-3', 5'-CTTTATCAGCTGCACATCACTCAGA-3'); lpl (5'-TCTGTACGGCACAGTGG-3', 5'-CCTCTCGATGACGAAGC-3'); cd36 (5'-ATGGGCTGTGATCGGAACTG-3', 5'-TTTGCCACGTCATCTGGGTTT-3'); vldlr (5'-CTCCCAGTTTCAGTGCACAA-3', 5'-ATCAGAACCGTCTTCGCAAT-3'); elovl6 (5'-TCAGCAAAGCAGCCGAAC-3', 5'-AGCGACCATGTCTTTGTAGGAG-3');

ap2 (5'-AAGGTGAAGAGCATCATAACCCT-3', 5'-TCACGCCTTTCATAACACATTCC-3'); pparg (5'-GGAAGACCACTCGCATTCCTT-3', 5'-GTAATCAGCAACCATTGGGTCA-3'); fasn (5'-GGAGGTGGTGATAGCCGGTAT-3', 5'-TGGGTAATCCATAGAGCCCAG-3'); glut4 (5'-GTGACTGGAACACTGGTCCTA-3', 5'-CCAGCCACGTTGCATTGTAG-3'); Scd1 (5'-TTCTTGCGATACACTCTGGTGC-3', 5'-CGGGATTGAATGTTCTTGTCGT-3'); dgat2 (5'-GCGCTACTTCCGAGACTACTT-3', 5'-GGGCCTTATGCCAGGAAACT-3')

Western blot: As described previously (**Chapter 3**).

Flow cytometry: SVF cells from mice treated with FITC-GeRPs were incubated for 20 min in blocking buffer containing 1% BSA and Fc block (eBioscience) for 15 min at 4°C to block nonspecific binding. Cells were then counted and incubated for an additional 20 min in the dark at 4°C with fluorophore-conjugated primary antibodies or isotype control antibodies (AbD Serotec). Antibodies used in these studies included F4/80-APC (AbD Serotec), CD11b-PerCP-Cy5.5 (BD bioscience), and Bodipy-FITC (Invitrogen). Subsequently, cells were analyzed by flow cytometry in an LSRII cytometer (BD Bioscience). FlowJo software (Treestar) was used to identify the different cell populations; 100,000 events were recorded. For sorting experiments, SVF cells were run through a FACS

Vantage (BD Bioscience). Both FITC_ and FITC_ populations were collected, and RNA was harvested for RT-PCR.

Microscopy: For SVF, fixed cells were incubated with rat anti-mouse F4/80 primary antibody (AbD-Serotec) followed by goat anti-rat Alexa fluor 594 secondary antibody (Invitrogen). Cells were mounted in Prolong Gold anti-fade with DAPI (Invitrogen). Cell images were obtained with a Solamere CSU10 Spinning Disk confocal system mounted on a Nikon TE2000-E2 inverted microscope. For tissues, fixed sections were stained with hematoxylin and eosin (H&E). Images were obtained using a Zeiss Axiovert 200 inverted microscope equipped with a Zeiss AxioCam HR CCD camera with 1,300 x 1,030 pixels basic resolution and a Zeiss Plan NeoFluar x20/0.50 Ph2 (DIC II) objective.

Transmission electron microscopy: Samples were processed and analyzed at the University of Massachusetts Medical School Electron Microscopy Core Facility according to standard procedures. Briefly, pieces of whole adipose tissue were fixed in 2.5% gluteraldehyde in 0.1 M sodium cacodylate buffer and left overnight at 4°C. The samples were then rinsed twice in the same fixation buffer and postfixed with 1% osmium tetroxide for 1 h at room temperature. Samples were then washed twice with DH2O for 5 min and then dehydrated through a graded ethanol series of 20% increments, before two changes in 100% ethanol. Samples were then infiltrated first with two changes of 100% propylene oxide and

then with a 50%/50% propylene oxide-SPI-Pon 812 resin mixture. The following day, three changes of fresh 100% SPI-Pon 812 resin were done before the samples were polymerized at 68°C in plastic capsules. The samples were then thin-sectioned, and the sections were placed on copper support grids and contrasted with lead citrate and uranyl acetate. Sections were examined using the FEI Tecani 12 BT with 80 Kv accelerating voltage, and images were captured using a Gatan TEM CCD camera.

TG, LDL/VLDL, HDL-cholesterol, and FFA measurements: TG, LDL/VLDL, HDL-cholesterol, and FFA concentrations in serum and liver homogenate were measured using commercial kits according to manufacturer's protocol (Cayman Chemical).

Glucose and pyruvate tolerance tests: Pyruvate and glucose tolerance tests were performed on ob/ob animals 5 days after GeRP treatment. Pyruvate (1 g/kg) and glucose (1 g/kg) were administered by intraperitoneal injection. Blood samples were withdrawn from the tail vein at the indicated time, and glycemia was determined using glucometers (Bayer-Breeze 2 and Abbott Alphatrak).

Statistics: Student's t-test, one-way or two-way ANOVA and Bonferroni, or Tukey's posttests using GraphPad Prism 5.0a software determined the statistical significance of the differences in the means of experimental groups. The data are

presented as means ± SE.

RESULTS

Lipid uptake by ATMs increases with obesity

To determine the role of ATM lipid handling in systemic metabolism, we first measured the effect of obesity on formation of lipid-laden macrophages in the AT. Flow cytometry was performed on the SVF of 6-wk-old obese ob/ob mice and wild-type (WT) lean controls, using antibodies against the macrophage markers F4/80 and CD11b and the lipid stain bodipy (**Figure 4.1**). Consistent with previous studies (134), the percentage of lipid-laden macrophages (defined as bodipy+F4/80+CD11b+) was significantly increased in the VAT of ob/ob compared with WT mice (**Figure 4.1A and B**). To confirm the presence of foam cells in AT, fluorescence and transmission electron microscopy (TEM) were performed on epididymal SVF of ob/ob mice (**Figure 4.1C and D**). **Figure 4.1C** shows a representative macrophage (F4/80, red) containing lipid droplets (bodipy, green). The TEM image presented shows a macrophage with characteristics described in previous studies (110, 246), with lipid droplets (arrows) confirming the presence of lipid-laden macrophages in the VAT of ob/ob mice (**Figure 4.1D**).

SVF contains multiple cell types; therefore to determine specific gene expression changes in macrophages, we isolated ATMs by using CD11b magnetic bead pull-down from WT and ob/ob AT. We then measured the expression of LPL as well as other genes involved in lipid metabolism, including

FASN, CD36, VLDL receptor (VLDLr), PPARγ, SCD1, and fatty acid-binding protein-4 (fabp4/aP2) (**Figure 4.1E**). Only the expression of LPL was significantly increased in epididymal ATMs of ob/ob mice compared with their lean WT littermates (**Figure 4.1E**). Together, the data confirms that obesity induces foam cell formation in VAT, and the accumulation of lipid is occurs via lipid uptake rather than de novo lipogenesis.

Figure 4.1 - Formation of lipid-laden macrophages in epididymal adipose tissue (AT) of obese mice.

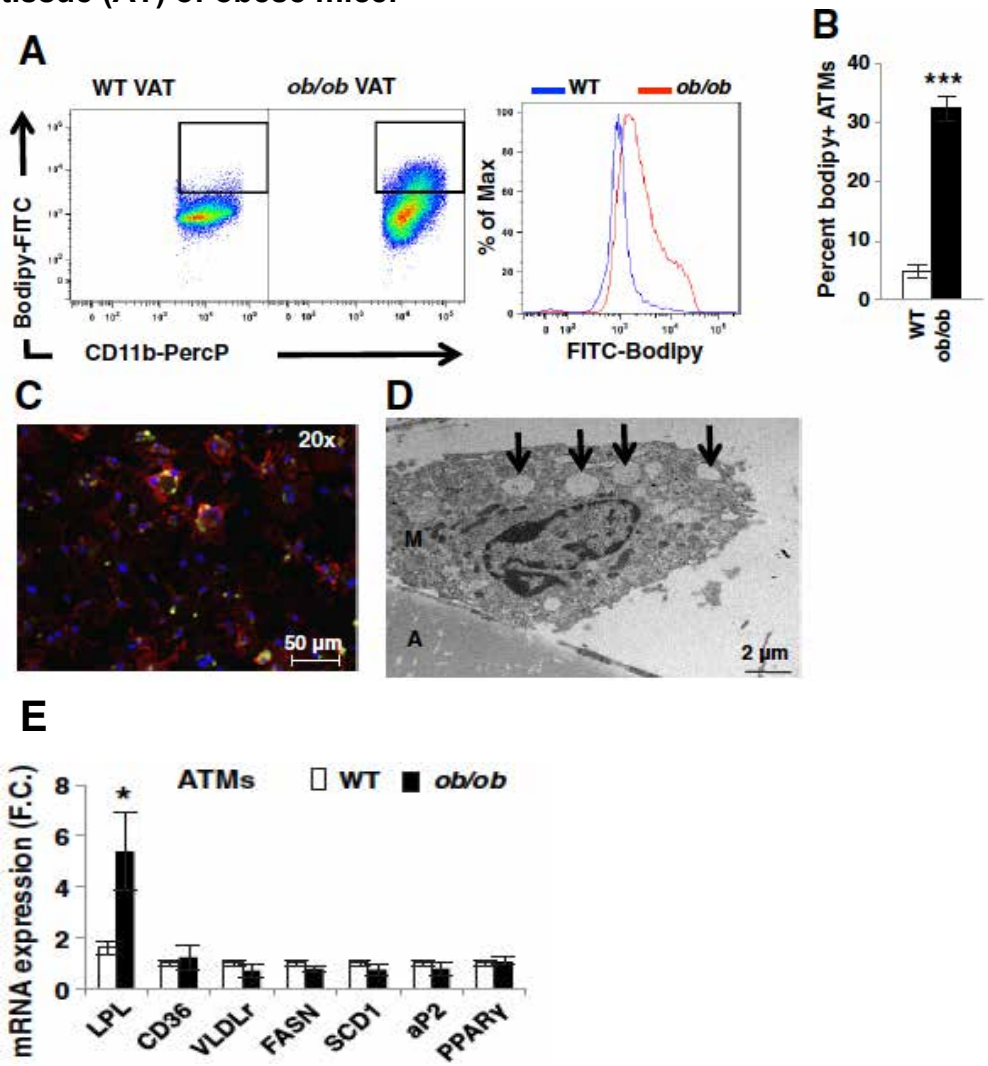

Figure 4.1 Formation of lipid-laden macrophages in epididymal adipose tissue of obese mice

Stromal vascular fraction (SVF) from epididymal AT (VAT) of WT and ob/ob mice was isolated and analyzed by flow cytometry. (**A**) Representative flow cytometry dot plots and mean fluorescence intensity (MFI) of AT macrophages (ATMs) stained with bodipy. (**B**) Percentage of macrophages stained with bodipy; n = 10. (**C**) microscopy of SVF isolated from ob/ob VAT stained with antibodies against F4/80 (red) and bodipy (green); x20 (scale bar, 50 µm). (**D**) TEM of whole VAT of ob/ob mice; A, adipocyte; M, macrophage; arrows, lipid droplet; scale bar, 2 µm. (**E**) Gene expression measured by RT-PCR in macrophages isolated using CD11b antibody bound to magnetic beads; n = 5. All graphs are expressed as means ± SE. Statistical significance was determined by Student's t-test. ***P < 0.001, **P < 0.01, *P < 0.05.

GeRP-mediated LPL silencing decreases lipid uptake by ATMs

To test the hypothesis that LPL is required for lipid uptake by macrophages in AT, LPL was selectively depleted in ATMs of obese mice by intraperitoneal injections with GeRPs loaded with SCR or LPL siRNA (see protocol outline in **Figure 4.2A**). As previously described (**Chapter 3**), silencing was specific to visceral phagocytes, as no depletion of the target gene products was observed in livers of GeRP-treated mice (**Figure 4.2B**). Other studies we have performed showed no gene silencing with this technique in macrophages present in other tissues of the obese mice, including lung, pancreas, spleen, and muscle (**Chapter 3**). LPL protein levels in SVF isolated from epididymal AT of mice treated with LPL-GeRPs were also significantly reduced compared with mice treated with SCR-GeRPs (**Figure 4.2C**). Importantly, flow cytometry showed that silencing LPL in ATMs significantly decreased lipid accumulation in VAT macrophages (**Figure 4.2D**). Careful analysis of epididymal AT sections by TEM showed lipid droplets in macrophages containing GeRPs within AT. Treatment with LPL-GeRPs reduced the presence of these lipid droplets in ATM (**Figure 4.2E**). These results suggested that ATM LPL contributes to obesity-induced lipid uptake by macrophages in VAT.

Figure 4.2 - GeRP-mediated ATM LPL silencing decreases formation of lipid-laden macrophages in VAT of obese mice.

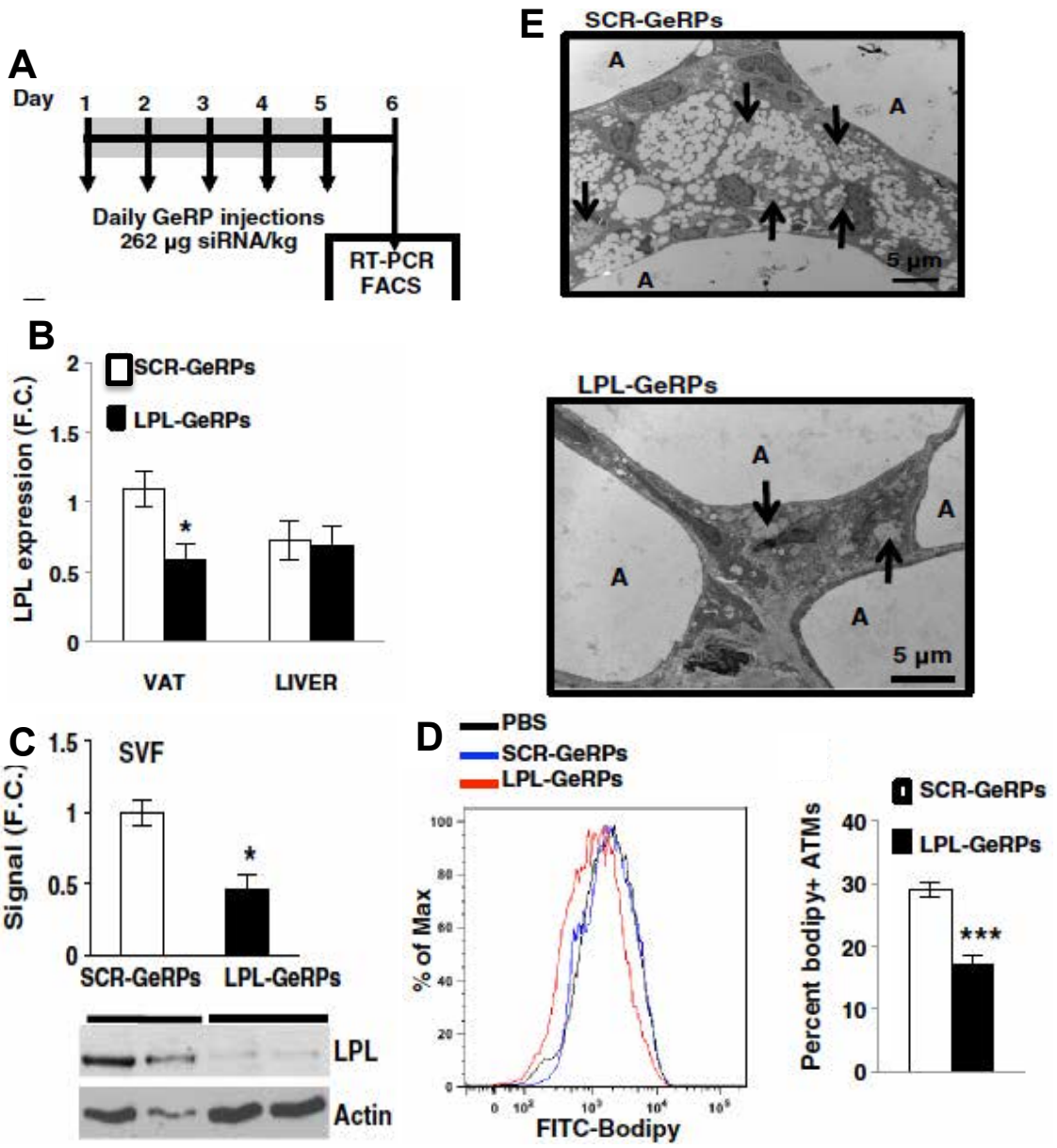

Figure 4.2 GeRP-mediated ATM LPL silencing decreases formation of lipid-laden macrophages in VAT of obese mice

(**A**) Outline of GeRP treatment given to mice. (**B**) mRNA expression of LPL in VAT and liver from mice treated with SCR- or LPL-GeRPs; n =14–15. (**C)** Representative LPL Western blot and densitometry using epididymal SVF lysates from mice treated with SCR- or LPL -GeRPs. Actin was used as a loading control. Statistical significance was determined by Student's t-test. ****P** <0.01, ***P** <0.05. (**D**) Percentage of macrophages expressing bodipy; **n** = 10. All graphs

are expressed as means ± SE. Statistical significance was determined by Student's **t**-test. ***$P < 0.001$, **$P < 0.01$, *$P < 0.05$. (**E**) TEM of whole VAT from ob/ob mice treated with SCR- or LPL-GeRPs; A, adipocyte; arrows, GeRPs. Scale bar, 5 μm.

LPL silencing in ATMs increases serum FFA levels

Treatment of ob/ob mice with LPL-GeRPs had no impact on serum TG levels, LDL/VLDL-cholesterol, and HDL-cholesterol (**Figure 4.3A and B**), consistent with a recent study showing that LPL depletion in the myeloid lineage has no effect on circulating TG and cholesterol levels (276). Therefore, steady-state circulating TG levels could be maintained in mice treated with LPL-GeRPs compared with SCR-GeRPs by the normal expression of LPL in other tissues. Although LPL silencing had no impact on serum TG and cholesterol levels, serum FFA levels were significantly increased following ATM LPL silencing (**Figure 4.3C**). One study suggested that ATMs can buffer local increases in lipid and suppress local adipocyte lipolysis, decreasing lipid levels in the circulation (268). In an effort to test whether LPL silencing in ATMs increased serum FFA levels through regulation of lipid release by adipocytes, we found that LPL depletion in ATMs had no effect on the expression of hormone-sensitive lipase (HSL) and adipose triglyceride lipase (ATGL), involved in lipolysis (**Figure 4.3D**).

LPL silencing in ATMs also resulted in a significant decrease of CD36 and diglyceride acyltransferase-2 (DGAT2) expression when measured in SVF cells isolated by fluorescence-activated cell sorting (FACS) on the basis of their FITC-GeRP signal. This was consistent with a decreased FFA uptake and esterification by ATMs following LPL silencing (**Figure 4.3E**). To confirm this hypothesis, we measured the percentage of foam cells in AT following fasting-induced lipolysis (**Figure 4.3F**). Consistent with the idea that ATMs take up FFA

released by adipocytes in fasting condition (268), in obese mice treated with PBS, fasting increased the percentage of bodipy+ ATMs (**Figure 4.3F**). Furthermore, flow cytometry analysis showed that the increase in bodipy+ ATMs under fasting condition was blocked following LPL silencing in ATMs (**Figure 4.3F**). Taken together, these results suggest that silencing LPL unexpectedly decreases the capacity of ATMs to take up the excess FFA released by adipocytes

Figure 4.3 - LPL silencing in ATMs increases plasma FFA

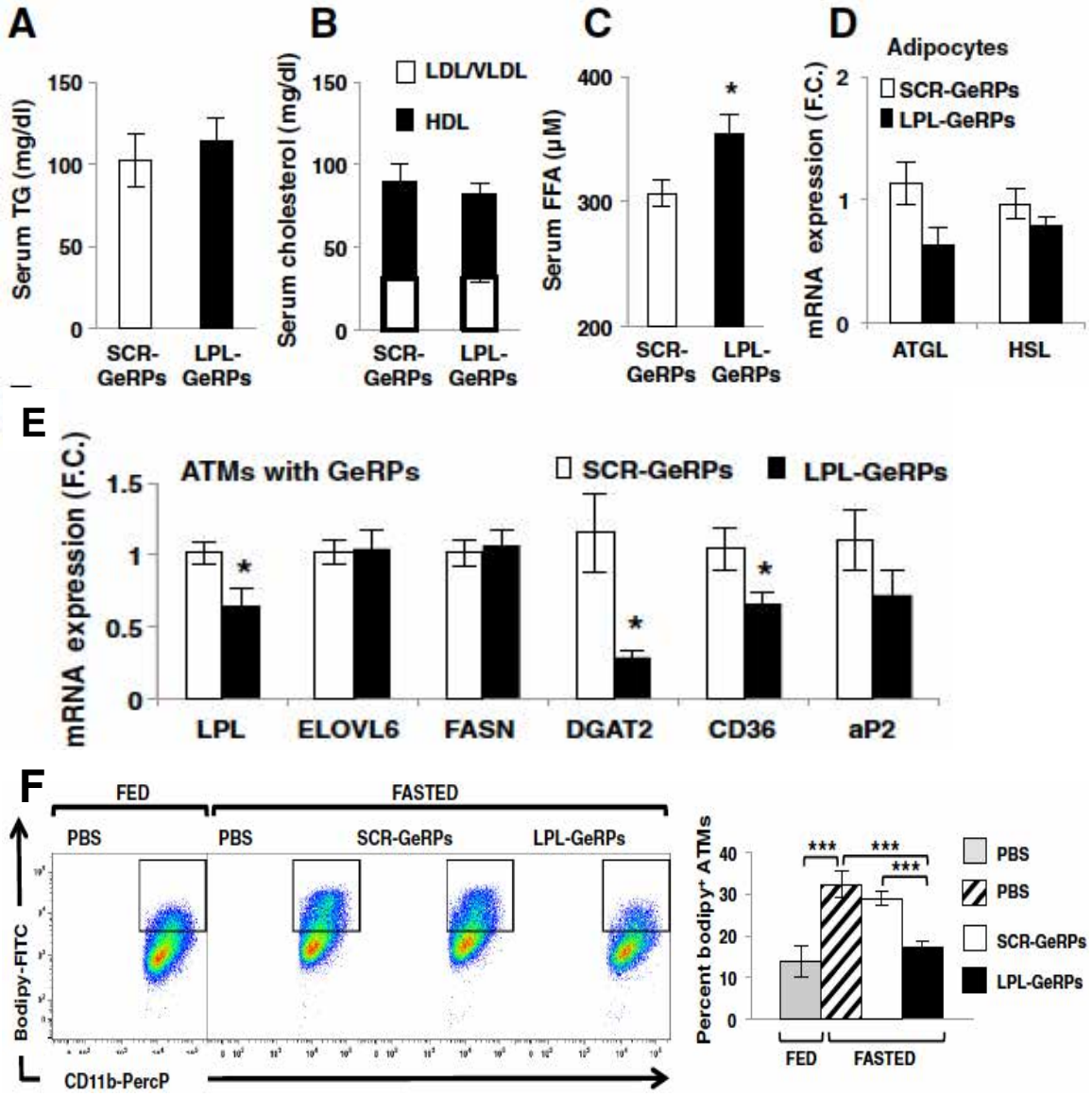

Figure 4.3 LPL silencing in ATMs increases plasma FFA

Serum triglyceride (TG; **A**) and LDL/VLDL and HDL cholesterol (**B**) in mice treated with scrambled SCR- or LPL-GeRPs; **n** = 10. (**C**) Serum FFA levels; **n** = 14-15. (**D**) ATGL and HSL expression in adipocytes isolated from ob/ob mice treated with SCR- or LPL-GeRPs; **n** = 14–15. (**E**) Gene expression measured by RT-PCR in ATMs containing GeRPs sorted by FACS; **n** = 5. (**F)** Representative dot-plot and percentage of ATMs expressing bodipy in fed and fasted states in VAT; **n** = 10. All graphs are expressed as means ± SE. Statistical significance was determined by Student's t-test. ***$P < 0.001$, *$P < 0.05$.

Silencing LPL in visceral ATMs exacerbates glucose intolerance in ob/ob mice

Increased serum FFA levels have been shown to positively regulate glucose production by liver (268, 277, 278). The expression of two gluconeogenic enzymes, phosphoenolpyruvate carboxykinase (PEPCK) and glucose-6-phosphatase (G6Pase), was significantly increased in livers from ob/ob mice treated with LPL-GeRPs compared with SCR-GeRPs (**Figure 4.4A**). To further assess hepatic glucose production, mice were challenged with the gluconeogenic precursor pyruvate (**Figure 4.4B**). Silencing LPL in visceral ATMs exacerbated pyruvate intolerance in mice treated with LPL- compared with SCR-GeRPs (**Figure 4.4B**). Given that increased hepatic glucose output often results in exacerbated systemic glucose tolerance, we performed glucose tolerance tests (GTT) in ob/ob mice treated with LPL-GeRPs or SCR-GeRPs (**Figure 4.4C**). Mice treated with LPL-GeRPs were significantly less glucose tolerant than mice treated with SCR-GeRPs (**Figure 4.4C**). This effect on glucose tolerance occurred independently of an effect on insulin tolerance, fasting glucose, or insulin levels, or islet morphology (data not shown). Interestingly, treatment of lean healthy mice with LPL-GeRPs had no significant effect on glucose tolerance or circulating FFA (**Figure 4.4D and E**).

Figure 4.4 - LPL silencing in ATMs exacerbates glucose intolerance in ob/ob mice.

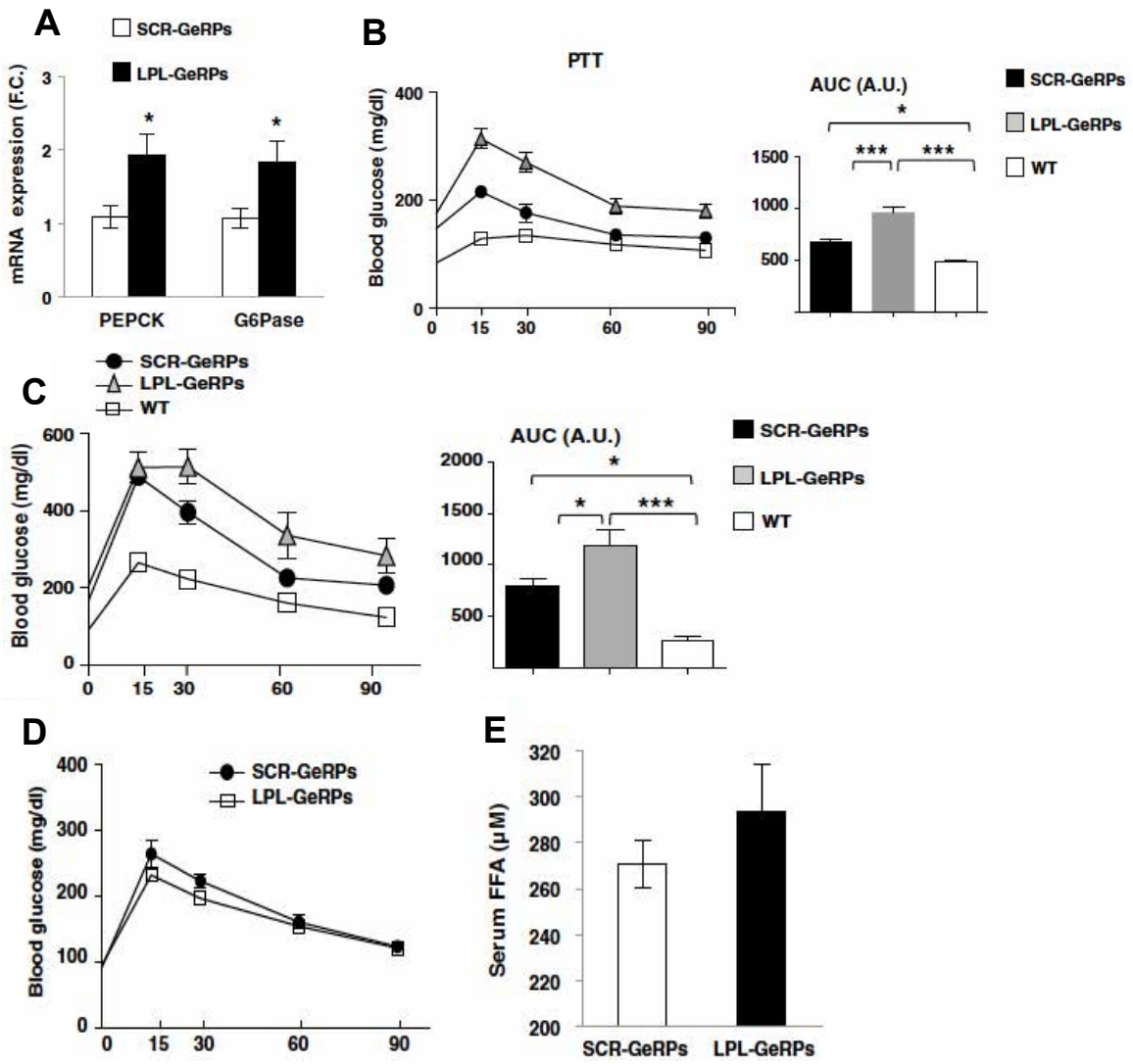

Figure 4.4 LPL silencing in ATMs exacerbates glucose intolerance in ob/ob mice

(**A**): PEPCK and G6Pase expression in liver of ob/ob mice treated with SCR- or LPL-GeRPs; n **=** 10. (**B**) Pyruvate tolerance test and area under the curve (AUC); n **=** 10. (**C**) Glucose tolerance tests (GTT) and AUC; n **=** 14-15, performed on mice fasted for 18 h. (**D**) GTT performed on 8-wk-old C57BL6 lean mice treated with SCR- or LPL-GeRPs; n **=** 5. (**E**) Serum FFA levels in lean mice treated with SCR- or LPL-GeRPs; n **=** 5. Results are means ± SE. Statistical significance was determined by t-test or ANOVA and Tukey's posttest. ***P < 0.001, *P **<** 0.05.

DISCUSSION

Most relevant literature describes ATMs as detrimental to whole body metabolism through secretion of inflammatory cytokines and other factors that may impair adipocyte function (32, 110, 111, 252). However, recent work has indicated a beneficial role of ATMs, for example in increasing adipose lipid storage (268). We therefore sought to investigate the importance of foam cell formation by ATMs. We were able to show that foam cells are present in the adipose tissue of mice, and their number increases with obesity (**Figure 4.1**). Interestingly, the lipid expression of LPL, which controls fatty acid uptake from the circulation into tissues (273, 274), was also significantly upregulated (**Figure 4.1**). Together, these data indicate that lipid uptake by macrophages in the VAT is increased with obesity and could be mediated by LPL.

To test our hypothesis of the role of LPL in foam cell formation, we specifically knocked down ATM LPL using GeRPs, and saw a marked decrease in the number of foam cells (**Figure 4.2**). This was re-enforced by microscopic analysis of VAT and a decrease in lipid-laden macrophages as determined by Bodipy+ staining of ATMs from SVF (**Figure 4.2**). Importantly, This finding is consistent with data showing that ATMs mostly accumulate lipids via activation of lipid uptake rather than de novo lipogenesis (134). Although lipid uptake by ATMs has been suggested to contribute to lipid storage in AT (4, 16), LPL deficiency in macrophages throughout the body did not regulate adiposity in mice fed a HFD (28). Similarly, we found that although serum FFA was increased, body weight

gain, epididymal fad pad weight, and adipocyte number and size were unchanged following ATM-specific LPL silencing over this 5 day period (**Figure 4.3**). A potential mechanism for this surprising effect may relate to studies suggesting that hydrolysis of TG by LPL releases ligands for PPARα/δ transcription factors known to drive the expression of lipogenic genes including DGAT2 and CD36, which are decreased by ATM LPL silencing (9, 32). However, LPL silencing decreased the expression of CD36 and DGAT2, while the expression of other PPAR target genes remained unchanged (**Figure 4.3**). Although additional work would be needed to unravel the mechanism whereby LPL silencing secondarily decreases CD36 and DGAT2 gene expression, previous studies (8, 22) as well as our work suggest that different transcription factors, coactivators, or repressors may be involved in the transcriptional regulation of lipogenic genes in macrophages deficient in LPL.

The impaired ability of ATMs to store lipids also resulted in increased levels of hepatic glucose output (**Figure 4.4**). GTT and PTT performed on obese mice that received LPL-GeRPs showed an inability of the liver to regulate systemic glucose levels, while lean mice treated with LPL-GeRPs were still able to respond within normal parameters compared to the controls (**Figure 4.4**). This confirmed the ability of AT in lean healthy mice to appropriately store lipids and the minimal role that ATMs play in this process in lean mice. All together, these data suggest ATMs may contribute to lipid storage in the AT of obese mice, thus preventing glucose intolerance induced by increased circulating FFA.

Chapter V: Activated Kupffer cells inhibit insulin sensitivity in obese mice

This chapter is derived from an article by the same name published in the

Federation of American Societies for Experimental Biology Journal.

Tencerova, M., Aouadi, M., Vangala, P., Nicoloro, S. M., Yawe, J. C., Cohen, J. L., Shen, Y., Garcia-Menendez, L., Pedersen, D. J., Gallagher-Dorval, K., Perugini, R. A., Gupta, O. T., and Czech, M. P. (2015) Activated Kupffer cells inhibit insulin sensitivity in obese mice. *FASEB J* **29**, 2959-2969

Author Contributions

- **Figure 5.1 and 5.2 NF-κB Knockdown and metabolic analyses –** Mice were maintained on a HFD by Michaela Tencerova. GeRP experiments were performed by Myriam Aouadi, Pranitha Vangala, Michaela Tencerova, Sarah Nicoloro, Jessica Cohen, Yuefei Shen, Lorena Garcia-Mendez and Joseph Yawe (GeRP team, Czech lab). Metabolic tests and AKT phosphorylation measurement were performed by Michaela Tencerova, Pranitha Vangala and Joseph Yawe.

SUMMARY

Obesity promotes insulin resistance associated with liver inflammation, elevated glucose production, and T2DM. Although insulin resistance is attenuated in genetic mouse models that suppress systemic inflammation, it is not clear whether local resident macrophages in liver, Kupffer cells (KCs), directly contribute to this syndrome. We addressed this question by selectively silencing the expression of the master regulator of inflammation, NF-κB, in KCs in obese mice. We used GeRPs that selectively silence gene expression in macrophages in vivo. Following intravenous injections, GeRPs containing siRNA against p65 of the NF-κB complex caused loss of NF-κB p65 expression in KCs without disrupting NF-κB in hepatocytes. Silencing of NF-κB expression in KCs in obese mice decreased cytokine secretion and improved insulin sensitivity and glucose tolerance. Thus, KCs are key contributors to hepatic insulin resistance in obesity and a potential therapeutic target for metabolic disease.

INTRODUCTION

Obesity impairs insulin responsiveness in the liver and is associated with the development of T2DM with severe comorbid conditions. Although hepatic lipid accumulation (77, 279), endoplasmic reticulum stress (280), and inflammation (281) have all been suggested as potential contributors to obesity induced insulin resistance, the relative causal roles of these factors are still unclear. For example, nonalcoholic fatty liver disease is a strong known risk

factor for insulin resistance and T2DM (282), but lipid accumulation in liver can be experimentally dissociated from insulin resistance under certain conditions (283), suggesting that other mechanisms are also involved. Kupffer cells are thought to be the major source of hepatic inflammation (284); however, their contribution to insulin resistance has not been directly tested because of the lack of technology to manipulate gene expression specifically in KCs. Here we used a new approach to ask whether these immune cells directly contribute to the development of insulin resistance associated with obesity.

To investigate the role of KC activation in obesity-induced insulin resistance, we developed a method to specifically silence gene expression in these hepatic macrophages *in vivo*. GeRPs loaded with an siRNA against a major regulator of inflammatory cytokine expression, NF-κB (191, 215), were delivered to KCs of obese mice by intravenous administration. Using this method, we demonstrate that silencing NF-k B selectively in KCs decreases liver inflammation and improves insulin sensitivity and glucose tolerance in obese mice.

MATERIALS AND METHODS

Animals and diet: Six-week-old male wild-type C57BL/6J (WT) and 5- and 7- to 8- week-old male B6.V-Lepob/J (ob/ob) mice were (Jackson Laboratory, Bar Harbor, ME, USA) maintained on a 12-hour light/dark cycle. Animals were given free access to food and water. C57BL/6J WT mice were fed a high-fat diet (HFD; 60%calories from lipids; D12492; Research Diets, New Brunswick, NJ, USA) for

14 or 24 weeks beginning at 6 weeks of age. All other mice were fed normal chow diet. All procedures were performed in accordance with protocols approved by the University of Massachusetts Institutional Animal Care and Use Committee.

GeRP administration by intravenous injection in vivo: GeRPs were prepared as previously described (**Chapter 3**). Seven- or 8-week-old genetically obese ob/ob mice were treated with 12.5 mg/kg GeRPs loaded with siRNA (247 **m**g/kg) and Endoporter (2.27 mg/kg). Seven-week-old ob/ob mice were used for 15-day treatment. They received 2 or 6 doses of fluorescently labeled GeRPs by intravenous injections over 5 or 15 days, respectively. In a model of diet-induced obesity, 6-week-old C57Bl/6J mice were fed a HFD for 14 or 24 weeks. They received 6 doses of fluorescently labeled GeRPs for 15 days by intravenous injections. siRNA sequences used are as follows: Scrambled (SCR) 5'-CAGUCGCGUUUGCGACUGGUU-3'; NF-κB/RelA 5'-GGAUUGAAGAGAAGCGCAAUU-3'

Isolation of KCs and hepatocytes: The liver of anesthetized mice was first perfused with calcium-free Hanks balanced salt solution, followed by collagenase digestion. After digestion, the hepatocytes were released by dissociation from the lobes and underwent several steps of filtration with calcium plus Hanks balanced salt solution and centrifugation at 50 g for 3 minutes at room temperature. The supernatant from the first centrifugation of hepatocytes was loaded on a Percoll

gradient (25%and 50%) and centrifuged for 30minutes, at 2300 rpm, at 4°C. The interphase ring with KCs was collected and washed 2 times with PBS. The cells were cultured overnight. The following day, primary cells were used for subsequent analyses.

Western blot: Cell lysates were separated on an 8% SDS-PAGE polyacrylamide gel, transferred to a PVDF membrane, and incubated overnight at 4°C with primary antibody against p65 (RelA), pSer473 protein kinase B (PKB/AKT), AKT, or actin as a loading control (Cell Signaling, Danvers, MA, USA). Anti-rabbit or anti-mouse IgG antibody conjugated with horseradish peroxidase was used as a secondary antibody. The levels of particular proteins were determined by chemiluminescence (Pierce, Rockford, IL, USA).

Isolation of RNA and real-time PCR: As previously described (**Chapter 2**). Primer sequences used are as follows: 36B4 (5'-TCCAGGCTTTGGGCATCA-3', 5'-CTTTATCAGCTGCACATCACTCAGA-3'); Clec4f (5'-GAGGCCGAGCTGAACAGAG-3', 5'-TGTGAAGCCACCACAAAAAGAG-3'); NF-κB/RelA (5'-ACTGCCGGGATGGCTACTAT-3', 5'-TCTGGATTCGCTGGCTAATGG-3'); TNF-a (5'-CCCTCACACTCAGATCATCTTCT-3', 5'-GCTACGACGTGGGCTACAG-3'); IL-1b (5'-GCAACTGTTCCTGAACTCAACT-3', 5'-ATCTTTTGGGGTCCGTCAACT-3'); IL-6 (5'-TAGTCCTTCCTACCCCAATTTCC-3', 5'-

TTGGTCCTTAGCCACTCCTTC-3'); PEPCK (5'-CTGCATAACGGTCTGGACTTC-3', 5'-CAGCAACTGCCCGTACTCC-3'); G6Pase (5'-GTTGAACCAGTCTCCGACCA-3', 5'-CGACTCGCTATCTCCAAGTGA-3')

Metabolic analyses:

Glucose and pyruvate tolerance tests (GTTs and PTTs) were performed after GeRP treatment (24 hours after last injection) and 6-hour food withdrawal. A dose of 1 g/kg glucose or pyruvate was intraperitoneally injected, and blood glucose levels were measured by glucometer at defined time points from the tail vein. The following day, the mice were killed to harvest tissues for subsequent analyses. Insulin-stimulated phosphorylation of AKT in vivo Insulin stimulated phosphorylation of AKT was performed after GeRP treatment (24 hours after last injection) and 4 hours food withdrawal. A dose of 0.75 U/kg insulin was intraperitoneally injected, and then adipose tissue and liver samples were harvested from GeRP-treated mice for subsequent analyses 15minutes after injection.

Statistical analyses:

The data were analyzed using GraphPad 5a software (GraphPad Software, La Jolla, CA, USA). The statistical significance of differences among groups was analyzed using Student t test or ANOVA as appropriate. Data were presented as

means ± SEM. $P < 0.05$ was considered statistically significant.

RESULTS

Specific silencing of NF-κB expression in KCs improves insulin sensitivity in genetic obesity mice

To test whether we could specifically target KCs for genetic knockdown using GeRPs, 8 week old ob/ob mice were injected with either SCR- or NF-κB-GeRPs for 5 days, after which KCs were isolated (see protocol scheme in **Figure 5.1A)**. RT-PCR analysis revealed almost a 50% knockdown of NF-κB in animals that received NF-κB-GeRPs compared to the SCR group (**Figure 5.1B**). Importantly, there was no knockdown of NF-κB observed in EPI AT, suggesting specific targeting of liver KCs (**Figure 5.1C**). Based on the ability of the intravenously delivered GeRPs to specifically silence genes in KCs but not in other cells or other organs, and without toxic effects (233), we assessed the effect of attenuating inflammation in KCs on insulin resistance in obese mice. Seven-week-old ob/ob mice were treated with SCR- or NF-κB-GeRPs for 5 or 15 days, and GTTs were performed at the end of the treatment (see protocol scheme in **Figure 5.1A**). Although NF-κB silencing in KCs showed no effect on glucose tolerance at day 5, we observed a significant improvement at day 16 (**Figure 5.1D**). This was accompanied by a decrease in inflammatory gene expression (**Figure 5.1E**). We also observed a decrease in basal fasting glycemia in mice after the 15-day treatment compared with 5-day treatment.

Although the length of the treatment itself could cause this, it could also be explained by the variability in basal glycemia often observed following a short 6-hour fast.

Consistent with the hypothesis that silencing NF-κB in KCs improves insulin sensitivity, we observed a significant decrease in the expression of enzymes involved in hepatic glucose production, including phosphoenolpyruvate carboxykinase and glucose 6-phosphatase expression in mice treated with NF-κB -GeRPs for compared with SCR-GeRPs for 15 days (**Figure 5.1F**). Consistently, biochemical studies showed an increased insulin-stimulated AKT phosphorylation in liver of mice treated with NF-κB -GeRPs at day 16 (**Figure 5.1G**). Importantly, silencing NF-κB specifically in KCs had no effect on insulin-stimulated AKT activation in adipose tissue (**Figure 5.1G**).

Figure 5.1 – Kupffer cell inflammation drives hepatic glucose output in ob/ob mice

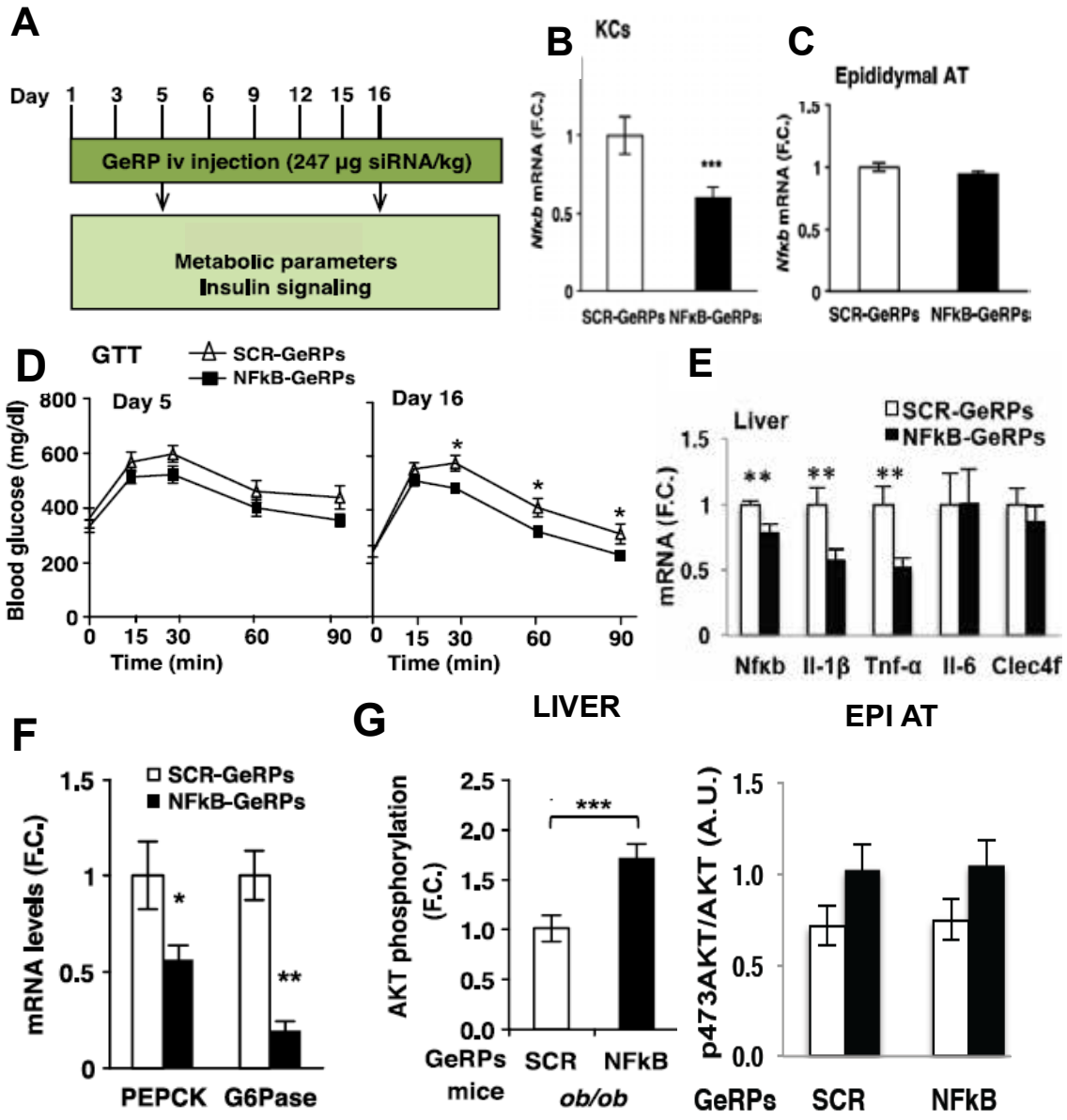

Figure 5.1 Kupffer cell activation drives hepatic glucose output in ob/ob mice

(**A**) Protocol of 5- and 15-day GeRP treatment. 8-week-old mice were used for the 5-day treatment and 7-week-old mice were used for the 15-day treatment. mRNA of NF-κB in (**B**) KCs and (**C**) EPI AT from mice treated with either SCR-GeRPs or NF-κB -GeRPs for 15 days (**n** = 11**–**13). (**D**) GTT (1 g/kg) were performed on mice treated with SCR- or NF-κB-GeRPs after withholding food for 6 hours. (**E**) mRNA levels of inflammatory genes in the liver of ob/ob mice treated

15 days with SCR-GeRPs and NF-κB-GeRPs (n= 11-13). (**F**) mRNA levels of gluconeogenic genes in liver from mice treated for 15 days with SCR- or NF-κB-GeRPs (n = 5). (**G**) F.C. of AKT phosphorylation by insulin in liver and EPI AT measured by densitometry of pSer473-AKT normalized to total AKT. For EPI AT, white bars represent saline, black bars represent insulin (ob/ob, n = 9–10). Results are presented as mean of fold change (F.C.) normalized to SCR-GeRPs–treated mice 6 SEM. *P < 0.05; **P < 0.01. The statistical significance was analyzed by t-test or ANOVA followed by Tukey posttest.

Specific silencing of NF-κB expression in KCs improves insulin sensitivity in diet-induced obesity

We next studied the effect of NF-κB-GeRPs in a model of diet-induced obesity, which also shows increased liver inflammation (**Figure 5.2A**). Six-week-old male C57Bl/6J mice were fed an HFD for 14 or 24 weeks and treated with SCR- or NF-κB-GeRPs for 15 days (see protocol scheme in **Figure 5.1A**) to study the effect of NF-κB silencing on liver metabolism at different stages of lipid accumulation in the liver. In the 24-week HFD-fed mouse model silencing of NF-κB in KCs improved fasting hyperglycemia, glucose tolerance, and lowered hepatic glucose production from pyruvate as measured by PTT (**Figure 5.2B and C**). Importantly, NF-κB silencing did not affect body weight (**Figure 5.2D**). Consistent with this concept, mice fed a HFD for 14 weeks with NF-κB**–** depleted KCs also exhibited improved glucose tolerance measured by GTT and enhanced insulin-stimulated AKT phosphorylation in the liver (**Figure 5.2E and F**).

Figure 5.2 – HFD feeding activates Kupffer cells and induces hepatic glucose production

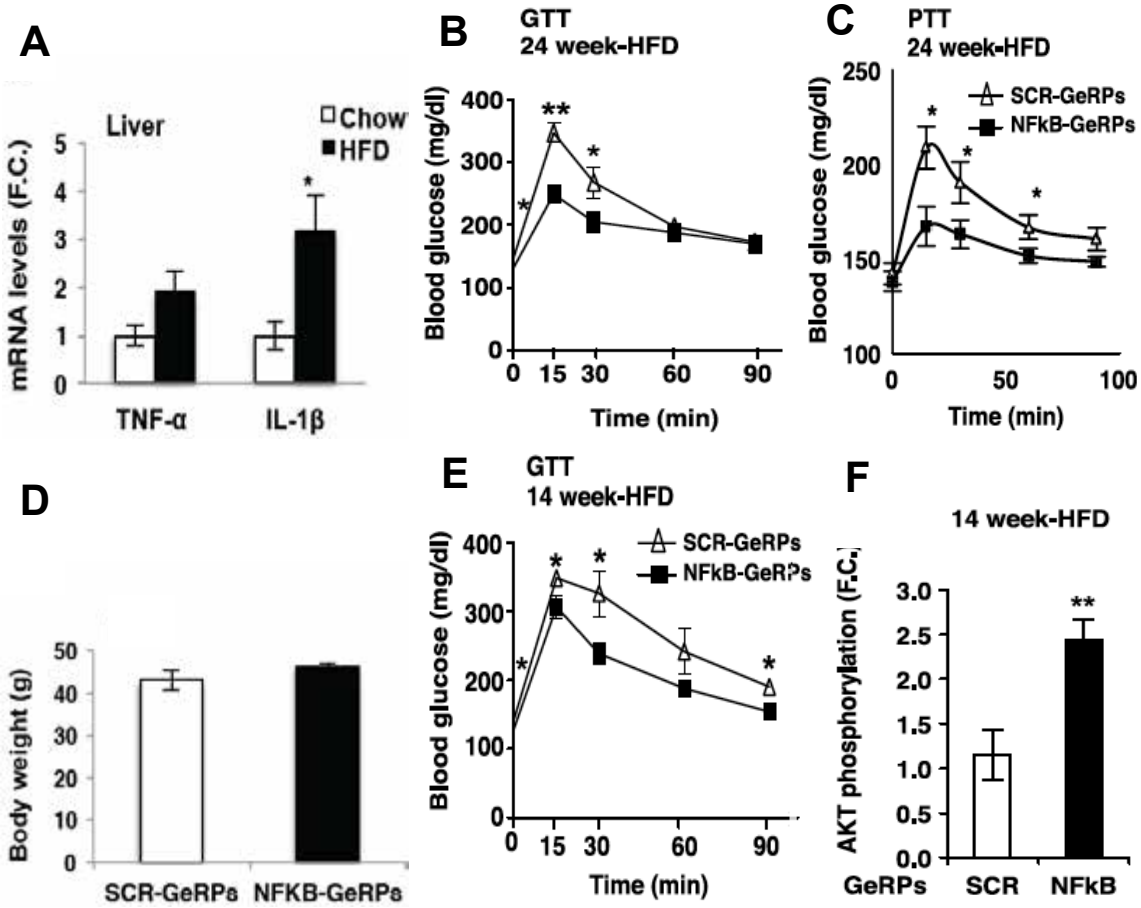

Figure 5.2 HFD feeding activates Kupffer cells and incudes hepatic glucose production

(A) Expression of inflammation genes in the liver of mice fed a chow or HFD for 24 weeks (n=5). (**B**) GTT (1 g/kg) was performed in mice fed 24 weeks of an HFD and treated with SCR- or NF-κB-GeRPs (**n** = 11**–**14). **(C**) PTT (1 g/kg) was performed in mice fed a 24-week HFD treated with SCR- or NF-κB-GeRPs after withholding food for 6 hours (**n** = 5). **(D)** Body weight of 24 week-HFD after a 15-day treatment with SCR- or NFkB-GeRPs (n=5). (**E**) GTT (1 g/kg) was performed in mice fed a 14-week HFD and treated with SCR- or NF-κB-GeRPs (n = 11**–**14). (**F**) F.C. of AKT phosphorylation by insulin measured by densitometry of pSer473-AKT normalized to total AKT (n = 9**–**10).

DISCUSSION

In the present study, we demonstrated that silencing NF-κB specifically in KCs improved insulin sensitivity independent in diet or genetically induced obesity. We used the GeRP technology, developed in our laboratory, to deliver siRNA and silence genes specifically in KCs without affecting nonimmune cells in the liver and cells in other organs in obese mice. Although various systems have been developed to deliver siRNA to the liver, none of these strategies has demonstrated the ability to specifically target KCs in liver without affecting hepatocytes. Previous studies showing siRNA delivery to KCs in vivo used carriers that were also internalized by non-phagocytic cells or phagocytic cells in organs other than liver (285-290). In the present study, we accomplished specific delivery of GSs to KCs in obese mice by taking advantage of the micrometer-size and Dectin 1 receptor-mediated recognition of GS (230). The treatment protocol developed for the subsequent experiments requires 15 days, with the administration of an injection every 2 days and analysis 24 hrs after the final injection. This protocol proved to be more effective in terms of both knockdown and improving glucose tolerance compared to a 5-day protocol in ob/ob mice (**Figure 5.1**).

In our study, we demonstrated that GeRP-mediated silencing of NF-κB in KCs decreased the expression of NF-κB (**Figure 5.1**). Several studies have investigated the role of KCs in insulin resistance in obese mice. These studies used systemic delivery of anti-inflammatory drugs, bone marrow transplantation,

or transgenic mice deficient in inflammatory genes, which had inhibitory effects on insulin resistance (215, 291-293). However, a direct role for inflammation could at most only be implied due to the nature of these approaches. Our data directly demonstrates that silencing NF-κB in KCs improves insulin sensitivity in obese mice (**Figure 5.1 and 2**). Indeed multiple studies have reported a beneficial effect of systemic inhibition of NF-κB or global knockout of its upstream activator on liver inflammation and steatosis (191, 291, 294, 295). Silencing NF-κB for 15 days resulted in a significant improvement of insulin sensitivity, measured by GTT, and increased AKT phosphorylation in the liver in ob/ob and HFD mice (**Figure 5.2**). Importantly, GeRPs do not have a toxic effect on the liver as determined by liver enzyme measurements (233). Although additional work would be needed to unravel the cross talk between KCs and parenchymal cells and its impact on liver diseases, the GeRP technology provides a unique tool for such studies.

Together, these data demonstrate that partial silencing of NF-κB specifically in KCs improves insulin sensitivity in diet or genetically induced obesity under our experimental conditions. Thus, KC activation and consequent liver inflammation play causal roles in the development of insulin resistance in mouse models of obesity.

CHAPTER VI: Final summary, conclusions and future directions

Macrophage infiltration into adipose tissue and activation of liver Kupffer cells are believed to play important roles in the pathology of obesity associated T2DM. However, there is lack of direct evidence to support ATM and KC involvement in the development of insulin resistance and dysregulated glucose metabolism. Our lab has therefore been interested in elucidating the role of resident tissue macrophages in the regulation of insulin signaling, the effect on energy homeostasis, and how the functions of adipose tissue and liver are altered. The work reported in this manuscript was aimed at answering three major questions:

1. **What is the source of macrophage accumulation in obese adipose tissue?**
2. **What is the effect of ATM-specific gene knockdown on the development of insulin resistance in obesity?**
3. **Does changing the activation state of Kupffer cells affect systemic insulin sensitivity in obesity?**

To address these questions, we employed a number of in vitro and in vivo techniques that allowed us to determine that (i) macrophages proliferate locally in VAT of genetic and diet-induced models of obesity and MCP-1 plays a direct role in promoting proliferation (Chapter2); (ii) GeRP-mediated knockdown of ATM-derived OPN improves glucose disposal and insulin signaling (Chapter 3); (iii) GeRP-mediated knockdown of LPL in ATMs results in impaired lipid buffering, increase in hepatic glucose output and decrease in hepatic insulin sensitivity

(Chapter 4); (iv) GeRP-mediated depletion of NF-κB in Kupffer cells decreases hepatic inflammation and improves insulin signaling in the liver (Chapter 5). Below is a schematic representation of these results, followed by discussions of my interpretations, potential pitfalls and future directions for the studies presented in the chapters above.

Figure 6.1 – Macrophages are regulators of whole body metabolism

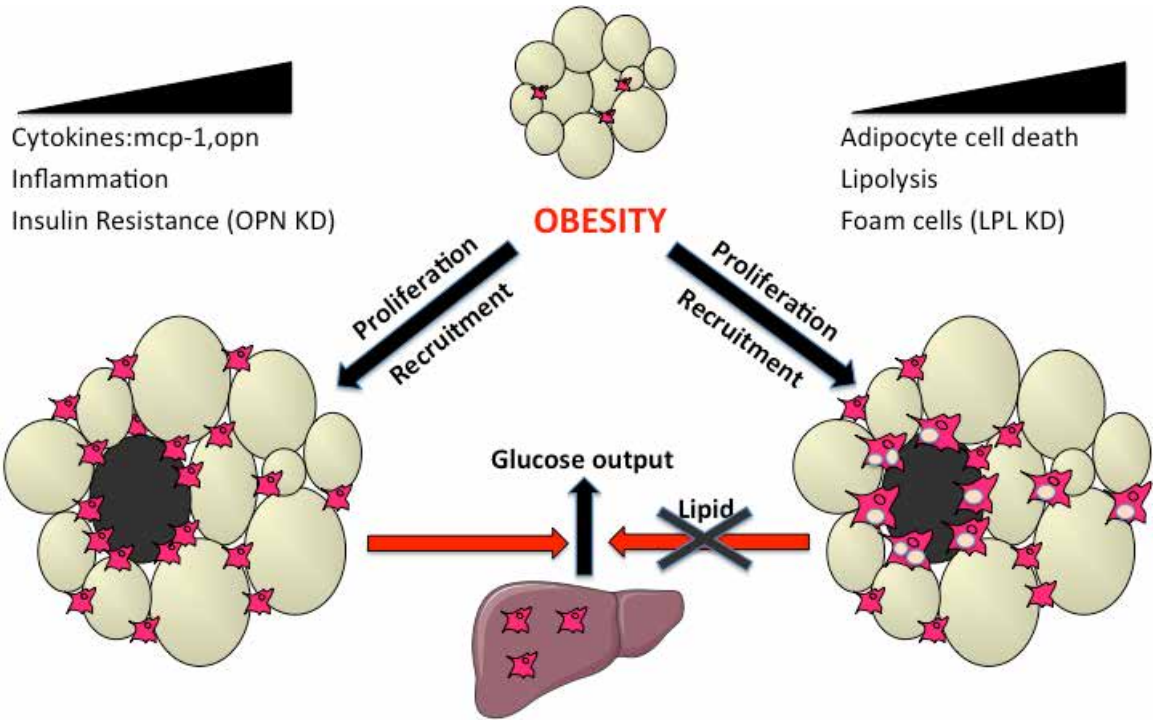

Figure 6.1 Macrophages are regulators of whole body metabolism
The data in this thesis show that the initial accumulation of macrophages in AT might be an adaptive response to AT remodeling and lipid spillover. However, with increasing accumulation, a chronic low-grade inflammation develops, exerting detrimental effects that lead to the development of insulin resistance. In the liver, activated Kupffer cells are responsible for hepatic inflammation, promoting hepatic dysfunction and insulin resistance.

Local macrophage proliferation in adipose tissue of obese mice

In the studies detailed in Chapter 2, we hypothesized that macrophages in adipose tissue could proliferate in the context of obesity. We confirmed by FACS analysis that the ATM population is indeed increased in both genetic and diet induced models of obesity, and this increase was specific to the visceral adipose depot (**Figure 2.1 and 2.2**). We further demonstrated that this increase was in part due to proliferation of resident macrophages by assessing Ki67 staining (**Figure 2.1 and 2.2**). However, the most important finding was the fact that macrophages were still able to proliferate without monocyte recruitment from the circulation, as demonstrated by depleting the circulating monocyte pool and measuring EdU incorporation into macrophage nuclei (**Figure 2.3**). Based on previous literature reports on M1 versus M2 macrophages in obesity, we expected the rate of proliferation to be higher in the M1 inflammatory CD11C+ cells versus the M2 anti-inflammatory CD11C- macrophages. However, we were surprised to observe no significant difference in proliferation rates between the two subtypes (data not shown). One could argue that the expansion of one subtype population over the other may be regulated by recruitment rather than proliferation. Perhaps recruited monocytes also proliferate, which may favor inflammatory over anti-inflammatory expansion (248). This would be an interesting area for follow up studies, especially to understand whether resident proliferating versus recruited proliferating, carry out specific roles within the adipose tissue.

By microscopy we determined that proliferating macrophages were primarily localized to crown-like structures (**Figure 2.3**). This could be an important indicator of the potential significance of locally proliferating macrophages. Adipose tissue is very plastic and therefore requires an efficient mechanism of clearing cellular debris as it undergoes rapid remodeling (55). During obesity-associated adipose expansion, necrotic adipocytes must be cleared to avoid local and potentially systemic toxicity. Therefore, resident macrophages may act as sentries that are stimulated to proliferate by dying adipocytes and thereby acting as a local response system. The localization of proliferating ATMs around individual cells also suggests a spatiotemporal specificity to promoting proliferation rather than relying on a system of mass recruitment, thereby conserving resources. It also implies that macrophage recruitment is a secondary response that is triggered by other secreted factors or the exacerbation of adipocyte death.

Finally, both MCP-1 and OPN were significantly increased in adipose tissue, although only MCP-1 stimulated macrophage proliferation in tissue explants from ob/ob mice (**Figure 2.4**). These results suggested that MCP-1, if not the proliferative signal, is at least important for promoting adipose tissue macrophage proliferation. One drawback of this approach, however, is the complex nature of the adipose tissue, as many different cell types are present. It is possible that MCP-1 triggers a paracrine response emanating from non-adipocytes within the AT, which subsequently triggers the proliferative response. However our data do

not support this hypothesis, as we were not able to detect increased in the expression of other important stimulators of proliferation such as M-CSF and IL-4 (**Figure 2.4**). Another aspect that requires careful consideration follows from the previous discussion about localization of this activity to crown-like structures. The effect of explant stimulation on proliferation might be biologically distinct from the metabolic response observed *in vivo*. Since we cannot isolate individual crown-like structures or necrotic adipocytes, we are unable to specifically recreate the *in vivo* phenomenon. However, such a reductionist approach is likely to also introduce confounding factors, since the adipose environment does involve the synergistic interaction of different cell types. Therefore, while imperfect, explant techniques still serve as the best technique until technological advancements allow for a more rigorous approach.

In summary, we demonstrated that local proliferation plays a significant role in obesity-induced macrophage accumulation in visceral adipose tissue independent of monocyte recruitment. Although some of the techniques employed are not transferrable to human studies, determining whether this observation is conserved in humans would help further our understanding of obesity associated inflammation. Additionally, this could impact future research involving the blockade of macrophage infiltration, emphasizing a dual approach that also takes into account proliferation.

ATM-specific gene knockdown affects whole body metabolism

In Chapters 3 and 4, we utilized a novel approach involving GeRPs, a tool developed by our laboratory, to specifically downregulate ATM gene expression. We first determined the biodistribution of GeRPs injected i.p. into obese mice, since we had previously observed that lean animals exhibited a systemic distribution (228, 230). Surprisingly, we found that in obese mice, GeRPs were localized to the epididymal adipose tissue (**Figure 3.1**). Upon sorting cells from this depot, we confirmed that GeRPs were specifically taken up by macrophages (**Figure 3.2**). Considering the obesity-induced accumulation of macrophages in VAT compared to other tissue types and fat depots, this specificity suggests that GeRPs localize to areas of inflammation or macrophage concentration. This property makes GeRPs uniquely suited for the targeting of macrophages, and particularly ATMs in the case of obesity-induced inflammation of adipose tissue. It is still unclear whether GeRPs are taken up by resident macrophages, or taken up first by circulating monocytes that subsequently infiltrate the adipose tissue. However, the latter is the most likely scenario given the route of administration. One way to answer this question would involve using the clodronate liposomes as employed in chapter 2, then injecting mice with GeRPs to determine whether they are still phagocytosed by ATMs.

OPN was selected as one of the target genes for GeRP-mediated silencing because its expression in VAT positively correlates with obesity in humans and rodents (209-211). We also confirmed this result by analyzing GeneChip® data in

our database of human and mouse adipose tissue samples (data not shown), and by measuring Opn gene expression in ob/ob mice (**Figure 3.3**). OPN-GeRP administration resulted in a 50% knockdown of OPN expression in adipose tissue and about a 90% knockdown in sorted macrophages (**Figure 3.4**). Importantly, a reduction in OPN protein was also observed. These data, together with the lack of significant changes in the expression of other macrophage genes, or changes in liver OPN expression, gave us confidence in the specificity of our knockdown (**Figure 3.4**). Knockdown resulted in a significant improvement in both glucose and insulin tolerance compared to mice that received SCR-GeRPs, without changes in weight gain or insulin secretion (**Figure 3.5**). Because OPN is a secreted protein that circulates at high concentrations, we determined whether knockdown in ATMs had altered circulating levels. This would perhaps indicate that serum OPN levels were regulating hepatic glucose output. However, there was no change in serum OPN concentrations after knockdown (**Figure 3.5**). This implies that OPN acts locally on adipose tissue to promote insulin resistance.

Indeed comparing AKT phosphorylation on serine 473 in adipose, muscle and liver tissues of mice that were treated with OPN-GeRPs revealed an increase in insulin signaling only in the adipose tissue (**Figure 3.6**). These data prompted further analysis of the adipose tissue, particularly looking at the expression of key adipocyte genes involved in adipogenesis and lipogenesis i.e., PPARγ, FASN, GLUT4, SCD1, Adiponectin, CPT1b and SREBP1c. I found that although there was a general trend toward an increase, only PPARγ and FASN

were significantly upregulated in adipocytes following OPN knockdown in ATMs (**Figure 3.6**). This suggested that depleting OPN was perhaps improving adipocyte dysfunction by promoting adipogenesis and lipogenesis. I tested this hypothesis by comparing fat pads taken from mice treated with SCR-GeRPs versus OPN-GeRPs, measuring mass, adipocyte size and adipocyte number. However, there were no differences observed in any of these parameters (data not shown). Functional assays using radiolabeled glucose to determine rates of glucose uptake or incorporation into triglycerides might provide more information moving forward.

One interesting observation after OPN knockdown was the lack of a significant effect on inflammatory gene expression in adipose tissue. Some pro-inflammatory genes trended toward a decrease while some anti-inflammatory genes trended toward an increase (**Figure 3.4**). Perhaps a longer treatment protocol would result in more pronounced and significant differences. Additionally, beta glucans themselves have shown glucose lowering effects in T2DM when administered orally, though the underlying mechanisms are not well understood (296). However, most studies have focused on oral administration of beta glucans. Liu *et al.* found oat beta glucan to have anti-inflammatory effects in ulcerative colitis by suppression of pro-inflammatory cytokine expression (297). Thus in our model the glucan shells might exert similar effects, although the observed improvement in glucose metabolism likely stems from OPN knockdown. As adipose inflammation is not significantly changed, OPN itself

must be interacting with adipocytes either indirectly or via a receptor. Indeed, OPN reportedly binds surface integrins and the CD44 receptor, causing downstream effects including activation of inflammatory pathways, decreased insulin stimulated glucose uptake and reduced adipocyte differentiation (298). Identifying an OPN receptor in our model would create a better understanding of how it affects adipocyte biology and the beneficial effects observed depletion of OPN.

LPL was the second ATM gene that was targeted using the GeRP technology, because of its role in foam cell formation (275, 276). Thus we assessed the effect of blocking foam cell formation in adipose tissue on systemic metabolic parameters. First, we confirmed the presence of foam cells in VAT of obese ob/ob mice by FACS analysis, immunofluorescence microscopy and transmission electron microscopy (TEM) (**Figure 4.1**). In addition, measurement of a number of lipid processing genes revealed that LPL was significantly upregulated in ATMs of obese mice compared to wild type controls (**Figure 4.1**). Using LPL-GeRPs via i.p. injection, foam cells were depleted. Using this method, ATMs were specifically targeted, resulting in reduced foam cell formation as determined by TEM and lipid staining (**Figure 4.2**). This ATM-specific knockdown also resulted in increased circulating FFA without affecting TAG or cholesterol levels. CD36 and DGAT2 expression were also decreased, implying a decrease in FFA uptake and TAG formation, similar to what was observed in a macrophage specific LPL KO model (**Figure 4.3**) (276). Foam cell formation was

also observed in fasted mice, likely because fasting results in lipid mobilization via TAG lipolysis and secretion of FFA. The decrease in foam cell formation in fasted LPL-GeRP treated animals confirms the role of ATMs in lipid buffering in adipose tissue (**Figure 4.3**).

The effect of LPL knockdown in ATMs on systemic glucose levels and hepatic gluconeogenic enzymes highlights the significance of adipose tissue in regulating glucose metabolism. Obese mice that were treated with LPL-GeRPs showed exacerbated glucose and pyruvate tolerance, as well as increased expression of the gluconeogenic enzymes PEPCK and G6Pase (**Figure 4.4**). Indeed a recent study by Perry *et al.* has linked increased hepatic glucose output to an increase in circulating FFA from adipose tissue, resulting from adipose tissue inflammation. Increased FFA flux to the liver results in increased hepatic acetyl CoA, which activates pyruvate carboxylase activity and thus drives glucose production (87).

In summary, the work detailed in Chapters 3 and 4 describes a method of reprogramming macrophages in the adipose tissue of obese mice. These methods reprogrammed ATMs via gene silencing to either improve metabolic homeostasis or exacerbate its dysregulation. Thus we have shown the advantage of GeRPs in specifically targeting ATMs, and more importantly the significance of ATMs in regulating whole body metabolism.

Kupffer cell activation promotes insulin resistance

In Chapter 5 we sought to apply the GeRP technology in a different manner by targeting hepatic Kupffer cells. Instead of the i.p. route used for ATM targeting, we used intravenous injections to deliver GeRPs to the liver. Indeed biodistribution studies of radiolabeled GeRPs confirmed that most GeRPs administered in this fashion were specifically delivered to the livers of ob/ob mice (233). We selected NF-κB as our target gene due to its role in macrophage activation as observed by cytokine production, and insulin resistance as determined by metabolic and molecular analysis (191, 215). We observed that NF-κB knockdown specifically in KCs, did not affect gene expression in VAT, and was accompanied by reduced expression of inflammatory cytokines such as IL-1β and TNFα (**Figure 5.1**). The improved hepatic insulin signaling and decrease in gluconeogenic enzyme expression following NF-κB knockdown suggest that Kupffer cell activation is responsible for stimulating hepatic glucose output in obese mice (**Figure 5.1**). Further studies will measure the protein levels and activity of these enzymes as well.

This work was replicated using a high fat diet model of obesity. Mice were placed on a 60% HFD for 24 weeks, and RT-PCR analysis of inflammatory genes revealed an increase in hepatic inflammatory gene expression, similar as others have shown (**Figure 5.2**). Therefore, we treated mice with NF-κB-GeRPs and assessed changes in metabolic parameters and hepatic insulin signaling. As with the ob/ob mice, a significant improvement in glucose tolerance as well as

reduced pyruvate conversion to glucose was observed. The improvement in glucose tolerance was observed as early as 14 weeks on HFD, a time point at which increased AKT phosphorylation, which is indicative of improved insulin signaling, was also observed (**Figure 5.2**). Similar to OPN knockdown in ATMs, NF-κB knockdown in KCs improved insulin signaling without affecting body weight (**Figure 5.2**). This is important because weight loss is an important factor in improving insulin sensitivity in humans. However, many are incapable of adopting long lasting lifestyle changes that prevent regaining weight. This treatment modality would be a promising avenue to explore in terms of developing therapies for obese human patients. In summary, GeRP technology was used to reprogram or “deactivate” liver Kupffer cells, thus reducing hepatic inflammation and improving hepatic insulin signaling.

Overall, this thesis illustrates the complex role of macrophages in metabolic tissues in obesity and metabolic disease. Using gene targeting metjods we have discovered that tissue specific macrophages play both pro and anti-inflammatory roles and can improve or worsen metabolic health depending on the genes expressed within. Further studies could be geared toward applying GeRP technology to further elucidate the role of macrophages in T2DM, as well as other clinical indications, without creating mutant strains. Naturally, such advancements would also facilitate the development of more effective therapies. It is also important to note that although our work shows that macrophages can be reprogrammed to affect changes in metabolism, there might be ways to affect

changes in the immune system, particularly the innate immune response. Macrophage research continues to be an active area of interest, and with the addition of GeRP technology to the tool kit we come one step further to better understanding the sum of their functions.

Bibliography

1. Kulkarni, R. N. (2004) The islet beta-cell. *Int J Biochem Cell Biol* **36**, 365-371
2. Hou, J. C., Min, L., and Pessin, J. E. (2009) Insulin granule biogenesis, trafficking and exocytosis. *Vitam Horm* **80**, 473-506
3. Dodson, G., and Steiner, D. (1998) The role of assembly in insulin's biosynthesis. *Curr Opin Struct Biol* **8**, 189-194
4. Daniel, S., Noda, M., Straub, S. G., and Sharp, G. W. (1999) Identification of the docked granule pool responsible for the first phase of glucose-stimulated insulin secretion. *Diabetes* **48**, 1686-1690
5. Straub, S. G., and Sharp, G. W. (2002) Glucose-stimulated signaling pathways in biphasic insulin secretion. *Diabetes Metab Res Rev* **18**, 451-463
6. Belfiore, A., Frasca, F., Pandini, G., Sciacca, L., and Vigneri, R. (2009) Insulin receptor isoforms and insulin receptor/insulin-like growth factor receptor hybrids in physiology and disease. *Endocr Rev* **30**, 586-623
7. Frasca, F., Pandini, G., Scalia, P., Sciacca, L., Mineo, R., Costantino, A., Goldfine, I. D., Belfiore, A., and Vigneri, R. (1999) Insulin receptor isoform A, a newly recognized, high-affinity insulin-like growth factor II receptor in fetal and cancer cells. *Mol Cell Biol* **19**, 3278-3288
8. Boucher, J., Kleinridders, A., and Kahn, C. R. (2014) Insulin receptor signaling in normal and insulin-resistant states. *Cold Spring Harb Perspect Biol* **6**
9. Sun, X. J., Crimmins, D. L., Myers, M. G., Jr., Miralpeix, M., and White, M. F. (1993) Pleiotropic insulin signals are engaged by multisite phosphorylation of IRS-1. *Mol Cell Biol* **13**, 7418-7428

10. Pearce, L. R., Komander, D., and Alessi, D. R. (2010) The nuts and bolts of AGC protein kinases. *Nat Rev Mol Cell Biol* **11**, 9-22
11. Schultze, S. M., Jensen, J., Hemmings, B. A., Tschopp, O., and Niessen, M. (2011) Promiscuous affairs of PKB/AKT isoforms in metabolism. *Arch Physiol Biochem* **117**, 70-77
12. Cho, H., Mu, J., Kim, J. K., Thorvaldsen, J. L., Chu, Q., Crenshaw, E. B., 3rd, Kaestner, K. H., Bartolomei, M. S., Shulman, G. I., and Birnbaum, M. J. (2001) Insulin resistance and a diabetes mellitus-like syndrome in mice lacking the protein kinase Akt2 (PKB beta). *Science* **292**, 1728-1731
13. Manning, B. D., and Cantley, L. C. (2007) AKT/PKB signaling: navigating downstream. *Cell* **129**, 1261-1274
14. Abdel-Misih, S. R., and Bloomston, M. (2010) Liver anatomy. *Surg Clin North Am* **90**, 643-653
15. Gayotto, L. C., and Scheuer, P. J. (1975) Letter: Liver-cell mass and nuclear-cytoplasmic ratio in human liver. *J Clin Pathol* **28**, 599
16. Racanelli, V., and Rehermann, B. (2006) The liver as an immunological organ. *Hepatology* **43**, S54-62
17. Miller, L. L., Bly, C. G., Watson, M. L., and Bale, W. F. (1951) The dominant role of the liver in plasma protein synthesis; a direct study of the isolated perfused rat liver with the aid of lysine-epsilon-C14. *J Exp Med* **94**, 431-453
18. Grant, D. M. (1991) Detoxification pathways in the liver. *J Inherit Metab Dis* **14**, 421-430
19. Roder, P. V., Wu, B., Liu, Y., and Han, W. (2016) Pancreatic regulation of glucose homeostasis. *Exp Mol Med* **48**, e219
20. Goke, B. (2008) Islet cell function: alpha and beta cells--partners towards normoglycaemia. *Int J Clin Pract Suppl*, 2-7
21. Magnuson, M. A., Quinn, P. G., and Granner, D. K. (1987) Multihormonal regulation of phosphoenolpyruvate carboxykinase-chloramphenicol acetyltransferase fusion genes. Insulin's effects oppose those of cAMP and dexamethasone. *J Biol Chem* **262**, 14917-14920
22. Pilkis, S. J., el-Maghrabi, M. R., and Claus, T. H. (1988) Hormonal regulation of hepatic gluconeogenesis and glycolysis. *Annu Rev Biochem* **57**, 755-783
23. Rui, L. (2014) Energy metabolism in the liver. *Compr Physiol* **4**, 177-197
24. Sasaki, K., Cripe, T. P., Koch, S. R., Andreone, T. L., Petersen, D. D., Beale, E. G., and Granner, D. K. (1984) Multihormonal regulation of phosphoenolpyruvate carboxykinase gene transcription. The dominant role of insulin. *J Biol Chem* **259**, 15242-15251
25. Hod, Y., and Hanson, R. W. (1988) Cyclic AMP stabilizes the mRNA for phosphoenolpyruvate carboxykinase (GTP) against degradation. *J Biol Chem* **263**, 7747-7752
26. Shapiro, B. (1967) Lipid metabolism. *Annu Rev Biochem* **36**, 247-270

27. Czech, M. P., Tencerova, M., Pedersen, D. J., and Aouadi, M. (2013) Insulin signalling mechanisms for triacylglycerol storage. *Diabetologia* **56**, 949-964
28. Matsuzaka, T., and Shimano, H. (2013) Insulin-dependent and -independent regulation of sterol regulatory element-binding protein-1c. *J Diabetes Investig* **4**, 411-412
29. Cinti, S. (2012) The adipose organ at a glance. *Dis Model Mech* **5**, 588-594
30. Kwok, K. H., Lam, K. S., and Xu, A. (2016) Heterogeneity of white adipose tissue: molecular basis and clinical implications. *Exp Mol Med* **48**, e215
31. Cereijo, R., Giralt, M., and Villarroya, F. (2015) Thermogenic brown and beige/brite adipogenesis in humans. *Ann Med* **47**, 169-177
32. Olefsky, J. M., and Glass, C. K. (2010) Macrophages, inflammation, and insulin resistance. *Annu Rev Physiol* **72**, 219-246
33. Giordano, A., Smorlesi, A., Frontini, A., Barbatelli, G., and Cinti, S. (2014) White, brown and pink adipocytes: the extraordinary plasticity of the adipose organ. *Eur J Endocrinol* **170**, R159-171
34. Garg, A. (2011) Clinical review#: Lipodystrophies: genetic and acquired body fat disorders. *J Clin Endocrinol Metab* **96**, 3313-3325
35. Scherer, P. E. (2016) The Multifaceted Roles of Adipose Tissue-Therapeutic Targets for Diabetes and Beyond: The 2015 Banting Lecture. *Diabetes* **65**, 1452-1461
36. Large, V., Peroni, O., Letexier, D., Ray, H., and Beylot, M. (2004) Metabolism of lipids in human white adipocyte. *Diabetes Metab* **30**, 294-309
37. Suzuki, K., and Kono, T. (1980) Evidence that insulin causes translocation of glucose transport activity to the plasma membrane from an intracellular storage site. *Proc Natl Acad Sci U S A* **77**, 2542-2545
38. Kohn, A. D., Summers, S. A., Birnbaum, M. J., and Roth, R. A. (1996) Expression of a constitutively active Akt Ser/Thr kinase in 3T3-L1 adipocytes stimulates glucose uptake and glucose transporter 4 translocation. *J Biol Chem* **271**, 31372-31378
39. Picard, F., Naimi, N., Richard, D., and Deshaies, Y. (1999) Response of adipose tissue lipoprotein lipase to the cephalic phase of insulin secretion. *Diabetes* **48**, 452-459
40. Semenkovich, C. F., Wims, M., Noe, L., Etienne, J., and Chan, L. (1989) Insulin regulation of lipoprotein lipase activity in 3T3-L1 adipocytes is mediated at posttranscriptional and posttranslational levels. *J Biol Chem* **264**, 9030-9038
41. Wu, Q., Ortegon, A. M., Tsang, B., Doege, H., Feingold, K. R., and Stahl, A. (2006) FATP1 is an insulin-sensitive fatty acid transporter involved in diet-induced obesity. *Mol Cell Biol* **26**, 3455-3467

42. Stahl, A., Evans, J. G., Pattel, S., Hirsch, D., and Lodish, H. F. (2002) Insulin causes fatty acid transport protein translocation and enhanced fatty acid uptake in adipocytes. *Dev Cell* **2**, 477-488
43. Nielsen, T. S., Jessen, N., Jorgensen, J. O., Moller, N., and Lund, S. (2014) Dissecting adipose tissue lipolysis: molecular regulation and implications for metabolic disease. *J Mol Endocrinol* **52**, R199-222
44. Robidoux, J., Martin, T. L., and Collins, S. (2004) Beta-adrenergic receptors and regulation of energy expenditure: a family affair. *Annu Rev Pharmacol Toxicol* **44**, 297-323
45. Sengenes, C., Bouloumie, A., Hauner, H., Berlan, M., Busse, R., Lafontan, M., and Galitzky, J. (2003) Involvement of a cGMP-dependent pathway in the natriuretic peptide-mediated hormone-sensitive lipase phosphorylation in human adipocytes. *J Biol Chem* **278**, 48617-48626
46. Greenberg, A. S., Egan, J. J., Wek, S. A., Garty, N. B., Blanchette-Mackie, E. J., and Londos, C. (1991) Perilipin, a major hormonally regulated adipocyte-specific phosphoprotein associated with the periphery of lipid storage droplets. *J Biol Chem* **266**, 11341-11346
47. Anthonsen, M. W., Ronnstrand, L., Wernstedt, C., Degerman, E., and Holm, C. (1998) Identification of novel phosphorylation sites in hormone-sensitive lipase that are phosphorylated in response to isoproterenol and govern activation properties in vitro. *J Biol Chem* **273**, 215-221
48. Langin, D., Holm, C., and Lafontan, M. (1996) Adipocyte hormone-sensitive lipase: a major regulator of lipid metabolism. *Proc Nutr Soc* **55**, 93-109
49. Granneman, J. G., Moore, H. P., Krishnamoorthy, R., and Rathod, M. (2009) Perilipin controls lipolysis by regulating the interactions of AB-hydrolase containing 5 (Abhd5) and adipose triglyceride lipase (Atgl). *J Biol Chem* **284**, 34538-34544
50. Choi, Y. H., Park, S., Hockman, S., Zmuda-Trzebiatowska, E., Svennelid, F., Haluzik, M., Gavrilova, O., Ahmad, F., Pepin, L., Napolitano, M., Taira, M., Sundler, F., Stenson Holst, L., Degerman, E., and Manganiello, V. C. (2006) Alterations in regulation of energy homeostasis in cyclic nucleotide phosphodiesterase 3B-null mice. *J Clin Invest* **116**, 3240-3251
51. Nedergaard, J., Bengtsson, T., and Cannon, B. (2007) Unexpected evidence for active brown adipose tissue in adult humans. *Am J Physiol Endocrinol Metab* **293**, E444-452
52. Cannon, B., and Nedergaard, J. (2004) Brown adipose tissue: function and physiological significance. *Physiol Rev* **84**, 277-359
53. Ricquier, D., and Bouillaud, F. (2000) The uncoupling protein homologues: UCP1, UCP2, UCP3, StUCP and AtUCP. *Biochem J* **345 Pt 2**, 161-179
54. Harms, M., and Seale, P. (2013) Brown and beige fat: development, function and therapeutic potential. *Nat Med* **19**, 1252-1263

55. Pellegrinelli, V., Carobbio, S., and Vidal-Puig, A. (2016) Adipose tissue plasticity: how fat depots respond differently to pathophysiological cues. *Diabetologia* **59**, 1075-1088
56. Guyenet, S. J., and Schwartz, M. W. (2012) Clinical review: Regulation of food intake, energy balance, and body fat mass: implications for the pathogenesis and treatment of obesity. *J Clin Endocrinol Metab* **97**, 745-755
57. Pi-Sunyer, F. X. (2000) Obesity: criteria and classification. *Proc Nutr Soc* **59**, 505-509
58. Duffey, K. J., and Popkin, B. M. (2011) Energy density, portion size, and eating occasions: contributions to increased energy intake in the United States, 1977-2006. *PLoS Med* **8**, e1001050
59. Lee, J. M., Pilli, S., Gebremariam, A., Keirns, C. C., Davis, M. M., Vijan, S., Freed, G. L., Herman, W. H., and Gurney, J. G. (2010) Getting heavier, younger: trajectories of obesity over the life course. *Int J Obes (Lond)* **34**, 614-623
60. Flegal, K. M., Graubard, B. I., Williamson, D. F., and Gail, M. H. (2007) Cause-specific excess deaths associated with underweight, overweight, and obesity. *JAMA* **298**, 2028-2037
61. Farooqi, I. S., and O'Rahilly, S. (2007) Genetic factors in human obesity. *Obes Rev* **8 Suppl 1**, 37-40
62. Matsuzawa, Y., Shimomura, I., Nakamura, T., Keno, Y., Kotani, K., and Tokunaga, K. (1995) Pathophysiology and pathogenesis of visceral fat obesity. *Obes Res* **3 Suppl 2**, 187S-194S
63. Despres, J. P. (2006) Is visceral obesity the cause of the metabolic syndrome? *Ann Med* **38**, 52-63
64. Palmer, B. F., and Clegg, D. J. (2015) The sexual dimorphism of obesity. *Mol Cell Endocrinol* **402**, 113-119
65. Joe, A. W., Yi, L., Even, Y., Vogl, A. W., and Rossi, F. M. (2009) Depot-specific differences in adipogenic progenitor abundance and proliferative response to high-fat diet. *Stem Cells* **27**, 2563-2570
66. Weyer, C., Foley, J. E., Bogardus, C., Tataranni, P. A., and Pratley, R. E. (2000) Enlarged subcutaneous abdominal adipocyte size, but not obesity itself, predicts type II diabetes independent of insulin resistance. *Diabetologia* **43**, 1498-1506
67. Skurk, T., Alberti-Huber, C., Herder, C., and Hauner, H. (2007) Relationship between adipocyte size and adipokine expression and secretion. *J Clin Endocrinol Metab* **92**, 1023-1033
68. Wang, Q. A., Tao, C., Gupta, R. K., and Scherer, P. E. (2013) Tracking adipogenesis during white adipose tissue development, expansion and regeneration. *Nat Med* **19**, 1338-1344
69. van Beek, L., van Klinken, J. B., Pronk, A. C., van Dam, A. D., Dirven, E., Rensen, P. C., Koning, F., Willems van Dijk, K., and van Harmelen, V. (2015) The limited storage capacity of gonadal adipose tissue directs the

development of metabolic disorders in male C57Bl/6J mice. *Diabetologia* **58**, 1601-1609
70. Guilherme, A., Virbasius, J. V., Puri, V., and Czech, M. P. (2008) Adipocyte dysfunctions linking obesity to insulin resistance and type 2 diabetes. *Nat Rev Mol Cell Biol* **9**, 367-377
71. de Ferranti, S., and Mozaffarian, D. (2008) The perfect storm: obesity, adipocyte dysfunction, and metabolic consequences. *Clin Chem* **54**, 945-955
72. Moreno-Indias, I., and Tinahones, F. J. (2015) Impaired adipose tissue expandability and lipogenic capacities as ones of the main causes of metabolic disorders. *J Diabetes Res* **2015**, 970375
73. Baron, A. D., Brechtel, G., Wallace, P., and Edelman, S. V. (1988) Rates and tissue sites of non-insulin- and insulin-mediated glucose uptake in humans. *Am J Physiol* **255**, E769-774
74. Gurley, J. M., Griesel, B. A., and Olson, A. L. (2016) Increased Skeletal Muscle Glut4 Expression in Obese Mice after Voluntary Wheel Running Exercise is Post-Transcriptional. *Diabetes*
75. Dimitriadis, G., Mitrou, P., Lambadiari, V., Maratou, E., and Raptis, S. A. (2011) Insulin effects in muscle and adipose tissue. *Diabetes Res Clin Pract* **93 Suppl 1**, S52-59
76. Amati, F., Dube, J. J., Alvarez-Carnero, E., Edreira, M. M., Chomentowski, P., Coen, P. M., Switzer, G. E., Bickel, P. E., Stefanovic-Racic, M., Toledo, F. G., and Goodpaster, B. H. (2011) Skeletal muscle triglycerides, diacylglycerols, and ceramides in insulin resistance: another paradox in endurance-trained athletes? *Diabetes* **60**, 2588-2597
77. Samuel, V. T., and Shulman, G. I. (2012) Mechanisms for insulin resistance: common threads and missing links. *Cell* **148**, 852-871
78. Nguyen, P., Leray, V., Diez, M., Serisier, S., Le Bloc'h, J., Siliart, B., and Dumon, H. (2008) Liver lipid metabolism. *J Anim Physiol Anim Nutr (Berl)* **92**, 272-283
79. Bechmann, L. P., Hannivoort, R. A., Gerken, G., Hotamisligil, G. S., Trauner, M., and Canbay, A. (2012) The interaction of hepatic lipid and glucose metabolism in liver diseases. *J Hepatol* **56**, 952-964
80. Stefan, N., and Haring, H. U. (2011) The metabolically benign and malignant fatty liver. *Diabetes* **60**, 2011-2017
81. Cohen, J. C., Horton, J. D., and Hobbs, H. H. (2011) Human fatty liver disease: old questions and new insights. *Science* **332**, 1519-1523
82. Gregg, E. W., Sattar, N., and Ali, M. K. (2016) The changing face of diabetes complications. *Lancet Diabetes Endocrinol* **4**, 537-547
83. Dresner, A., Laurent, D., Marcucci, M., Griffin, M. E., Dufour, S., Cline, G. W., Slezak, L. A., Andersen, D. K., Hundal, R. S., Rothman, D. L., Petersen, K. F., and Shulman, G. I. (1999) Effects of free fatty acids on glucose transport and IRS-1-associated phosphatidylinositol 3-kinase activity. *J Clin Invest* **103**, 253-259

84. Yu, C., Chen, Y., Cline, G. W., Zhang, D., Zong, H., Wang, Y., Bergeron, R., Kim, J. K., Cushman, S. W., Cooney, G. J., Atcheson, B., White, M. F., Kraegen, E. W., and Shulman, G. I. (2002) Mechanism by which fatty acids inhibit insulin activation of insulin receptor substrate-1 (IRS-1)-associated phosphatidylinositol 3-kinase activity in muscle. *J Biol Chem* **277**, 50230-50236
85. Itani, S. I., Ruderman, N. B., Schmieder, F., and Boden, G. (2002) Lipid-induced insulin resistance in human muscle is associated with changes in diacylglycerol, protein kinase C, and IkappaB-alpha. *Diabetes* **51**, 2005-2011
86. Szendroedi, J., Yoshimura, T., Phielix, E., Koliaki, C., Marcucci, M., Zhang, D., Jelenik, T., Muller, J., Herder, C., Nowotny, P., Shulman, G. I., and Roden, M. (2014) Role of diacylglycerol activation of PKCtheta in lipid-induced muscle insulin resistance in humans. *Proc Natl Acad Sci U S A* **111**, 9597-9602
87. Perry, R. J., Camporez, J. P., Kursawe, R., Titchenell, P. M., Zhang, D., Perry, C. J., Jurczak, M. J., Abudukadier, A., Han, M. S., Zhang, X. M., Ruan, H. B., Yang, X., Caprio, S., Kaech, S. M., Sul, H. S., Birnbaum, M. J., Davis, R. J., Cline, G. W., Petersen, K. F., and Shulman, G. I. (2015) Hepatic acetyl CoA links adipose tissue inflammation to hepatic insulin resistance and type 2 diabetes. *Cell* **160**, 745-758
88. Ximenes, H. M., Hirata, A. E., Rocha, M. S., Curi, R., and Carpinelli, A. R. (2007) Propionate inhibits glucose-induced insulin secretion in isolated rat pancreatic islets. *Cell Biochem Funct* **25**, 173-178
89. Gupta, D., Krueger, C. B., and Lastra, G. (2012) Over-nutrition, obesity and insulin resistance in the development of beta-cell dysfunction. *Curr Diabetes Rev* **8**, 76-83
90. Jourdan, T., Godlewski, G., Cinar, R., Bertola, A., Szanda, G., Liu, J., Tam, J., Han, T., Mukhopadhyay, B., Skarulis, M. C., Ju, C., Aouadi, M., Czech, M. P., and Kunos, G. (2013) Activation of the Nlrp3 inflammasome in infiltrating macrophages by endocannabinoids mediates beta cell loss in type 2 diabetes. *Nat Med* **19**, 1132-1140
91. Pedersen, D. J., Guilherme, A., Danai, L. V., Heyda, L., Matevossian, A., Cohen, J., Nicoloro, S. M., Straubhaar, J., Noh, H. L., Jung, D., Kim, J. K., and Czech, M. P. (2015) A major role of insulin in promoting obesity-associated adipose tissue inflammation. *Mol Metab* **4**, 507-518
92. Mraz, M., and Haluzik, M. (2014) The role of adipose tissue immune cells in obesity and low-grade inflammation. *J Endocrinol* **222**, R113-127
93. Schipper, H. S., Prakken, B., Kalkhoven, E., and Boes, M. (2012) Adipose tissue-resident immune cells: key players in immunometabolism. *Trends Endocrinol Metab* **23**, 407-415
94. Cildir, G., Akincilar, S. C., and Tergaonkar, V. (2013) Chronic adipose tissue inflammation: all immune cells on the stage. *Trends Mol Med* **19**, 487-500

95. Lee, B. C., and Lee, J. (2014) Cellular and molecular players in adipose tissue inflammation in the development of obesity-induced insulin resistance. *Biochim Biophys Acta* **1842**, 446-462
96. Medzhitov, R. (2008) Origin and physiological roles of inflammation. *Nature* **454**, 428-435
97. Feingold, K. R., Soued, M., Staprans, I., Gavin, L. A., Donahue, M. E., Huang, B. J., Moser, A. H., Gulli, R., and Grunfeld, C. (1989) Effect of tumor necrosis factor (TNF) on lipid metabolism in the diabetic rat. Evidence that inhibition of adipose tissue lipoprotein lipase activity is not required for TNF-induced hyperlipidemia. *J Clin Invest* **83**, 1116-1121
98. Hotamisligil, G. S., Arner, P., Caro, J. F., Atkinson, R. L., and Spiegelman, B. M. (1995) Increased adipose tissue expression of tumor necrosis factor-alpha in human obesity and insulin resistance. *J Clin Invest* **95**, 2409-2415
99. Hotamisligil, G. S., Shargill, N. S., and Spiegelman, B. M. (1993) Adipose expression of tumor necrosis factor-alpha: direct role in obesity-linked insulin resistance. *Science* **259**, 87-91
100. Uysal, K. T., Wiesbrock, S. M., Marino, M. W., and Hotamisligil, G. S. (1997) Protection from obesity-induced insulin resistance in mice lacking TNF-alpha function. *Nature* **389**, 610-614
101. Shoelson, S. E., Lee, J., and Yuan, M. (2003) Inflammation and the IKK beta/I kappa B/NF-kappa B axis in obesity- and diet-induced insulin resistance. *Int J Obes Relat Metab Disord* **27 Suppl 3**, S49-52
102. Yuan, M., Konstantopoulos, N., Lee, J., Hansen, L., Li, Z. W., Karin, M., and Shoelson, S. E. (2001) Reversal of obesity- and diet-induced insulin resistance with salicylates or targeted disruption of Ikkbeta. *Science* **293**, 1673-1677
103. Hirosumi, J., Tuncman, G., Chang, L., Gorgun, C. Z., Uysal, K. T., Maeda, K., Karin, M., and Hotamisligil, G. S. (2002) A central role for JNK in obesity and insulin resistance. *Nature* **420**, 333-336
104. Solinas, G., Vilcu, C., Neels, J. G., Bandyopadhyay, G. K., Luo, J. L., Naugler, W., Grivennikov, S., Wynshaw-Boris, A., Scadeng, M., Olefsky, J. M., and Karin, M. (2007) JNK1 in hematopoietically derived cells contributes to diet-induced inflammation and insulin resistance without affecting obesity. *Cell Metab* **6**, 386-397
105. Wensveen, F. M., Valentic, S., Sestan, M., Turk Wensveen, T., and Polic, B. (2015) The "Big Bang" in obese fat: Events initiating obesity-induced adipose tissue inflammation. *Eur J Immunol* **45**, 2446-2456
106. Mraz, M., Lacinova, Z., Drapalova, J., Haluzikova, D., Horinek, A., Matoulek, M., Trachta, P., Kavalkova, P., Svacina, S., and Haluzik, M. (2011) The effect of very-low-calorie diet on mRNA expression of inflammation-related genes in subcutaneous adipose tissue and peripheral monocytes of obese patients with type 2 diabetes mellitus. *J Clin Endocrinol Metab* **96**, E606-613

107. Masoodi, M., Kuda, O., Rossmeisl, M., Flachs, P., and Kopecky, J. (2015) Lipid signaling in adipose tissue: Connecting inflammation & metabolism. *Biochim Biophys Acta* **1851**, 503-518
108. Knight, S. C. (2008) Specialized perinodal fat fuels and fashions immunity. *Immunity* **28**, 135-138
109. Chawla, A., Nguyen, K. D., and Goh, Y. P. (2011) Macrophage-mediated inflammation in metabolic disease. *Nat Rev Immunol* **11**, 738-749
110. Weisberg, S. P., McCann, D., Desai, M., Rosenbaum, M., Leibel, R. L., and Ferrante, A. W., Jr. (2003) Obesity is associated with macrophage accumulation in adipose tissue. *J Clin Invest* **112**, 1796-1808
111. Xu, H., Barnes, G. T., Yang, Q., Tan, G., Yang, D., Chou, C. J., Sole, J., Nichols, A., Ross, J. S., Tartaglia, L. A., and Chen, H. (2003) Chronic inflammation in fat plays a crucial role in the development of obesity-related insulin resistance. *J Clin Invest* **112**, 1821-1830
112. Harman-Boehm, I., Bluher, M., Redel, H., Sion-Vardy, N., Ovadia, S., Avinoach, E., Shai, I., Kloting, N., Stumvoll, M., Bashan, N., and Rudich, A. (2007) Macrophage infiltration into omental versus subcutaneous fat across different populations: effect of regional adiposity and the comorbidities of obesity. *J Clin Endocrinol Metab* **92**, 2240-2247
113. Apovian, C. M., Bigornia, S., Mott, M., Meyers, M. R., Ulloor, J., Gagua, M., McDonnell, M., Hess, D., Joseph, L., and Gokce, N. (2008) Adipose macrophage infiltration is associated with insulin resistance and vascular endothelial dysfunction in obese subjects. *Arterioscler Thromb Vasc Biol* **28**, 1654-1659
114. Cancello, R., Tordjman, J., Poitou, C., Guilhem, G., Bouillot, J. L., Hugol, D., Coussieu, C., Basdevant, A., Bar Hen, A., Bedossa, P., Guerre-Millo, M., and Clement, K. (2006) Increased infiltration of macrophages in omental adipose tissue is associated with marked hepatic lesions in morbid human obesity. *Diabetes* **55**, 1554-1561
115. Lumeng, C. N., Deyoung, S. M., Bodzin, J. L., and Saltiel, A. R. (2007) Increased inflammatory properties of adipose tissue macrophages recruited during diet-induced obesity. *Diabetes* **56**, 16-23
116. Curat, C. A., Miranville, A., Sengenes, C., Diehl, M., Tonus, C., Busse, R., and Bouloumie, A. (2004) From blood monocytes to adipose tissue-resident macrophages: induction of diapedesis by human mature adipocytes. *Diabetes* **53**, 1285-1292
117. Cancello, R., Henegar, C., Viguerie, N., Taleb, S., Poitou, C., Rouault, C., Coupaye, M., Pelloux, V., Hugol, D., Bouillot, J. L., Bouloumie, A., Barbatelli, G., Cinti, S., Svensson, P. A., Barsh, G. S., Zucker, J. D., Basdevant, A., Langin, D., and Clement, K. (2005) Reduction of macrophage infiltration and chemoattractant gene expression changes in white adipose tissue of morbidly obese subjects after surgery-induced weight loss. *Diabetes* **54**, 2277-2286

118. Osborn, O., and Olefsky, J. M. (2012) The cellular and signaling networks linking the immune system and metabolism in disease. *Nat Med* **18**, 363-374
119. Christiansen, T., Richelsen, B., and Bruun, J. M. (2005) Monocyte chemoattractant protein-1 is produced in isolated adipocytes, associated with adiposity and reduced after weight loss in morbid obese subjects. *Int J Obes (Lond)* **29**, 146-150
120. Kanda, H., Tateya, S., Tamori, Y., Kotani, K., Hiasa, K., Kitazawa, R., Kitazawa, S., Miyachi, H., Maeda, S., Egashira, K., and Kasuga, M. (2006) MCP-1 contributes to macrophage infiltration into adipose tissue, insulin resistance, and hepatic steatosis in obesity. *J Clin Invest* **116**, 1494-1505
121. Hashimoto, I., Wada, J., Hida, A., Baba, M., Miyatake, N., Eguchi, J., Shikata, K., and Makino, H. (2006) Elevated serum monocyte chemoattractant protein-4 and chronic inflammation in overweight subjects. *Obesity (Silver Spring)* **14**, 799-811
122. Vasudevan, A. R., Wu, H., Xydakis, A. M., Jones, P. H., Smith, E. O., Sweeney, J. F., Corry, D. B., and Ballantyne, C. M. (2006) Eotaxin and obesity. *J Clin Endocrinol Metab* **91**, 256-261
123. Huber, J., Kiefer, F. W., Zeyda, M., Ludvik, B., Silberhumer, G. R., Prager, G., Zlabinger, G. J., and Stulnig, T. M. (2008) CC chemokine and CC chemokine receptor profiles in visceral and subcutaneous adipose tissue are altered in human obesity. *J Clin Endocrinol Metab* **93**, 3215-3221
124. Doulatov, S., Notta, F., Eppert, K., Nguyen, L. T., Ohashi, P. S., and Dick, J. E. (2010) Revised map of the human progenitor hierarchy shows the origin of macrophages and dendritic cells in early lymphoid development. *Nat Immunol* **11**, 585-593
125. Geissmann, F., Manz, M. G., Jung, S., Sieweke, M. H., Merad, M., and Ley, K. (2010) Development of monocytes, macrophages, and dendritic cells. *Science* **327**, 656-661
126. Gordon, S., and Taylor, P. R. (2005) Monocyte and macrophage heterogeneity. *Nat Rev Immunol* **5**, 953-964
127. Geissmann, F., Gordon, S., Hume, D. A., Mowat, A. M., and Randolph, G. J. (2010) Unravelling mononuclear phagocyte heterogeneity. *Nat Rev Immunol* **10**, 453-460
128. Wynn, T. A., and Barron, L. (2010) Macrophages: master regulators of inflammation and fibrosis. *Semin Liver Dis* **30**, 245-257
129. Murray, P. J., and Wynn, T. A. (2011) Obstacles and opportunities for understanding macrophage polarization. *J Leukoc Biol* **89**, 557-563
130. Mosser, D. M., and Edwards, J. P. (2008) Exploring the full spectrum of macrophage activation. *Nat Rev Immunol* **8**, 958-969
131. Nguyen, K. D., Qiu, Y., Cui, X., Goh, Y. P., Mwangi, J., David, T., Mukundan, L., Brombacher, F., Locksley, R. M., and Chawla, A. (2011) Alternatively activated macrophages produce catecholamines to sustain adaptive thermogenesis. *Nature* **480**, 104-108

132. Sun, K., Kusminski, C. M., and Scherer, P. E. (2011) Adipose tissue remodeling and obesity. *J Clin Invest* **121**, 2094-2101
133. Nguyen, M. T., Favelyukis, S., Nguyen, A. K., Reichart, D., Scott, P. A., Jenn, A., Liu-Bryan, R., Glass, C. K., Neels, J. G., and Olefsky, J. M. (2007) A subpopulation of macrophages infiltrates hypertrophic adipose tissue and is activated by free fatty acids via Toll-like receptors 2 and 4 and JNK-dependent pathways. *J Biol Chem* **282**, 35279-35292
134. Prieur, X., Mok, C. Y., Velagapudi, V. R., Nunez, V., Fuentes, L., Montaner, D., Ishikawa, K., Camacho, A., Barbarroja, N., O'Rahilly, S., Sethi, J. K., Dopazo, J., Oresic, M., Ricote, M., and Vidal-Puig, A. (2011) Differential lipid partitioning between adipocytes and tissue macrophages modulates macrophage lipotoxicity and M2/M1 polarization in obese mice. *Diabetes* **60**, 797-809
135. Patsouris, D., Li, P. P., Thapar, D., Chapman, J., Olefsky, J. M., and Neels, J. G. (2008) Ablation of CD11c-positive cells normalizes insulin sensitivity in obese insulin resistant animals. *Cell Metab* **8**, 301-309
136. Fujisaka, S., Usui, I., Bukhari, A., Ikutani, M., Oya, T., Kanatani, Y., Tsuneyama, K., Nagai, Y., Takatsu, K., Urakaze, M., Kobayashi, M., and Tobe, K. (2009) Regulatory mechanisms for adipose tissue M1 and M2 macrophages in diet-induced obese mice. *Diabetes* **58**, 2574-2582
137. Lumeng, C. N., Deyoung, S. M., and Saltiel, A. R. (2007) Macrophages block insulin action in adipocytes by altering expression of signaling and glucose transport proteins. *Am J Physiol Endocrinol Metab* **292**, E166-174
138. Khan, T., Muise, E. S., Iyengar, P., Wang, Z. V., Chandalia, M., Abate, N., Zhang, B. B., Bonaldo, P., Chua, S., and Scherer, P. E. (2009) Metabolic dysregulation and adipose tissue fibrosis: role of collagen VI. *Mol Cell Biol* **29**, 1575-1591
139. Sun, S., Ji, Y., Kersten, S., and Qi, L. (2012) Mechanisms of inflammatory responses in obese adipose tissue. *Annu Rev Nutr* **32**, 261-286
140. Creely, S. J., McTernan, P. G., Kusminski, C. M., Fisher f, M., Da Silva, N. F., Khanolkar, M., Evans, M., Harte, A. L., and Kumar, S. (2007) Lipopolysaccharide activates an innate immune system response in human adipose tissue in obesity and type 2 diabetes. *Am J Physiol Endocrinol Metab* **292**, E740-747
141. Saberi, M., Woods, N. B., de Luca, C., Schenk, S., Lu, J. C., Bandyopadhyay, G., Verma, I. M., and Olefsky, J. M. (2009) Hematopoietic cell-specific deletion of toll-like receptor 4 ameliorates hepatic and adipose tissue insulin resistance in high-fat-fed mice. *Cell Metab* **10**, 419-429
142. Dasu, M. R., Devaraj, S., Park, S., and Jialal, I. (2010) Increased toll-like receptor (TLR) activation and TLR ligands in recently diagnosed type 2 diabetic subjects. *Diabetes Care* **33**, 861-868
143. Erbay, E., Babaev, V. R., Mayers, J. R., Makowski, L., Charles, K. N., Snitow, M. E., Fazio, S., Wiest, M. M., Watkins, S. M., Linton, M. F., and

Hotamisligil, G. S. (2009) Reducing endoplasmic reticulum stress through a macrophage lipid chaperone alleviates atherosclerosis. *Nat Med* **15**, 1383-1391

144. Vandanmagsar, B., Youm, Y. H., Ravussin, A., Galgani, J. E., Stadler, K., Mynatt, R. L., Ravussin, E., Stephens, J. M., and Dixit, V. D. (2011) The NLRP3 inflammasome instigates obesity-induced inflammation and insulin resistance. *Nat Med* **17**, 179-188
145. Ohashi, K., Parker, J. L., Ouchi, N., Higuchi, A., Vita, J. A., Gokce, N., Pedersen, A. A., Kalthoff, C., Tullin, S., Sams, A., Summer, R., and Walsh, K. (2010) Adiponectin promotes macrophage polarization toward an anti-inflammatory phenotype. *J Biol Chem* **285**, 6153-6160
146. Bourlier, V., Zakaroff-Girard, A., Miranville, A., De Barros, S., Maumus, M., Sengenes, C., Galitzky, J., Lafontan, M., Karpe, F., Frayn, K. N., and Bouloumie, A. (2008) Remodeling phenotype of human subcutaneous adipose tissue macrophages. *Circulation* **117**, 806-815
147. Shaul, M. E., Bennett, G., Strissel, K. J., Greenberg, A. S., and Obin, M. S. (2010) Dynamic, M2-like remodeling phenotypes of CD11c+ adipose tissue macrophages during high-fat diet--induced obesity in mice. *Diabetes* **59**, 1171-1181
148. Zeyda, M., Farmer, D., Todoric, J., Aszmann, O., Speiser, M., Gyori, G., Zlabinger, G. J., and Stulnig, T. M. (2007) Human adipose tissue macrophages are of an anti-inflammatory phenotype but capable of excessive pro-inflammatory mediator production. *Int J Obes (Lond)* **31**, 1420-1428
149. Bouhlel, M. A., Derudas, B., Rigamonti, E., Dievart, R., Brozek, J., Haulon, S., Zawadzki, C., Jude, B., Torpier, G., Marx, N., Staels, B., and Chinetti-Gbaguidi, G. (2007) PPARgamma activation primes human monocytes into alternative M2 macrophages with anti-inflammatory properties. *Cell Metab* **6**, 137-143
150. Li, P., Lu, M., Nguyen, M. T., Bae, E. J., Chapman, J., Feng, D., Hawkins, M., Pessin, J. E., Sears, D. D., Nguyen, A. K., Amidi, A., Watkins, S. M., Nguyen, U., and Olefsky, J. M. (2010) Functional heterogeneity of CD11c-positive adipose tissue macrophages in diet-induced obese mice. *J Biol Chem* **285**, 15333-15345
151. Oh, D. Y., Talukdar, S., Bae, E. J., Imamura, T., Morinaga, H., Fan, W., Li, P., Lu, W. J., Watkins, S. M., and Olefsky, J. M. (2010) GPR120 is an omega-3 fatty acid receptor mediating potent anti-inflammatory and insulin-sensitizing effects. *Cell* **142**, 687-698
152. Steinman, R. M. (2008) Dendritic cells in vivo: a key target for a new vaccine science. *Immunity* **29**, 319-324
153. Hashimoto, D., Miller, J., and Merad, M. (2011) Dendritic cell and macrophage heterogeneity in vivo. *Immunity* **35**, 323-335
154. Bertola, A., Ciucci, T., Rousseau, D., Bourlier, V., Duffaut, C., Bonnafous, S., Blin-Wakkach, C., Anty, R., Iannelli, A., Gugenheim, J., Tran, A.,

Bouloumie, A., Gual, P., and Wakkach, A. (2012) Identification of adipose tissue dendritic cells correlated with obesity-associated insulin-resistance and inducing Th17 responses in mice and patients. *Diabetes* **61**, 2238-2247

155. Abraham, S. N., and St John, A. L. (2010) Mast cell-orchestrated immunity to pathogens. *Nat Rev Immunol* **10**, 440-452
156. Liu, J., Divoux, A., Sun, J., Zhang, J., Clement, K., Glickman, J. N., Sukhova, G. K., Wolters, P. J., Du, J., Gorgun, C. Z., Doria, A., Libby, P., Blumberg, R. S., Kahn, B. B., Hotamisligil, G. S., and Shi, G. P. (2009) Genetic deficiency and pharmacological stabilization of mast cells reduce diet-induced obesity and diabetes in mice. *Nat Med* **15**, 940-945
157. Amulic, B., Cazalet, C., Hayes, G. L., Metzler, K. D., and Zychlinsky, A. (2012) Neutrophil function: from mechanisms to disease. *Annu Rev Immunol* **30**, 459-489
158. Nijhuis, J., Rensen, S. S., Slaats, Y., van Dielen, F. M., Buurman, W. A., and Greve, J. W. (2009) Neutrophil activation in morbid obesity, chronic activation of acute inflammation. *Obesity (Silver Spring)* **17**, 2014-2018
159. Elgazar-Carmon, V., Rudich, A., Hadad, N., and Levy, R. (2008) Neutrophils transiently infiltrate intra-abdominal fat early in the course of high-fat feeding. *J Lipid Res* **49**, 1894-1903
160. Talukdar, S., Oh da, Y., Bandyopadhyay, G., Li, D., Xu, J., McNelis, J., Lu, M., Li, P., Yan, Q., Zhu, Y., Ofrecio, J., Lin, M., Brenner, M. B., and Olefsky, J. M. (2012) Neutrophils mediate insulin resistance in mice fed a high-fat diet through secreted elastase. *Nat Med* **18**, 1407-1412
161. Spencer, L. A., and Weller, P. F. (2010) Eosinophils and Th2 immunity: contemporary insights. *Immunol Cell Biol* **88**, 250-256
162. Wu, D., Molofsky, A. B., Liang, H. E., Ricardo-Gonzalez, R. R., Jouihan, H. A., Bando, J. K., Chawla, A., and Locksley, R. M. (2011) Eosinophils sustain adipose alternatively activated macrophages associated with glucose homeostasis. *Science* **332**, 243-247
163. Ricardo-Gonzalez, R. R., Red Eagle, A., Odegaard, J. I., Jouihan, H., Morel, C. R., Heredia, J. E., Mukundan, L., Wu, D., Locksley, R. M., and Chawla, A. (2010) IL-4/STAT6 immune axis regulates peripheral nutrient metabolism and insulin sensitivity. *Proc Natl Acad Sci U S A* **107**, 22617-22622
164. Oestreich, K. J., and Weinmann, A. S. (2012) Master regulators or lineage-specifying? Changing views on CD4+ T cell transcription factors. *Nat Rev Immunol* **12**, 799-804
165. Rocha, V. Z., Folco, E. J., Sukhova, G., Shimizu, K., Gotsman, I., Vernon, A. H., and Libby, P. (2008) Interferon-gamma, a Th1 cytokine, regulates fat inflammation: a role for adaptive immunity in obesity. *Circ Res* **103**, 467-476
166. Winer, S., Chan, Y., Paltser, G., Truong, D., Tsui, H., Bahrami, J., Dorfman, R., Wang, Y., Zielenski, J., Mastronardi, F., Maezawa, Y.,

Drucker, D. J., Engleman, E., Winer, D., and Dosch, H. M. (2009) Normalization of obesity-associated insulin resistance through immunotherapy. *Nat Med* **15**, 921-929
167. Rausch, M. E., Weisberg, S., Vardhana, P., and Tortoriello, D. V. (2008) Obesity in C57BL/6J mice is characterized by adipose tissue hypoxia and cytotoxic T-cell infiltration. *Int J Obes (Lond)* **32**, 451-463
168. Nishimura, S., Manabe, I., Nagasaki, M., Eto, K., Yamashita, H., Ohsugi, M., Otsu, M., Hara, K., Ueki, K., Sugiura, S., Yoshimura, K., Kadowaki, T., and Nagai, R. (2009) CD8+ effector T cells contribute to macrophage recruitment and adipose tissue inflammation in obesity. *Nat Med* **15**, 914-920
169. Zuniga, L. A., Shen, W. J., Joyce-Shaikh, B., Pyatnova, E. A., Richards, A. G., Thom, C., Andrade, S. M., Cua, D. J., Kraemer, F. B., and Butcher, E. C. (2010) IL-17 regulates adipogenesis, glucose homeostasis, and obesity. *J Immunol* **185**, 6947-6959
170. Jagannathan-Bogdan, M., McDonnell, M. E., Shin, H., Rehman, Q., Hasturk, H., Apovian, C. M., and Nikolajczyk, B. S. (2011) Elevated proinflammatory cytokine production by a skewed T cell compartment requires monocytes and promotes inflammation in type 2 diabetes. *J Immunol* **186**, 1162-1172
171. Goossens, G. H., Blaak, E. E., Theunissen, R., Duijvestijn, A. M., Clement, K., Tervaert, J. W., and Thewissen, M. M. (2012) Expression of NLRP3 inflammasome and T cell population markers in adipose tissue are associated with insulin resistance and impaired glucose metabolism in humans. *Mol Immunol* **50**, 142-149
172. Zhu, L., Wu, Y., Wei, H., Yang, S., Zhan, N., Xing, X., and Peng, B. (2012) Up-regulation of IL-23 p19 expression in human periodontal ligament fibroblasts by IL-1beta via concurrent activation of the NF-kappaB and MAPKs/AP-1 pathways. *Cytokine* **60**, 171-178
173. Feuerer, M., Herrero, L., Cipolletta, D., Naaz, A., Wong, J., Nayer, A., Lee, J., Goldfine, A. B., Benoist, C., Shoelson, S., and Mathis, D. (2009) Lean, but not obese, fat is enriched for a unique population of regulatory T cells that affect metabolic parameters. *Nat Med* **15**, 930-939
174. Deiuliis, J., Shah, Z., Shah, N., Needleman, B., Mikami, D., Narula, V., Perry, K., Hazey, J., Kampfrath, T., Kollengode, M., Sun, Q., Satoskar, A. R., Lumeng, C., Moffatt-Bruce, S., and Rajagopalan, S. (2011) Visceral adipose inflammation in obesity is associated with critical alterations in tregulatory cell numbers. *PLoS One* **6**, e16376
175. Wu, L., Parekh, V. V., Gabriel, C. L., Bracy, D. P., Marks-Shulman, P. A., Tamboli, R. A., Kim, S., Mendez-Fernandez, Y. V., Besra, G. S., Lomenick, J. P., Williams, B., Wasserman, D. H., and Van Kaer, L. (2012) Activation of invariant natural killer T cells by lipid excess promotes tissue inflammation, insulin resistance, and hepatic steatosis in obese mice. *Proc Natl Acad Sci U S A* **109**, E1143-1152

176. Ohmura, K., Ishimori, N., Ohmura, Y., Tokuhara, S., Nozawa, A., Horii, S., Andoh, Y., Fujii, S., Iwabuchi, K., Onoe, K., and Tsutsui, H. (2010) Natural killer T cells are involved in adipose tissues inflammation and glucose intolerance in diet-induced obese mice. *Arterioscler Thromb Vasc Biol* **30**, 193-199
177. Kotas, M. E., Lee, H. Y., Gillum, M. P., Annicelli, C., Guigni, B. A., Shulman, G. I., and Medzhitov, R. (2011) Impact of CD1d deficiency on metabolism. *PLoS One* **6**, e25478
178. Mantell, B. S., Stefanovic-Racic, M., Yang, X., Dedousis, N., Sipula, I. J., and O'Doherty, R. M. (2011) Mice lacking NKT cells but with a complete complement of CD8+ T-cells are not protected against the metabolic abnormalities of diet-induced obesity. *PLoS One* **6**, e19831
179. Schipper, H. S., Rakhshandehroo, M., van de Graaf, S. F., Venken, K., Koppen, A., Stienstra, R., Prop, S., Meerding, J., Hamers, N., Besra, G., Boon, L., Nieuwenhuis, E. E., Elewaut, D., Prakken, B., Kersten, S., Boes, M., and Kalkhoven, E. (2012) Natural killer T cells in adipose tissue prevent insulin resistance. *J Clin Invest* **122**, 3343-3354
180. Lynch, L., Nowak, M., Varghese, B., Clark, J., Hogan, A. E., Toxavidis, V., Balk, S. P., O'Shea, D., O'Farrelly, C., and Exley, M. A. (2012) Adipose tissue invariant NKT cells protect against diet-induced obesity and metabolic disorder through regulatory cytokine production. *Immunity* **37**, 574-587
181. DeFuria, J., Belkina, A. C., Jagannathan-Bogdan, M., Snyder-Cappione, J., Carr, J. D., Nersesova, Y. R., Markham, D., Strissel, K. J., Watkins, A. A., Zhu, M., Allen, J., Bouchard, J., Toraldo, G., Jasuja, R., Obin, M. S., McDonnell, M. E., Apovian, C., Denis, G. V., and Nikolajczyk, B. S. (2013) B cells promote inflammation in obesity and type 2 diabetes through regulation of T-cell function and an inflammatory cytokine profile. *Proc Natl Acad Sci U S A* **110**, 5133-5138
182. Duffaut, C., Galitzky, J., Lafontan, M., and Bouloumie, A. (2009) Unexpected trafficking of immune cells within the adipose tissue during the onset of obesity. *Biochem Biophys Res Commun* **384**, 482-485
183. Baratta, J. L., Ngo, A., Lopez, B., Kasabwalla, N., Longmuir, K. J., and Robertson, R. T. (2009) Cellular organization of normal mouse liver: a histological, quantitative immunocytochemical, and fine structural analysis. *Histochem Cell Biol* **131**, 713-726
184. Jager, J., Aparicio-Vergara, M., and Aouadi, M. (2016) Liver innate immune cells and insulin resistance: the multiple facets of Kupffer cells. *J Intern Med* **280**, 209-220
185. Baffy, G. (2009) Kupffer cells in non-alcoholic fatty liver disease: the emerging view. *J Hepatol* **51**, 212-223
186. Kolios, G., Valatas, V., and Kouroumalis, E. (2006) Role of Kupffer cells in the pathogenesis of liver disease. *World J Gastroenterol* **12**, 7413-7420

187. Bilzer, M., Roggel, F., and Gerbes, A. L. (2006) Role of Kupffer cells in host defense and liver disease. *Liver Int* **26**, 1175-1186
188. Swirski, F. K., Libby, P., Aikawa, E., Alcaide, P., Luscinskas, F. W., Weissleder, R., and Pittet, M. J. (2007) Ly-6Chi monocytes dominate hypercholesterolemia-associated monocytosis and give rise to macrophages in atheromata. *J Clin Invest* **117**, 195-205
189. Odegaard, J. I., and Chawla, A. (2011) Alternative macrophage activation and metabolism. *Annu Rev Pathol* **6**, 275-297
190. Dey, A., Allen, J., and Hankey-Giblin, P. A. (2014) Ontogeny and polarization of macrophages in inflammation: blood monocytes versus tissue macrophages. *Front Immunol* **5**, 683
191. Cai, D., Yuan, M., Frantz, D. F., Melendez, P. A., Hansen, L., Lee, J., and Shoelson, S. E. (2005) Local and systemic insulin resistance resulting from hepatic activation of IKK-beta and NF-kappaB. *Nat Med* **11**, 183-190
192. Huang, W., Metlakunta, A., Dedousis, N., Zhang, P., Sipula, I., Dube, J. J., Scott, D. K., and O'Doherty, R. M. (2010) Depletion of liver Kupffer cells prevents the development of diet-induced hepatic steatosis and insulin resistance. *Diabetes* **59**, 347-357
193. Morinaga, H., Mayoral, R., Heinrichsdorff, J., Osborn, O., Franck, N., Hah, N., Walenta, E., Bandyopadhyay, G., Pessentheiner, A. R., Chi, T. J., Chung, H., Bogner-Strauss, J. G., Evans, R. M., Olefsky, J. M., and Oh da, Y. (2015) Characterization of distinct subpopulations of hepatic macrophages in HFD/obese mice. *Diabetes* **64**, 1120-1130
194. Obstfeld, A. E., Sugaru, E., Thearle, M., Francisco, A. M., Gayet, C., Ginsberg, H. N., Ables, E. V., and Ferrante, A. W., Jr. (2010) C-C chemokine receptor 2 (CCR2) regulates the hepatic recruitment of myeloid cells that promote obesity-induced hepatic steatosis. *Diabetes* **59**, 916-925
195. Fink, L. N., Oberbach, A., Costford, S. R., Chan, K. L., Sams, A., Bluher, M., and Klip, A. (2013) Expression of anti-inflammatory macrophage genes within skeletal muscle correlates with insulin sensitivity in human obesity and type 2 diabetes. *Diabetologia* **56**, 1623-1628
196. Esser, N., Legrand-Poels, S., Piette, J., Scheen, A. J., and Paquot, N. (2014) Inflammation as a link between obesity, metabolic syndrome and type 2 diabetes. *Diabetes Res Clin Pract* **105**, 141-150
197. Donath, M. Y., and Shoelson, S. E. (2011) Type 2 diabetes as an inflammatory disease. *Nat Rev Immunol* **11**, 98-107
198. Maedler, K., Sergeev, P., Ris, F., Oberholzer, J., Joller-Jemelka, H. I., Spinas, G. A., Kaiser, N., Halban, P. A., and Donath, M. Y. (2002) Glucose-induced beta cell production of IL-1beta contributes to glucotoxicity in human pancreatic islets. *J Clin Invest* **110**, 851-860
199. Dinarello, C. A. (2009) Immunological and inflammatory functions of the interleukin-1 family. *Annu Rev Immunol* **27**, 519-550

200. Tran, D. Q., Tse, E. K., Kim, M. H., and Belsham, D. D. (2016) Diet-induced cellular neuroinflammation in the hypothalamus: Mechanistic insights from investigation of neurons and microglia. *Mol Cell Endocrinol*
201. Schwartz, M. W., Woods, S. C., Porte, D., Jr., Seeley, R. J., and Baskin, D. G. (2000) Central nervous system control of food intake. *Nature* **404**, 661-671
202. Thaler, J. P., Yi, C. X., Schur, E. A., Guyenet, S. J., Hwang, B. H., Dietrich, M. O., Zhao, X., Sarruf, D. A., Izgur, V., Maravilla, K. R., Nguyen, H. T., Fischer, J. D., Matsen, M. E., Wisse, B. E., Morton, G. J., Horvath, T. L., Baskin, D. G., Tschop, M. H., and Schwartz, M. W. (2012) Obesity is associated with hypothalamic injury in rodents and humans. *J Clin Invest* **122**, 153-162
203. Araujo, E. P., Moraes, J. C., Cintra, D. E., and Velloso, L. (2016) MECHANISMS IN ENDOCRINOLOGY: Hypothalamic inflammation and nutrition. *Eur J Endocrinol*
204. Romeo, G. R., Lee, J., and Shoelson, S. E. (2012) Metabolic syndrome, insulin resistance, and roles of inflammation--mechanisms and therapeutic targets. *Arterioscler Thromb Vasc Biol* **32**, 1771-1776
205. Dominguez, H., Storgaard, H., Rask-Madsen, C., Steffen Hermann, T., Ihlemann, N., Baunbjerg Nielsen, D., Spohr, C., Kober, L., Vaag, A., and Torp-Pedersen, C. (2005) Metabolic and vascular effects of tumor necrosis factor-alpha blockade with etanercept in obese patients with type 2 diabetes. *J Vasc Res* **42**, 517-525
206. Weisberg, S. P., Hunter, D., Huber, R., Lemieux, J., Slaymaker, S., Vaddi, K., Charo, I., Leibel, R. L., and Ferrante, A. W., Jr. (2006) CCR2 modulates inflammatory and metabolic effects of high-fat feeding. *J Clin Invest* **116**, 115-124
207. Rittling, S. R. (2011) Osteopontin in macrophage function. *Expert Rev Mol Med* **13**, e15
208. Nomiyama, T., Perez-Tilve, D., Ogawa, D., Gizard, F., Zhao, Y., Heywood, E. B., Jones, K. L., Kawamori, R., Cassis, L. A., Tschop, M. H., and Bruemmer, D. (2007) Osteopontin mediates obesity-induced adipose tissue macrophage infiltration and insulin resistance in mice. *J Clin Invest* **117**, 2877-2888
209. Kiefer, F. W., Zeyda, M., Todoric, J., Huber, J., Geyeregger, R., Weichhart, T., Aszmann, O., Ludvik, B., Silberhumer, G. R., Prager, G., and Stulnig, T. M. (2008) Osteopontin expression in human and murine obesity: extensive local up-regulation in adipose tissue but minimal systemic alterations. *Endocrinology* **149**, 1350-1357
210. Gomez-Ambrosi, J., Catalan, V., Ramirez, B., Rodriguez, A., Colina, I., Silva, C., Rotellar, F., Mugueta, C., Gil, M. J., Cienfuegos, J. A., Salvador, J., and Fruhbeck, G. (2007) Plasma osteopontin levels and expression in adipose tissue are increased in obesity. *J Clin Endocrinol Metab* **92**, 3719-3727

211. Bertola, A., Deveaux, V., Bonnafous, S., Rousseau, D., Anty, R., Wakkach, A., Dahman, M., Tordjman, J., Clement, K., McQuaid, S. E., Frayn, K. N., Huet, P. M., Gugenheim, J., Lotersztajn, S., Le Marchand-Brustel, Y., Tran, A., and Gual, P. (2009) Elevated expression of osteopontin may be related to adipose tissue macrophage accumulation and liver steatosis in morbid obesity. *Diabetes* **58**, 125-133
212. Kiefer, F. W., Zeyda, M., Gollinger, K., Pfau, B., Neuhofer, A., Weichhart, T., Saemann, M. D., Geyeregger, R., Schlederer, M., Kenner, L., and Stulnig, T. M. (2010) Neutralization of osteopontin inhibits obesity-induced inflammation and insulin resistance. *Diabetes* **59**, 935-946
213. Kiefer, F. W., Neschen, S., Pfau, B., Legerer, B., Neuhofer, A., Kahle, M., Hrabe de Angelis, M., Schlederer, M., Mair, M., Kenner, L., Plutzky, J., Zeyda, M., and Stulnig, T. M. (2011) Osteopontin deficiency protects against obesity-induced hepatic steatosis and attenuates glucose production in mice. *Diabetologia* **54**, 2132-2142
214. Vallerie, S. N., Furuhashi, M., Fucho, R., and Hotamisligil, G. S. (2008) A predominant role for parenchymal c-Jun amino terminal kinase (JNK) in the regulation of systemic insulin sensitivity. *PLoS One* **3**, e3151
215. Arkan, M. C., Hevener, A. L., Greten, F. R., Maeda, S., Li, Z. W., Long, J. M., Wynshaw-Boris, A., Poli, G., Olefsky, J., and Karin, M. (2005) IKK-beta links inflammation to obesity-induced insulin resistance. *Nat Med* **11**, 191-198
216. Hume, D. A. (2011) Applications of myeloid-specific promoters in transgenic mice support in vivo imaging and functional genomics but do not support the concept of distinct macrophage and dendritic cell lineages or roles in immunity. *J Leukoc Biol* **89**, 525-538
217. Mauer, J., Chaurasia, B., Plum, L., Quast, T., Hampel, B., Bluher, M., Kolanus, W., Kahn, C. R., and Bruning, J. C. (2010) Myeloid cell-restricted insulin receptor deficiency protects against obesity-induced inflammation and systemic insulin resistance. *PLoS Genet* **6**, e1000938
218. Clementi, A. H., Gaudy, A. M., van Rooijen, N., Pierce, R. H., and Mooney, R. A. (2009) Loss of Kupffer cells in diet-induced obesity is associated with increased hepatic steatosis, STAT3 signaling, and further decreases in insulin signaling. *Biochim Biophys Acta* **1792**, 1062-1072
219. Lanthier, N., Molendi-Coste, O., Horsmans, Y., van Rooijen, N., Cani, P. D., and Leclercq, I. A. (2010) Kupffer cell activation is a causal factor for hepatic insulin resistance. *Am J Physiol Gastrointest Liver Physiol* **298**, G107-116
220. Lanthier, N., Molendi-Coste, O., Cani, P. D., van Rooijen, N., Horsmans, Y., and Leclercq, I. A. (2011) Kupffer cell depletion prevents but has no therapeutic effect on metabolic and inflammatory changes induced by a high-fat diet. *FASEB J* **25**, 4301-4311
221. Bu, L., Gao, M., Qu, S., and Liu, D. (2013) Intraperitoneal injection of clodronate liposomes eliminates visceral adipose macrophages and

blocks high-fat diet-induced weight gain and development of insulin resistance. *AAPS J* **15**, 1001-1011
222. Choe, S. S., Shin, K. C., Ka, S., Lee, Y. K., Chun, J. S., and Kim, J. B. (2014) Macrophage HIF-2alpha ameliorates adipose tissue inflammation and insulin resistance in obesity. *Diabetes* **63**, 3359-3371
223. Negrin, K. A., Roth Flach, R. J., DiStefano, M. T., Matevossian, A., Friedline, R. H., Jung, D., Kim, J. K., and Czech, M. P. (2014) IL-1 signaling in obesity-induced hepatic lipogenesis and steatosis. *PLoS One* **9**, e107265
224. Navarro, L. A., Wree, A., Povero, D., Berk, M. P., Eguchi, A., Ghosh, S., Papouchado, B. G., Erzurum, S. C., and Feldstein, A. E. (2015) Arginase 2 deficiency results in spontaneous steatohepatitis: a novel link between innate immune activation and hepatic de novo lipogenesis. *J Hepatol* **62**, 412-420
225. Zeng, T. S., Liu, F. M., Zhou, J., Pan, S. X., Xia, W. F., and Chen, L. L. (2015) Depletion of Kupffer cells attenuates systemic insulin resistance, inflammation and improves liver autophagy in high-fat diet fed mice. *Endocr J* **62**, 615-626
226. Sakamoto, T., Nitta, T., Maruno, K., Yeh, Y. S., Kuwata, H., Tomita, K., Goto, T., Takahashi, N., and Kawada, T. (2016) Macrophage infiltration into obese adipose tissues suppresses the induction of UCP1 expression in mice. *Am J Physiol Endocrinol Metab*, ajpendo 00028 02015
227. Van Rooijen, N., and Sanders, A. (1994) Liposome mediated depletion of macrophages: mechanism of action, preparation of liposomes and applications. *J Immunol Methods* **174**, 83-93
228. Aouadi, M., Tesz, G. J., Nicoloro, S. M., Wang, M., Chouinard, M., Soto, E., Ostroff, G. R., and Czech, M. P. (2009) Orally delivered siRNA targeting macrophage Map4k4 suppresses systemic inflammation. *Nature* **458**, 1180-1184
229. Huang, W., Ghisletti, S., Saijo, K., Gandhi, M., Aouadi, M., Tesz, G. J., Zhang, D. X., Yao, J., Czech, M. P., Goode, B. L., Rosenfeld, M. G., and Glass, C. K. (2011) Coronin 2A mediates actin-dependent de-repression of inflammatory response genes. *Nature* **470**, 414-418
230. Tesz, G. J., Aouadi, M., Prot, M., Nicoloro, S. M., Boutet, E., Amano, S. U., Goller, A., Wang, M., Guo, C. A., Salomon, W. E., Virbasius, J. V., Baum, R. A., O'Connor, M. J., Jr., Soto, E., Ostroff, G. R., and Czech, M. P. (2011) Glucan particles for selective delivery of siRNA to phagocytic cells in mice. *Biochem J* **436**, 351-362
231. Aouadi, M., Tencerova, M., Vangala, P., Yawe, J. C., Nicoloro, S. M., Amano, S. U., Cohen, J. L., and Czech, M. P. (2013) Gene silencing in adipose tissue macrophages regulates whole-body metabolism in obese mice. *Proc Natl Acad Sci U S A* **110**, 8278-8283
232. Aouadi, M., Vangala, P., Yawe, J. C., Tencerova, M., Nicoloro, S. M., Cohen, J. L., Shen, Y., and Czech, M. P. (2014) Lipid storage by adipose

tissue macrophages regulates systemic glucose tolerance. *Am J Physiol Endocrinol Metab* **307**, E374-383
233. Tencerova, M., Aouadi, M., Vangala, P., Nicoloro, S. M., Yawe, J. C., Cohen, J. L., Shen, Y., Garcia-Menendez, L., Pedersen, D. J., Gallagher-Dorval, K., Perugini, R. A., Gupta, O. T., and Czech, M. P. (2015) Activated Kupffer cells inhibit insulin sensitivity in obese mice. *FASEB J* **29**, 2959-2969
234. Herre, J., Gordon, S., and Brown, G. D. (2004) Dectin-1 and its role in the recognition of beta-glucans by macrophages. *Mol Immunol* **40**, 869-876
235. Hotamisligil, G. S. (2006) Inflammation and metabolic disorders. *Nature* **444**, 860-867
236. Daems, W. T., and de Bakker, J. M. (1982) Do resident macrophages proliferate? *Immunobiology* **161**, 204-211
237. Hume, D. A., Ross, I. L., Himes, S. R., Sasmono, R. T., Wells, C. A., and Ravasi, T. (2002) The mononuclear phagocyte system revisited. *J Leukoc Biol* **72**, 621-627
238. Chorro, L., Sarde, A., Li, M., Woollard, K. J., Chambon, P., Malissen, B., Kissenpfennig, A., Barbaroux, J. B., Groves, R., and Geissmann, F. (2009) Langerhans cell (LC) proliferation mediates neonatal development, homeostasis, and inflammation-associated expansion of the epidermal LC network. *J Exp Med* **206**, 3089-3100
239. Jenkins, S. J., Ruckerl, D., Cook, P. C., Jones, L. H., Finkelman, F. D., van Rooijen, N., MacDonald, A. S., and Allen, J. E. (2011) Local macrophage proliferation, rather than recruitment from the blood, is a signature of TH2 inflammation. *Science* **332**, 1284-1288
240. Rosenfeld, M. E., and Ross, R. (1990) Macrophage and smooth muscle cell proliferation in atherosclerotic lesions of WHHL and comparably hypercholesterolemic fat-fed rabbits. *Arteriosclerosis* **10**, 680-687
241. Yang, N., Wu, L. L., Nikolic-Paterson, D. J., Ng, Y. Y., Yang, W. C., Mu, W., Gilbert, R. E., Cooper, M. E., Atkins, R. C., and Lan, H. Y. (1998) Local macrophage and myofibroblast proliferation in progressive renal injury in the rat remnant kidney. *Nephrol Dial Transplant* **13**, 1967-1974
242. Hashimoto, D., Chow, A., Noizat, C., Teo, P., Beasley, M. B., Leboeuf, M., Becker, C. D., See, P., Price, J., Lucas, D., Greter, M., Mortha, A., Boyer, S. W., Forsberg, E. C., Tanaka, M., van Rooijen, N., Garcia-Sastre, A., Stanley, E. R., Ginhoux, F., Frenette, P. S., and Merad, M. (2013) Tissue-resident macrophages self-maintain locally throughout adult life with minimal contribution from circulating monocytes. *Immunity* **38**, 792-804
243. Liddiard, K., Rosas, M., Davies, L. C., Jones, S. A., and Taylor, P. R. (2011) Macrophage heterogeneity and acute inflammation. *Eur J Immunol* **41**, 2503-2508
244. Page, D. T., and Garvey, J. S. (1979) Isolation and characterization of hepatocytes and Kupffer cells. *J Immunol Methods* **27**, 159-173

245. Scholzen, T., and Gerdes, J. (2000) The Ki-67 protein: from the known and the unknown. *J Cell Physiol* **182**, 311-322
246. Murano, I., Barbatelli, G., Parisani, V., Latini, C., Muzzonigro, G., Castellucci, M., and Cinti, S. (2008) Dead adipocytes, detected as crown-like structures, are prevalent in visceral fat depots of genetically obese mice. *J Lipid Res* **49**, 1562-1568
247. Lumeng, C. N., DelProposto, J. B., Westcott, D. J., and Saltiel, A. R. (2008) Phenotypic switching of adipose tissue macrophages with obesity is generated by spatiotemporal differences in macrophage subtypes. *Diabetes* **57**, 3239-3246
248. Oh, D. Y., Morinaga, H., Talukdar, S., Bae, E. J., and Olefsky, J. M. (2012) Increased macrophage migration into adipose tissue in obese mice. *Diabetes* **61**, 346-354
249. Chen, L., Magliano, D. J., and Zimmet, P. Z. (2012) The worldwide epidemiology of type 2 diabetes mellitus--present and future perspectives. *Nat Rev Endocrinol* **8**, 228-236
250. Kusminski, C. M., Shetty, S., Orci, L., Unger, R. H., and Scherer, P. E. (2009) Diabetes and apoptosis: lipotoxicity. *Apoptosis* **14**, 1484-1495
251. Samuel, V. T., Petersen, K. F., and Shulman, G. I. (2010) Lipid-induced insulin resistance: unravelling the mechanism. *Lancet* **375**, 2267-2277
252. Lumeng, C. N., and Saltiel, A. R. (2011) Inflammatory links between obesity and metabolic disease. *J Clin Invest* **121**, 2111-2117
253. Bluher, M. (2010) The distinction of metabolically 'healthy' from 'unhealthy' obese individuals. *Curr Opin Lipidol* **21**, 38-43
254. Hardy, O. T., Perugini, R. A., Nicoloro, S. M., Gallagher-Dorval, K., Puri, V., Straubhaar, J., and Czech, M. P. (2011) Body mass index-independent inflammation in omental adipose tissue associated with insulin resistance in morbid obesity. *Surg Obes Relat Dis* **7**, 60-67
255. Alvehus, M., Buren, J., Sjostrom, M., Goedecke, J., and Olsson, T. (2010) The human visceral fat depot has a unique inflammatory profile. *Obesity (Silver Spring)* **18**, 879-883
256. Fontana, L., Eagon, J. C., Trujillo, M. E., Scherer, P. E., and Klein, S. (2007) Visceral fat adipokine secretion is associated with systemic inflammation in obese humans. *Diabetes* **56**, 1010-1013
257. Chen, A., Mumick, S., Zhang, C., Lamb, J., Dai, H., Weingarth, D., Mudgett, J., Chen, H., MacNeil, D. J., Reitman, M. L., and Qian, S. (2005) Diet induction of monocyte chemoattractant protein-1 and its impact on obesity. *Obes Res* **13**, 1311-1320
258. Kamei, N., Tobe, K., Suzuki, R., Ohsugi, M., Watanabe, T., Kubota, N., Ohtsuka-Kowatari, N., Kumagai, K., Sakamoto, K., Kobayashi, M., Yamauchi, T., Ueki, K., Oishi, Y., Nishimura, S., Manabe, I., Hashimoto, H., Ohnishi, Y., Ogata, H., Tokuyama, K., Tsunoda, M., Ide, T., Murakami, K., Nagai, R., and Kadowaki, T. (2006) Overexpression of monocyte

chemoattractant protein-1 in adipose tissues causes macrophage recruitment and insulin resistance. *J Biol Chem* **281**, 26602-26614
259. Binkhathlan, Z., and Alshamsan, A. (2012) Emerging nanodelivery strategies of RNAi molecules for colon cancer therapy: preclinical developments. *Ther Deliv* **3**, 1117-1130
260. Gavrilov, K., and Saltzman, W. M. (2012) Therapeutic siRNA: principles, challenges, and strategies. *Yale J Biol Med* **85**, 187-200
261. Leuschner, F., Dutta, P., Gorbatov, R., Novobrantseva, T. I., Donahoe, J. S., Courties, G., Lee, K. M., Kim, J. I., Markmann, J. F., Marinelli, B., Panizzi, P., Lee, W. W., Iwamoto, Y., Milstein, S., Epstein-Barash, H., Cantley, W., Wong, J., Cortez-Retamozo, V., Newton, A., Love, K., Libby, P., Pittet, M. J., Swirski, F. K., Koteliansky, V., Langer, R., Weissleder, R., Anderson, D. G., and Nahrendorf, M. (2011) Therapeutic siRNA silencing in inflammatory monocytes in mice. *Nat Biotechnol* **29**, 1005-1010
262. Larsen, C. M., Faulenbach, M., Vaag, A., Volund, A., Ehses, J. A., Seifert, B., Mandrup-Poulsen, T., and Donath, M. Y. (2007) Interleukin-1-receptor antagonist in type 2 diabetes mellitus. *N Engl J Med* **356**, 1517-1526
263. Ofei, F., Hurel, S., Newkirk, J., Sopwith, M., and Taylor, R. (1996) Effects of an engineered human anti-TNF-alpha antibody (CDP571) on insulin sensitivity and glycemic control in patients with NIDDM. *Diabetes* **45**, 881-885
264. van Asseldonk, E. J., Stienstra, R., Koenen, T. B., Joosten, L. A., Netea, M. G., and Tack, C. J. (2011) Treatment with Anakinra improves disposition index but not insulin sensitivity in nondiabetic subjects with the metabolic syndrome: a randomized, double-blind, placebo-controlled study. *J Clin Endocrinol Metab* **96**, 2119-2126
265. van Asseldonk, E. J., van Poppel, P. C., Ballak, D. B., Stienstra, R., Netea, M. G., and Tack, C. J. (2015) One week treatment with the IL-1 receptor antagonist anakinra leads to a sustained improvement in insulin sensitivity in insulin resistant patients with type 1 diabetes mellitus. *Clin Immunol* **160**, 155-162
266. Di Rocco, P., Manco, M., Rosa, G., Greco, A. V., and Mingrone, G. (2004) Lowered tumor necrosis factor receptors, but not increased insulin sensitivity, with infliximab. *Obes Res* **12**, 734-739
267. Boulange, C. L., Neves, A. L., Chilloux, J., Nicholson, J. K., and Dumas, M. E. (2016) Impact of the gut microbiota on inflammation, obesity, and metabolic disease. *Genome Med* **8**, 42
268. Kosteli, A., Sugaru, E., Haemmerle, G., Martin, J. F., Lei, J., Zechner, R., and Ferrante, A. W., Jr. (2010) Weight loss and lipolysis promote a dynamic immune response in murine adipose tissue. *J Clin Invest* **120**, 3466-3479
269. Cao, Y. (2007) Angiogenesis modulates adipogenesis and obesity. *J Clin Invest* **117**, 2362-2368

270. Christiaens, V., and Lijnen, H. R. (2010) Angiogenesis and development of adipose tissue. *Mol Cell Endocrinol* **318**, 2-9
271. Pang, C., Gao, Z., Yin, J., Zhang, J., Jia, W., and Ye, J. (2008) Macrophage infiltration into adipose tissue may promote angiogenesis for adipose tissue remodeling in obesity. *Am J Physiol Endocrinol Metab* **295**, E313-322
272. Halberg, N., Khan, T., Trujillo, M. E., Wernstedt-Asterholm, I., Attie, A. D., Sherwani, S., Wang, Z. V., Landskroner-Eiger, S., Dineen, S., Magalang, U. J., Brekken, R. A., and Scherer, P. E. (2009) Hypoxia-inducible factor 1alpha induces fibrosis and insulin resistance in white adipose tissue. *Mol Cell Biol* **29**, 4467-4483
273. Adeyo, O., Goulbourne, C. N., Bensadoun, A., Beigneux, A. P., Fong, L. G., and Young, S. G. (2012) Glycosylphosphatidylinositol-anchored high-density lipoprotein-binding protein 1 and the intravascular processing of triglyceride-rich lipoproteins. *J Intern Med* **272**, 528-540
274. Obunike, J. C., Lutz, E. P., Li, Z., Paka, L., Katopodis, T., Strickland, D. K., Kozarsky, K. F., Pillarisetti, S., and Goldberg, I. J. (2001) Transcytosis of lipoprotein lipase across cultured endothelial cells requires both heparan sulfate proteoglycans and the very low density lipoprotein receptor. *J Biol Chem* **276**, 8934-8941
275. Babaev, V. R., Patel, M. B., Semenkovich, C. F., Fazio, S., and Linton, M. F. (2000) Macrophage lipoprotein lipase promotes foam cell formation and atherosclerosis in low density lipoprotein receptor-deficient mice. *J Biol Chem* **275**, 26293-26299
276. Takahashi, M., Yagyu, H., Tazoe, F., Nagashima, S., Ohshiro, T., Okada, K., Osuga, J., Goldberg, I. J., and Ishibashi, S. (2013) Macrophage lipoprotein lipase modulates the development of atherosclerosis but not adiposity. *J Lipid Res* **54**, 1124-1134
277. Chen, X., Iqbal, N., and Boden, G. (1999) The effects of free fatty acids on gluconeogenesis and glycogenolysis in normal subjects. *J Clin Invest* **103**, 365-372
278. Donnelly, K. L., Smith, C. I., Schwarzenberg, S. J., Jessurun, J., Boldt, M. D., and Parks, E. J. (2005) Sources of fatty acids stored in liver and secreted via lipoproteins in patients with nonalcoholic fatty liver disease. *J Clin Invest* **115**, 1343-1351
279. Chavez, J. A., and Summers, S. A. (2012) A ceramide-centric view of insulin resistance. *Cell Metab* **15**, 585-594
280. Fu, S., Watkins, S. M., and Hotamisligil, G. S. (2012) The role of endoplasmic reticulum in hepatic lipid homeostasis and stress signaling. *Cell Metab* **15**, 623-634
281. Glass, C. K., and Olefsky, J. M. (2012) Inflammation and lipid signaling in the etiology of insulin resistance. *Cell Metab* **15**, 635-645

282. Perry, R. J., Samuel, V. T., Petersen, K. F., and Shulman, G. I. (2014) The role of hepatic lipids in hepatic insulin resistance and type 2 diabetes. *Nature* **510**, 84-91
283. Sun, Z., and Lazar, M. A. (2013) Dissociating fatty liver and diabetes. *Trends Endocrinol Metab* **24**, 4-12
284. Ramadori, G., and Armbrust, T. (2001) Cytokines in the liver. *Eur J Gastroenterol Hepatol* **13**, 777-784
285. Dolina, J. S., Sung, S. S., Novobrantseva, T. I., Nguyen, T. M., and Hahn, Y. S. (2013) Lipidoid Nanoparticles Containing PD-L1 siRNA Delivered In Vivo Enter Kupffer Cells and Enhance NK and CD8(+) T Cell-mediated Hepatic Antiviral Immunity. *Mol Ther Nucleic Acids* **2**, e72
286. Hoffmann, F., Sass, G., Zillies, J., Zahler, S., Tiegs, G., Hartkorn, A., Fuchs, S., Wagner, J., Winter, G., Coester, C., Gerbes, A. L., and Vollmar, A. M. (2009) A novel technique for selective NF-kappaB inhibition in Kupffer cells: contrary effects in fulminant hepatitis and ischaemia-reperfusion. *Gut* **58**, 1670-1678
287. Jing, Y., Shishkov, A., and Ponnappa, B. C. (2008) Inhibition of tumor necrosis factor alpha secretion in rat Kupffer cells by siRNA: in vivo efficacy of siRNA-liposomes. *Biochim Biophys Acta* **1780**, 34-40
288. Lee, S., Yang, S. C., Kao, C. Y., Pierce, R. H., and Murthy, N. (2009) Solid polymeric microparticles enhance the delivery of siRNA to macrophages in vivo. *Nucleic Acids Res* **37**, e145
289. Ogushi, I., Iimuro, Y., Seki, E., Son, G., Hirano, T., Hada, T., Tsutsui, H., Nakanishi, K., Morishita, R., Kaneda, Y., and Fujimoto, J. (2003) Nuclear factor kappa B decoy oligodeoxynucleotides prevent endotoxin-induced fatal liver failure in a murine model. *Hepatology* **38**, 335-344
290. Tosello-Trampont, A. C., Landes, S. G., Nguyen, V., Novobrantseva, T. I., and Hahn, Y. S. (2012) Kuppfer cells trigger nonalcoholic steatohepatitis development in diet-induced mouse model through tumor necrosis factor-alpha production. *J Biol Chem* **287**, 40161-40172
291. Beraza, N., Malato, Y., Vander Borght, S., Liedtke, C., Wasmuth, H. E., Dreano, M., de Vos, R., Roskams, T., and Trautwein, C. (2008) Pharmacological IKK2 inhibition blocks liver steatosis and initiation of non-alcoholic steatohepatitis. *Gut* **57**, 655-663
292. Stienstra, R., Saudale, F., Duval, C., Keshtkar, S., Groener, J. E., van Rooijen, N., Staels, B., Kersten, S., and Muller, M. (2010) Kupffer cells promote hepatic steatosis via interleukin-1beta-dependent suppression of peroxisome proliferator-activated receptor alpha activity. *Hepatology* **51**, 511-522
293. Han, M. S., Jung, D. Y., Morel, C., Lakhani, S. A., Kim, J. K., Flavell, R. A., and Davis, R. J. (2013) JNK expression by macrophages promotes obesity-induced insulin resistance and inflammation. *Science* **339**, 218-222

294. Chiang, S. H., Bazuine, M., Lumeng, C. N., Geletka, L. M., Mowers, J., White, N. M., Ma, J. T., Zhou, J., Qi, N., Westcott, D., Delproposto, J. B., Blackwell, T. S., Yull, F. E., and Saltiel, A. R. (2009) The protein kinase IKKepsilon regulates energy balance in obese mice. *Cell* **138**, 961-975
295. Reilly, S. M., Chiang, S. H., Decker, S. J., Chang, L., Uhm, M., Larsen, M. J., Rubin, J. R., Mowers, J., White, N. M., Hochberg, I., Downes, M., Yu, R. T., Liddle, C., Evans, R. M., Oh, D., Li, P., Olefsky, J. M., and Saltiel, A. R. (2013) An inhibitor of the protein kinases TBK1 and IKK-varepsilon improves obesity-related metabolic dysfunctions in mice. *Nat Med* **19**, 313-321
296. Chen, J., and Raymond, K. (2008) Beta-glucans in the treatment of diabetes and associated cardiovascular risks. *Vasc Health Risk Manag* **4**, 1265-1272
297. Liu, B., Lin, Q., Yang, T., Zeng, L., Shi, L., Chen, Y., and Luo, F. (2015) Oat beta-glucan ameliorates dextran sulfate sodium (DSS)-induced ulcerative colitis in mice. *Food Funct* **6**, 3454-3463
298. Zeyda, M., Gollinger, K., Todoric, J., Kiefer, F. W., Keck, M., Aszmann, O., Prager, G., Zlabinger, G. J., Petzelbauer, P., and Stulnig, T. M. (2011) Osteopontin is an activator of human adipose tissue macrophages and directly affects adipocyte function. *Endocrinology* **152**, 2219-2227